



ADVANCED MASTERS IN STRUCTURAL ANALYSIS OF MONUMENTS AND HISTORICAL CONSTRUCTIONS

# Master's Thesis

Carolina Manrique Hoyos

## Limit Analysis: Collection of Examples of Applications



UNIVERSITAT POLITÈCNICA DE CATALUNYA



University of Minho



Education and Culture

# Erasmus Mundus



ADVANCED MASTERS IN STRUCTURAL ANALYSIS  
OF MONUMENTS AND HISTORICAL CONSTRUCTIONS



# Master's Thesis

Carolina Manrique Hoyos

## Limit Analysis: Collection of Examples of Applications

This Masters Course has been funded with support from the European Commission. This publication reflects the views only of the author, and the Commission cannot be held responsible for any use which may be made of the information contained therein.

## DECLARATION

Name: Carolina Manrique Hoyos

Email: carquicol@gmail.com

Title of the Msc Dissertation: Limit Analysis: Collection of Examples of Applications

Supervisor(s): Climent Molins

Year: 2010

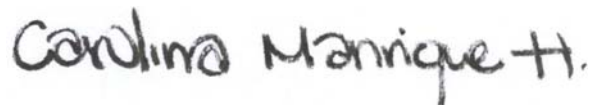
I hereby declare that all information in this document has been obtained and presented in accordance with academic rules and ethical conduct. I also declare that, as required by these rules and conduct, I have fully cited and referenced all material and results that are not original to this work.

I hereby declare that the MSc Consortium responsible for the Advanced Masters in Structural Analysis of Monuments and Historical Constructions is allowed to store and make available electronically the present MSc Dissertation.

University: Universitat Politècnica de Catalunya

Date: 12th of July of 2010

Signature:



---



To the mighty tower that kept me safe.



## ACKNOWLEDGEMENTS

I want to give a special acknowledgement to the European Commission and the Master Consortium for the Erasmus Mundus scholarship that allowed me to have the experience of pursuing this master course in two different countries.

To professors Paulo Lourenço and Daniel Abrams for the amazing lectures at Universidade do Minho.

To professors Pere Roca and Climent Molins for their guidance in Barcelona.

To Elisa Poletti, Joao Leite, Leonardo Avila and Ines Costa for all the precious PhD hours spent in helping me understand greek.

To Pinar Abacilar for being my sister architect during the struggle for understanding what was going on during the courses and daily life. I hope we can meet in Istanbul in the near future.

To Gonzalo Roberts for his patience and unbelievable clarity when answering my endless questions during the program, for saving me when I was completely lost, and for inspiring me to do things better with his enthusiasm for structures. I know he has an architect inside of him, I hope he finds it.

To Cem Taneri for making me laugh during difficult times.

To Susana Moreira and Clive Allen for their generosity sharing knowledge always with a smile.

To Shouquan Zhu, Gibson Craig, Luana Boromeo, Peter Vonk, Dora Coehlo, Mateus Oliveira, Amr Fangary, Amol Varshney and Diogo Coutinho for the time shared in Guimarães and Barcelona.

To Mauricio Otero for waking me up.

To Rodrigo Vargas for keeping in contact during all these months, for making me aware of the real life, for his silly comments that cheered me up, for his inspirational talent as an architect, and for reminding me I have to write. ¡Suerte en Georgia Tech!

To Diego Javier Lotero for being the mighty tower that has kept me safe during all these years, for sharing my interest in structures from an architecture point of view, and for understanding more than I why I came to this program. ¡Te quiero mucho y te he extrañado un montón!

To my aunt Constanza and grandmother Olga for their love since I can remember.

To my brother Juan Carlos and his new family Margarita, Valentina and Tomas for all the joy this year.

To my sister Natalia for coming to visit me in both countries, for all the important conversations we have always had, for the love we have for our family and beloved pets, and for the pain we share of being far away. ¡Ánimo Nati, nos vemos en Cali para Navidad!

To my parents Fabiola and Alfonso for their unconditional love and support in every new adventure I decide to start, for giving me strength during challenging times, for learning every technology available in order to keep in contact, and for reminding me their house is always mine. Me han hecho mucha falta, ¡Los quiero mucho!





## **ABSTRACT**

Limit Analysis constitutes a simplified method for the assessment of masonry historical constructions.

A series of examples of application of both static and kinematic limit analysis are presented with detailed explanations so as to be used by future SAHC students and others interested in understanding the principles and operation of these approaches.

A state of art on the concepts underlying limit analysis is presented as well as a selection of real case studies of different typology of structures such as a single span arch bridge, a barrel vault over buttresses, a multi-span two level arch bridge (aqueduct), the last arch in a series of arches façade, and a tower.

Each case is shown in a step-by-step scheme following the sequence of assumptions and procedures followed with the use of graphic statics.

The examples include cases of structures subjected to dead loading, live loading and earthquake.

For each case a specific objective was defined which included verifying an experimentally known solution for an arch bridge that was tested to failure, comparing two mechanisms in the kinematic approach and finding a safe condition for the most critical one in the case of a convent church, obtaining a thrust line for the exterior buttress of a four story building, evaluating the seismic behavior for the transversal section of an aqueduct, and applying the kinematic approach for designing the strengthening with tie rods of a façade in a tower.



## RESUMEN

*Análisis Límite: Colección de ejemplos de aplicación.*

El Análisis Límite constituye un método simplificado para la evaluación de construcciones históricas de mampostería.

Una serie de ejemplos de aplicación utilizando las aproximaciones estática y cinemática del análisis límite son presentadas con explicaciones detalladas para ser utilizadas por futuros estudiantes del programa SAHC, y por aquellos interesados en los principios y procedimientos de éstos métodos.

El estado del arte de los conceptos que subyacen el análisis límite es presentado así como una selección de casos de estudio reales de diferente tipología estructural tales como un puente de arco de luz simple, una bóveda de cañón apoyada en contrafuertes, un puente de arco de dos niveles y múltiples luces (acueducto), el último arco en una fachada de series de arcos, y una torre.

Cada caso es mostrado en un esquema paso a paso, siguiendo la secuencia de suposiciones y procedimientos llevados a cabo con el uso de la estática gráfica.

Los ejemplos incluyen casos de estructuras solicitadas a cargas permanentes, cargas vivas y sismo.

Para cada caso un objetivo específico fue definido incluyendo la verificación de una solución conocida para una prueba de colapso en un puente de arco, la comparación entre dos mecanismos siguiendo la aproximación cinemática y la búsqueda de una condición segura para el caso encontrado como más crítico en el caso de una iglesia, la obtención de una línea de empuje para el contrafuerte exterior de un edificio de cuatro plantas, la evaluación del comportamiento sísmico para la sección transversal de un acueducto, y la aplicación de la aproximación cinemática para el diseño del reforzamiento con tensores de una de las fachadas en una torre.



## RESUMO

### *Análise Limite: Compilação de Exemplos de Aplicação*

A Análise Limite constitui um método simplificado para a avaliação de construções históricas de alvenaria.

São apresentados vários exemplos de aplicação de ambas as análises limite estática e cinemática, com explicações detalhadas de forma a serem usados no futuro por alunos do curso SAHC e por outros interessados em entender os princípios e procedimento destas abordagens.

É apresentado o estado de arte dos conceitos subjacentes à análise limite, bem como uma selecção de casos de estudo reais de diferentes tipologias de estruturas, como uma ponte em arco de vão único, uma abóbada de berço apoiada em contrafortes, uma ponte em arco com vários vãos e de dois níveis (aqueduto), o último arco numa fachada composta por uma série de arcos, e uma torre.

Cada caso é apresentado num esquema passo por passo, seguindo a sequência de suposições e procedimentos, e seguido pelo uso de estáticas gráficas.

Os exemplos incluem casos de estruturas sujeitas a cargas permanentes, cargas variáveis e sismos.

Para cada caso é definido um objectivo específico que inclui verificar uma solução conhecida experimentalmente para uma ponte em arco que foi testado até ao colapso, comparar dois mecanismos da estrutura de um convento através da abordagem cinemática e encontrar uma condição de segurança para o mais crítico, obter uma linha de impulso para os contrafortes exteriores de um edifício de quatro pisos, avaliar o comportamento sísmico da secção transversal de um aqueduto, e aplicar a abordagem cinemática para o projecto de reforço de tirantes para a fachada de uma torre.



## TABLE OF CONTENTS

DECLARATION .....	i
ACKNOWLEDGEMENTS .....	v
ABSTRACT.....	vii
RESUMEN.....	ix
RESUMO.....	xi
LIST OF FIGURES.....	xv
LIST OF TABLES .....	xix
1. INTRODUCTION.....	1
2. STATE OF ART.....	3
2.1 General aspects .....	3
2.2 Masonry.....	3
2.3 Structural Analysis.....	4
2.3.1 Graphic statics.....	4
2.3.2 Plastic theory .....	6
2.4 Limit Analysis.....	7
2.4.1 Static approach.....	9
2.4.2 Kinematic approach.....	11
2.5 Computational limit analysis.....	12
3. EXAMPLES OF APPLICATION OF LIMIT ANALYSIS METHODS .....	15
3.1 Arch Bridge (Bridgemill Bridge in UK) .....	17
3.1.1 Kinematic Approach .....	18
3.1.2 Static Approach .....	28
3.2 Continuous barrel vault with buttresses (Cuernavaca Church in Mexico) .....	35
3.2.1 Kinematic Approach .....	39
3.2.1.1 Mechanism – 1: Five hinges in isolated arch. ....	39
3.2.1.2 Mechanism – 2: Three hinges in arch and two hinges in buttresses. ....	48
3.2.2 Static Approach .....	59
3.2.2.1 5 hinges in arch (no contribution of buttresses) .....	59
3.3 Multiple span one level arch façade (Plaza Real in Spain) .....	65
3.3.1 Static Approach .....	67
3.4 Multiple span arch bridge (Devil Bridge in Spain) .....	77
3.4.1 Kinematic approach.....	80
3.5 Façade wall (Quintela Tower in Portugal) .....	87
3.5.1 Kinematic approach.....	88
4. CONCLUSIONS .....	97
5. REFERENCES .....	99
6. ANNEXES .....	103

6.1.	Limit Analysis using RING© .....	103
6.1.1.	Bridgemill bridge: Limit Analysis using RING© .....	103
6.1.2.	Cuernavaca Church: Limit Analysis using RING© .....	106



## LIST OF FIGURES

Fig. 1 – Different types of masonry arrangements. (Huerta Fernández, 2004) .....	3
Fig. 2 – (a) Funicular construction for a set of loads; (b) magnitude of forces in funicular polygon. (Block P. , Equilibrium systems: Studies in Masonry Structure, 2005) .....	5
Fig. 3 – Left, force equilibrium of hanging weights on a string (Stevin, 1586); right, graphical analysis of a funicular shape (Varignon, 1725) (Block, DeJong, & Ochsendorf, As Hangs the Flexible Line:Equilibrium of Masonry Arches, 2006) .....	5
Fig. 4 – Gaudi’s graphical design for the columns and retaining wall of Park Guell, from Rubió, 1913. (Block P. , Equilibrium systems: Studies in Masonry Structure, 2005) .....	6
Fig. 5 – Thrust lines in masonry (Huerta Fernández, 2004) .....	8
Fig. 6 – Semicircular arch under selfweight application of the uniqueness theorem (a) Minimum thrust (b) Maximum thrust. (Heyman, The Stone Skeleton: Structural Engineering of Masonry Architecture, 1995). .....	9
Fig. 7 – Computer optimization for alternate solutions in Maynou, 1998 (Roca, Ancient Rules and Classical Approaches- Part 1-4. SA1 Lectures., 2009-2010) .....	9
Fig. 8 – Thrust line falls within the boundaries of the structure. (Roca, Ancient Rules and Classical Approaches- Part 1-4. SA1 Lectures., 2009-2010).....	10
Fig. 9 - The relationship between upper and lower bound solutions (Gilbert, Limit analysis applied to masonry arch bridges: state-of-the-art and recent developments, 2007) .....	13
Fig. 10 – Geometry of Bridgemill Bridge (Molins, June 1998) .....	17
Fig. 11 – Scaled geometry of Bridgemill Bridge with position of the vertical load V at $\frac{1}{4}$ of the span. .	19
Fig. 12 - Expressions for TOTAL WORK (Roca, Ancient Rules and Classical Approaches- Part 1-4. SA1 Lectures., 2009-2010) .....	19
Fig. 13 – Bridgemill Bridge with location of the four hinges. ....	20
Fig. 14 - Overlapped mechanism from RING© in order to identify the movement of each block. ....	21
Fig. 15 – Sign criteria. ....	21
Fig. 16 - Location of rotation centers for the three blocks in a four-hinge collapse mechanism in arch	21
Fig. 17 - Identification of the rotations, displacements and correlations with the hinges and centers of rotation.....	22
Fig. 18 - Identification of the signs of the angles of rotation of the blocks. ....	22
Fig. 19 - Displacements and rotations determined in sequence. ....	23
Fig. 20 - Measuring the horizontal component distance from centroid of initial block to rotation center (in red). Verification of vertical displacement between centroids of initial blocks and rotated blocks (in green). ....	25
Fig. 21 - Discretization of arch, Location of centroids and vertical forces.....	30
Fig. 22 - Funicular polygon and resultant force.....	31
Fig. 23 - Selection of three hinges for the thrust line to pass through and projection on the funicular polygon. ....	32

Fig. 24 - Defining the new origin for the force polygon.....	33
Fig. 25 - A thrust line passing through ALL hinges is found inside the arch. ....	33
Fig. 26 - Map of the distribution of convent compounds in Mexico and in the State of Morelos (Meli, 2009).....	35
Fig. 27 – Continuous barrel vault of Cuernavaca convent church (Meli, 2009) .....	35
Fig. 28 – Typical ground plan of a convent compound and its church (Meli, 2009).....	35
Fig. 29 – Buttress depth verification with Blondel’s Rule to Cuernavaca church.....	36
Fig. 30 – Geometrical properties for the plan view of Cuernavaca Church. The thickness of the buttress was assumed.....	37
Fig. 31 – Geometrical properties for the vertical section of Cuernavaca Church.....	38
Fig. 32 - Expressions for TOTAL WORK (Roca, Ancient Rules and Classical Approaches- Part 1-4. SA1 Lectures., 2009-2010).....	39
Fig. 33 – Overlapped mechanism from RING© in order to identify the movement of each block.....	40
Fig. 34 – Sign criteria.....	40
Fig. 35 - Location of rotation centers for the four blocks in a symmetrical five-hinge collapse mechanism in arch.....	41
Fig. 36 - Identification of the rotations, displacements and correlations with the hinges and centers of rotation.....	42
Fig. 37 - Identification of the signs of the angles of rotation of the blocks.....	42
Fig. 38 – Displacements and rotations determined in sequence. ....	43
Fig. 39 – Measuring the horizontal component distance from centroid of initial block to rotation center (in red). ....	45
Fig. 40 - Expressions for TOTAL WORK (Roca, Ancient Rules and Classical Approaches- Part 1-4. SA1 Lectures., 2009-2010).....	48
Fig. 41 - Identification of the movement of each block for the defined mechanism .....	49
Fig. 42 – Sign criteria.....	49
Fig. 43 - Location of rotation centers for the four blocks in a symmetrical five-hinge collapse mechanism in arch.....	50
Fig. 44 - Identification of the rotations, displacements and correlations with the hinges and centers of rotation.....	51
Fig. 45 - Identification of the signs of the angles of rotation of the blocks.....	52
Fig. 46 - Displacements and rotations determined in sequence according to the following procedure.53	
Fig. 47 - Measuring the horizontal component distance from centroid of initial block to rotation center, and distance from point of application of the external vertical force V to the nearest centroid (in red). Measuring the vertical component distance between the centroids of the initial and the rotated blocks (in green). ....	56
Fig. 48 – Areas and widths considered for calculating the volume of arches and buttresses.....	57
Fig. 49 – Discretization of arch, location of centroids and vertical forces. ....	61

Fig. 50 - Funicular polygon and resultant force.....	62
Fig. 51 - Selection of three hinges for the thrust line to pass through and projection on the funicular polygon.....	63
Fig. 52 - Defining the new origin for the force polygon.....	64
Fig. 53 – A thrust line passing through ALL hinges is found inside the arch.....	64
Fig. 54 – Façade with series of arches in the Plaça Reial. (La Plaça Reial) .....	65
Fig. 55 – Aerial view Plaça Reial. (Aero-plano).....	65
Fig. 56 – View of the arches. (Alcolea Antigüedades) .....	65
Fig. 57 – Arch in corner of Plaça Reial.....	65
Fig. 58 – Arch in corner of Carrer de Colom .....	65
Fig. 59 - Geometry of last arch in carrer de Colom.....	66
Fig. 60 – Blondel rule applied to the external buttress of the last arch.....	66
Fig. 61 - Vertical and horizontal areas for calculating the permanent and live loads.....	68
Fig. 62 - Permanent and live loads applied on each segment as point loads.....	69
Fig. 63 - Discretization of arch, location of centroids and vertical forces.....	71
Fig. 64 - Sum of the weight vectors.....	72
Fig. 65 - Position of the resultant force.....	72
Fig. 66 – Location of forces and distances from centroids to point A from where the moments are evaluated.....	73
Fig. 67 – Results for H through both analytical and graphical procedures.....	74
Fig. 68 – Magnitud of vectors (analytical) .....	75
Fig. 69 – Magnitud of vectors (graphical).....	75
Fig. 70 – Thrust line with H found analytically.....	75
Fig. 71 – Thrustline with H found graphically.....	75
Fig. 72 – Map of the aqueduct of Tarragona (Schram & Passchier, 2005) .....	77
Fig. 73 - Drawing of the Puente de Ferreras bridge of one of the aqueducts of Tarragona (D. Soberano and A&C Reus/casado1972) (Schram & Passchier, 2005) .....	77
Fig. 74 – Aqueduct of las Ferreras (Ajuntament de Tarragona) .....	77
Fig. 75 – Aqueduct of Las Ferreras in Tarragona (The History of the Spanish Architecture).....	78
Fig. 76 – Aqueduct of Las Ferreras detail view (Ajuntament de Tarragona) .....	78
Fig. 77 – Aqueduct of Las Ferreras view from the bottom (Ajuntament de Tarragona).....	78
Fig. 78 – Aqueduct of Las Ferreras (Ajuntament de Tarragona) .....	78
Fig. 79 – Section of Pillars A15-A30. Source: Eng. Pere Roca (UPC) .....	79
Fig. 80 – Detail of superior arches (Schram & Passchier, 2005).....	79
Fig. 81 – Detail. (Schram & Passchier, 2005).....	79
Fig. 82 – Detail of <i>specus</i> (Schram & Passchier, 2005) .....	79
Fig. 83 – Section profile of the Devil’s Bridge. Source: Eng. Pere Roca (Universitat Politècnica de Catalunya).....	79

Fig. 84 – ULS verification (Franchetti, 2009).....	80
Fig. 85 – Geometry of the transversal section and corresponding area in the longitudinal section.....	81
Fig. 86 - Positive Reacting Moment (RM) and negative Acting Moment (AM).....	82
Fig. 87 – Spectral acceleration for the activation of the mechanism $a_0^*$ . (Franchetti, 2009).....	84
Fig. 88 – Participation mass $M^*$ (Franchetti, 2009) .....	84
Fig. 89 – Distances from centroids of blocks to hinge-A; Virtual displacements with rotation of structure.....	85
Fig. 90 – mass participant to the kinematism ( $e^*$ ) .....	85
Fig. 91 – Spectral acceleration for the activation of the mechanism ( $a_0^*$ ).....	85
Fig. 92 – Safety verification for Ultimate Limit State (ULS) .....	86
Fig. 93 – Section (SIPA - Sistema de Informação para o Património Arquitectónico (IHRU, Instituto da Habitação e Reabilitação Urbana, IP)).....	87
Fig. 94 – Quintela Tower in 1907 (Museu de Arqueologia e Numismática de Vila Real) .....	87
Fig. 95 – Orientation and plan geometry (IGESPAR IP - Instituto de Gestão do Património Arquitectónico e Arqueológico (former IPPAR)).....	87
Fig. 96 – ULS verification (Franchetti, 2009).....	88
Fig. 97 – Plan and section view of Quintela Tower showing the wall that will be verified.....	89
Fig. 98 – Geometry of the cross section with location of the center of masses .....	91
Fig. 99 - Location of the vertical and horizontal forces acting in the mechanism.....	91
Fig. 100 – Spectral acceleration for the activation of the mechanism $a_0^*$ . (Franchetti, 2009) .....	92
Fig. 101 – Participation mass $M^*$ (Franchetti, 2009) .....	93
Fig. 102 - Distances from centroids of blocks to hinge-A; Virtual displacements with rotation of structure.....	93
Fig. 103 – mass participant to the kinematism ( $e^*$ ) .....	94
Fig. 104 – Spectral acceleration for the activation of the mechanism ( $a_0^*$ ).....	94
Fig. 105 – Safety verification for Ultimate Limit State (ULS) .....	94
Fig. 106 – RING© output showing a four-hinge mechanism and the corresponding thrust line. ....	103
Fig. 107 – Bridgemill bridge geometry with an axle width of 0.75 meters (Meli, 2009).....	104
Fig. 108 - RING© output showing the same four-hinge mechanism with a modified axle width for the vertical load.....	104
Fig. 109 - RING© output showing the relocation of the third hinge for the arch without infill.....	105
Fig. 110 - RING© output showing the mechanism obtained for the load applied in the center of the arch.....	105
Fig. 111 - RING© output showing the mechanism obtained for the load applied in the center of the arch.....	107

## LIST OF TABLES

Table 1 - Load Factor table from Excel© .....	27
Table 2 – Geometric characteristics of the Cuernavaca Convent Church (Meli, 2009).....	36
Table 3 - Mechanical properties of stone masonries. ....	37
Table 4 - Load Factor table from Excel© .....	47
Table 5 - Load Factor table from Excel© .....	58
Table 6 – Loads above the half of the arch and buttress analyzed. ....	69
Table 7 – Total weights in structure .....	70
Table 9 – Horizontal and vertical distances of centroids from hinge.....	83
Table 10 – Results of the verification without tie-rods and five tryout for strengthening with tie-rods modifying the hinge of the mechanism proposed.....	95



## 1. INTRODUCTION

The concept of the “gentleman” architect developed during the Renaissance has defined the division in the education of architects and engineers in the modern Western Europe (Heyman, *The Stone Skeleton: Structural Engineering of Masonry Architecture*, 1995). This has led to a step back when comparing the practice of architects in the medieval ages and before where the aesthetic aspects were integrated with the technical knowledge. There was no sacrifice on one or other aspects as the variations from one heritage building to the other share a common feature that defines an essence: the nature of a material. This essence defined how a structure was built but also challenges the understanding of how it is still standing up and if it will be able to withstand actual conditions.

Assessing heritage buildings implies the need of recovering the integrated view of buildings and structures that was present before the separation in the Renaissance. This is a major challenge as it requires being able to combine contemporary knowledge with the understanding of the concepts used in the past. Engineers interested in heritage preservation have the challenge of studying the historic, philosophic and aesthetic issues present, while architects must make an effort to understand the structural concepts underlying the behavior of a building.

As an architect my interest in the SAHC Master program was related to this concern. I am convinced that this separation is generating negative consequences in the intervention in heritage buildings, and it is also affecting the process of design of contemporary architecture.

However, I am aware of the difficulties that each professional has in the attempt of fully understanding the complexities of the other area of expertise without the basic background required to control a different method of approach. For this reason, I have chosen a topic for the thesis that I knew will help me start with understanding the basics of structural analysis and material behavior. It was also of my interest to be able to learn a method that requires the use of graphic tools which constitute one of the main tools of my profession. This is my first step towards integration.

The topic selected, preparing a set of examples of both static and kinematic limit analysis, obliges understanding the principles and operation applied in each case study selected. The examples that were chosen are existing masonry structures in different regions of the world (with the exception of a bridge that existed but was tested to failure). Different typologies were selected as well: a bridge, an aqueduct, a tower, a church and a four story building. The case studies evaluated include the analysis for dead loading, live loading and earthquake. The variety of cases and the approach in each one allows observing the wide applicability of this simplified method of structural analysis.

The methodology used consisted in four steps: First, a literature review was performed in order to understand the theoretical principles of limit analysis applied to masonry structures. Second, an identification of the examples that have been done by other others was done. Third, the new examples

were selected, the conditions for the analysis were established for each approach defined, and the solutions were developed. Finally, the procedure of each analysis was organized in a step-by-step scheme within each of the chapters of this document.



## 2. STATE OF ART

### 2.1 General aspects

Masonry structures constitute the majority of the heritage buildings that remain until today considering that the other traditional material, wood, is subjected to the natural decay of living things. The fact of the existence of masonry heritage buildings surviving after the effects produced by time and the conditions of a particular geographical context, suggests *“an extreme stability of their structure”*. Stability refers to the fact that the structure *must not develop large unstable displacements (locally or overall)*. (Heyman, *The Stone Skeleton: Structural Engineering of Masonry Architecture*, 1995).

The other two structural criteria strength (capacity to withstand the imposed loads) and stiffness (excessive deflection should not occur) are not of main relevance for the assessment of historical masonry buildings, considering that for the process of building a structure the proportions of the elements were defined and once constructed and standing up it will not crush or deflect excessively.

On the other hand, sudden changes of the structural conditions can put an end on the stability of the structure, even though the strength capacity and the stiffness parameters are not affected.

These conditions define that the main concern for safety assessment of masonry structures is mainly related to the relationship between stability and geometrical characteristics (that were defined by rules of proportion until the theory of elasticity was developed).

### 2.2 Masonry

*“Masonry is an assemblage of stones – or bricks, or indeed sun-dried mud (adobe) – classified for convenience with certain distinct labels, as Byzantine, Romanesque, Gothic, but recognized by engineers as having a common structural action. This action arises directly from the properties of the material.”* (Heyman, *The Stone Skeleton: Structural Engineering of Masonry Architecture*, 1995)

Masonry has heterogeneous characteristics of the units and is subjected to modifications of the joints (with or without mortar) throughout time. The stability of the whole is assured by the compaction under gravity of its elements.

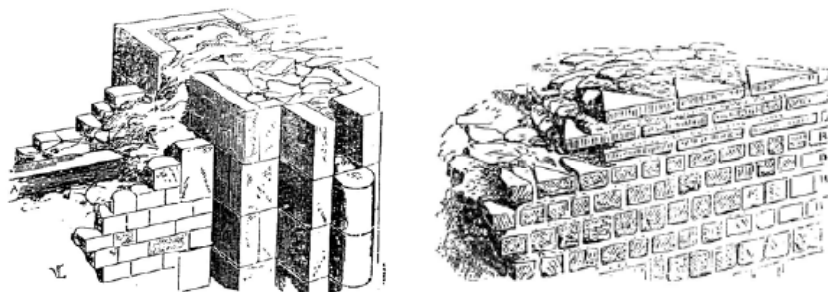


Fig. 1 – Different types of masonry arrangements. (Huerta Fernández, 2004)

The anisotropic and discontinuous characteristics of masonry oblige a different characterization compared to isotropic and homogeneous materials such as steel and reinforced concrete which are

defined by “*certain elastic constants*” (*Young and Poisson Modulus*). This difference obliges a shift in the structural analysis approach, as the elastic approach is interested in knowing the stresses within the structure in order to compare it with the admissible values obtained experimentally; therefore strength is the main concern in the elastic analysis. (Huerta Fernández, 2004)

Considering that strength is not the most important parameter for the analysis of masonry structures, a characterization of the mechanical behavior of masonry is done with the following considerations:

- Masonry has high capacity for compressive stresses.
- Masonry has very low capacity for tensile stresses.
- Failure by sliding of the units is very rare due to the high friction coefficients between them.

With these parameters, it can be observed that the weak aspect of masonry is due to the incapability of resisting tensile stresses. This parameter has been observed in the existence of cracks in masonry constructions that have appeared caused by changes in external boundary or load conditions without causing the collapse of the structure. This property of the material to deform and withstand structural damage without collapsing is known as ductility (the opposite concept is brittleness). Ductility of masonry structures “*ensure inelastic redistribution of actions among the components*”, therefore it constitutes a positive quality when subjected to seismic actions as the structure “*allows large absorption and dissipation of earthquake-induced energy*” (Marcari, Maca, & Oliveira, 2009).

The capacity to deform without rupture of the masonry allows the assumption of small displacements as a hypothesis that is used for the application of Limit Analysis (Orduña & Lourenço, 2001)

## **2.3 Structural Analysis**

“*The aim of structural theory is to be able to design safe buildings or to estimate the safety of existing ones*” (Huerta, *Mechanics of masonry vaults: The equilibrium approach*, 2001). Masonry structures have particular characteristics which have obliged specific applications of the analysis techniques that have been developed.

The traditional “geometrical” theory of the old master builders and the scientific theory developed afterwards are integrated today in order to understand “*what makes a structure safe (or unsafe)*”. Furthermore both theories arrive to the same conclusion: “*the safety of a masonry structure is a matter of geometry*”. (Huerta, *Mechanics of masonry vaults: The equilibrium approach*, 2001)

A brief reference to the evolution of these theories is presented connecting graphic statics with the plastic theory which are integrated to understand the methods of limit analysis.

### **2.3.1 Graphic statics**

Graphic statics refers to the method for equilibrium analysis developed as the attempt to calculate structures fundamentally by the use of graphic techniques throughout the process of constructing

funicular shapes (only tension or compression) for a certain set of loads. (Block P. , Equilibrium systems: Studies in Masonry Structure, 2005)

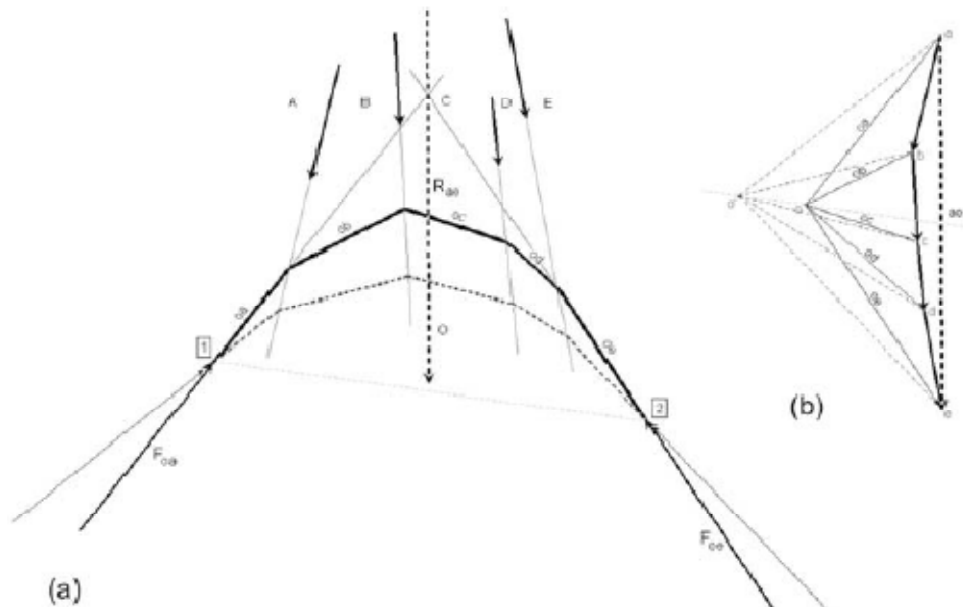


Fig. 2 – (a) Funicular construction for a set of loads; (b) magnitude of forces in funicular polygon. (Block P. , Equilibrium systems: Studies in Masonry Structure, 2005)

The use of Graphic statics for structural engineering was formalized by Culmann in 1866. However the theories and the notion of vectors existed previously since the introduction of Stevin's parallelogram rule (1586) where "equilibrium could be described graphically using force vectors and closed force polygons". (Block, DeJong, & Ochsendorf, As Hangs the Flexible Line:Equilibrium of Masonry Arches, 2006)

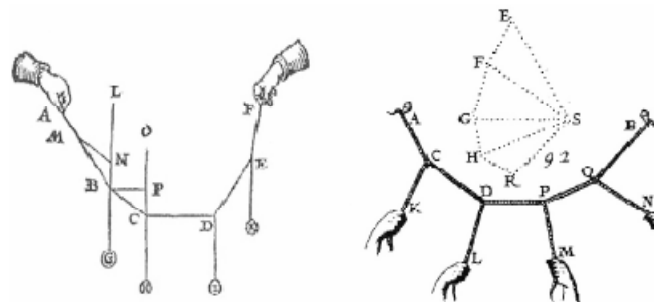


Fig. 3 – Left, force equilibrium of hanging weights on a string (Stevin, 1586); right, graphical analysis of a funicular shape (Varignon, 1725) (Block, DeJong, & Ochsendorf, As Hangs the Flexible Line:Equilibrium of Masonry Arches, 2006)

An extensive use of the methods of graphic statics started in 1870. Gaudi was the first one to apply the equilibrium approach since the beginning of the design process; until then the common practice was the verification of the structures after the design was developed (Huerta, 2003). Other master builders such as Robert Maillart and Gustave Eiffel used the graphic static method for some of their works. (Block P. , Equilibrium systems: Studies in Masonry Structure, 2005)

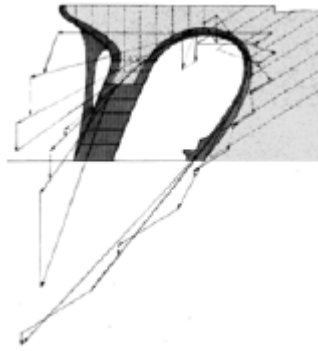


Fig. 4 – Gaudí's graphical design for the columns and retaining wall of Park Guell, from Rubió, 1913. (Block P. , Equilibrium systems: Studies in Masonry Structure, 2005)

Even though at the end of the 19<sup>th</sup> and beginning of the 20<sup>th</sup> century the most common method used for determining the equilibrium of structures was the graphic statics, by 1920 it was replaced by the theory of elasticity based on the quest for analytical solutions to obtain the stresses within the structure.

### 2.3.2 Plastic theory

Before the plastic theory, designers were interested in the quest for the actual (or working) state of the structure by calculating the stresses of its elements. The objective was to guarantee that the stresses obtained "*do not exceed a safe fraction of their ultimate values*" (Heyman, *The Stone Skeleton: Structural Engineering of Masonry Architecture*, 1995). However, it was noted that not all the structures could be solved with the equations of statics as there are many ways in which the structure can carry the loads, therefore many possible equilibrium states exist. This leads to the fact of needing additional information in order to be able to establish the actual state.

With elasticity two assumptions were introduced: a law of deformation which considered that the structure is a deformable body, and the determination of boundary conditions. However, with these considerations it was observed that the "actual" state that was obtained was ephemeral as it was affected by small modifications in reality concerning boundary conditions; Furthermore, if material properties were needed to be included, this was an additional problem taking into account that for some heterogeneous materials such as masonry a realistic characterization is very difficult to be done.

From experimental reports on steel structures in the 1930's a philosophical shift occurred in engineering design. It was observed that the stresses measured on real structures were very different from those calculated with elastic parameters. (Heyman, *Elements of the Theory of Structures*, 1996) The conclusion was that the mistake was the attempt of engineering design to obtain an "actual" state of a structure. A new concept was developed abandoning the quest for the actual state of a structure and replacing this target with the objective of examining how the structure might collapse. This new approach is applicable to materials with a ductile plastic collapse process (steel, timber, wrought iron, aluminum alloy and masonry), and cannot be considered to materials with a brittle behavior (cast iron or glass). (Heyman, *The Stone Skeleton: Structural Engineering of Masonry Architecture*, 1995)

The difference between the two approximations is that during the calculation of a hypothetical collapse of the structure, when an equilibrium state is achieved for the structure subjected to specific loading conditions, the elastic approach will consider this as the “actual” state, whereas the plastic approach will consider having found one particular state out of the infinite possible options. In both cases the master safe theorem of plasticity is being applied: *“If any equilibrium state can be found, that is, one for which a set of internal forces is in equilibrium with the external loads, and, further, for which every internal portion of the structure satisfies a strength criterion, then the structure is safe.”* *“In masonry the strength criterion is effectively that the forces should lie within the boundaries of the material”*. (Heyman, *The Stone Skeleton: Structural Engineering of Masonry Architecture*, 1995)

Considering the above, Heyman has pointed out that for the analysis of masonry structures plastic theory should be used with limit analysis methods considering the structure only in relation to its ultimate state, with the additional advantage that few material parameters and no prior knowledge of the initial stress state are required, (Gilbert, *Limit analysis applied to masonry arch bridges: state-of-the-art and recent developments*, 2007) being particularly appropriate for the usual lack of information regarding historical constructions.

*“Plastic methods are concerned with estimates of the strength of structures and they make use of the fact that any practical material has good ductile properties. Such materials allow internal forces in a structure to redistribute themselves; as loads are slowly increased, their final collapse values are predictable, and reproducible, with spectacular accuracy. The small imperfections of fabrication and erection of hyperstatic structures, which alter so markedly the elastic distribution of internal forces, have no effect on ultimate carrying capacity”*. *“The plastic designer imagines a hypothetical increase in loading”*. (Heyman, *Elements of the Theory of Structures*, 1996)

For the case of masonry, the limit condition of the material is the requirement of being always under a compression state, therefore the stresses must be always between the boundaries of the structure. (Huerta, 2003)

## **2.4 Limit Analysis**

Limit Analysis (or collapsing mechanism analysis) (Molins, June 1998) developed within the modern theory of plasticity during the 20<sup>th</sup> century when Jacques Heyman, in 1966, applied this approach to evaluate the load capacity and failure mechanisms of masonry arches which today are known as macro-elements. Heyman related the limit analysis theory with the rigid-perfectly plastic material model considering three hypotheses (Heyman, 1995):

- (i) Masonry has no tensile strength,
- (ii) Masonry has infinite compressive strength
- (iii) Sliding between stone blocks does not occur

With these considerations, the limit condition of the macro-element analyzed will be reached if two situations are found that comply with the following theorems (Roca, Ancient Rules and Classical Approaches- Part 1-4. SA1 Lectures., 2009-2010):

- (i) Static approach (Lower Bound): The structure is safe, meaning that the collapse will not occur, if a statically admissible state of equilibrium can be found.
- (ii) Kinematic approach (Upper Bound): If a kinematically admissible mechanism can be found, for which the work developed by external forces is positive or zero, then the structure will collapse.

The statically admissible state referred in the Lower Bound Theorem occurs when a thrust line can be determined, in equilibrium with the external loads, which falls within the boundaries of the structure. The load applied is a “lower bound” of the actual ultimate load that causes the failure. A thrust line is defined as *“the geometric locus of the point where stresses pass through a system of segmented planes”* (Huerta Fernández, 2004).

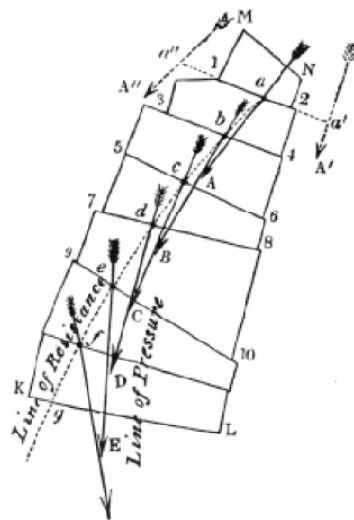


Fig. 5 – Thrust lines in masonry (Huerta Fernández, 2004)

The kinematically admissible mechanism referred in the Upper Bound Theorem occurs when assuming a mechanism (by arbitrarily placing a sufficient number of hinges) to obtain a load which results from equating the work of the external forces to zero. The load obtained is an “upper bound” of the actual ultimate load that causes the failure.

Both static and kinematic admissible collapse mechanisms are found (the limit condition of the macro-element is reached, meaning that the structure will be about to collapse) when a thrust line can be found causing as many hinges as needed to develop a mechanism. Plastic hinges are caused by the thrust line becoming tangent to the boundaries of the macro-element’s geometry. When this occurs *the load is the true ultimate load, the mechanism the true ultimate mechanism, and the thrust line is the only possible one* (Uniqueness Theorem) (Roca, Ancient Rules and Classical Approaches- Part 1-4. SA1 Lectures., 2009-2010).

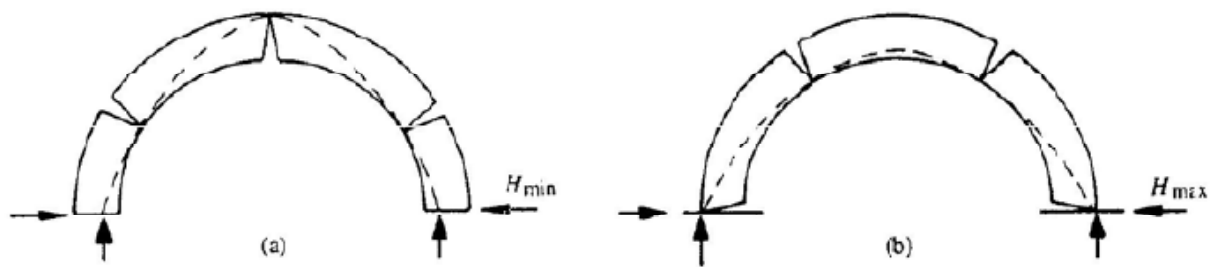


Fig. 6 – Semicircular arch under selfweight application of the uniqueness theorem (a) Minimum thrust (b) Maximum thrust. (Heyman, *The Stone Skeleton: Structural Engineering of Masonry Architecture*, 1995).

### 2.4.1 Static approach

The objective of finding a *statically admissible state of equilibrium* means obtaining at least one of the many possible “paths” the loads follow when being carried by the structure. The paths are represented by the geometry of a thrust line that lies within the boundaries of the masonry structure.

The infinite positions of the thrust lines are located within a range defined by a maximum and minimum position of the resultant force representing the thrust. This approach will give a *lower bound of the collapse load*, therefore in order to search for the ultimate collapse load several tryouts must be performed to find the maximum value obtained for thrust lines inside the boundaries of the structure.

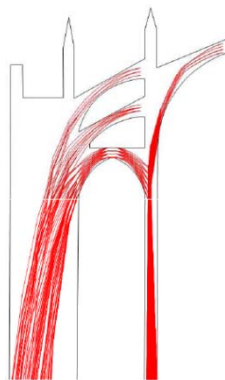


Fig. 7 – Computer optimization for alternate solutions in Maynou, 1998 (Roca, *Ancient Rules and Classical Approaches- Part 1-4. SA1 Lectures.*, 2009-2010)

This approach is referred as “the safe theorem” because even though it is not possible to know exactly how the loads in the masonry structure are being transferred to the supports, the fact is that it is enough to determine the structure is safe if it is possible to find one way the structure could be standing in equilibrium with the external forces.

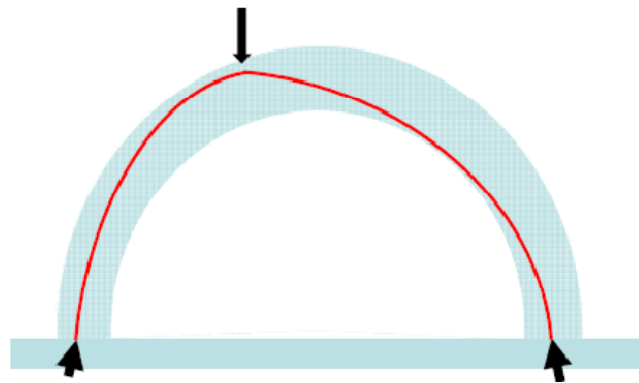


Fig. 8 – Thrust line falls within the boundaries of the structure. (Roca, Ancient Rules and Classical Approaches- Part 1-4. SA1 Lectures., 2009-2010)

The static approach involves the following procedure:

The equilibrium of the structure between external and internal loads is established. The objective is to find a thrust line within the structure for a lower bound of the collapse load. If this is achieved, the structure is safe. This load is a vector with orientation and position that is defined according to what needs to be analyzed and the unknown magnitude of the external force can be obtained analytically by the equations of equilibrium, or can be obtained as a reduced value from the magnitude of the load obtained if a previous kinematic analysis has been performed.

First the geometry of the structure is simplified and discretized into segments according to the convenience of shape of the components involved. For example, a buttress that has a changing cross section should be divided into fragments considering the “stepped” form, whereas a buttress with a “straight” cross section can be considered as only one element in order to reduce steps in the process with too much fragmentation. However it is important to consider that the more amount of segments in which the structure is divided, the smoother the thrust line obtained will be. This has to be decided for every specific case.

Second, the internal forces are calculated including dead and live loads, and are represented as point load vectors applied in the centroid of each segment.

Third, the magnitude, position and orientation of the resultant force for the internal loads is calculated applying the method of graphic statics. The individual weight-force vectors from each segment are summed as vectors determining the magnitude and orientation of the resultant force vector. The position is found by constructing a force polygon from which a funicular polygon is obtained. The extreme vectors of the funicular polygon are extended until they intersect. The point of intersection is the position of the resultant force. At this point two principal vectors are obtained: The horizontal thrust defined analytically or as a reduced value from the kinematic approach, and the resultant force.

However, the value of the horizontal thrust can also be determined graphically by defining the position of a third vector, the resultant vector ( $R$ ) from the sum of the horizontal thrust vector ( $H$ ) and the weight-force resultant vector ( $P$ ). Extending reference lines until intersection is obtained of the horizontal thrust vector and the weight-force resultant vector results in the second point from which the



orientation of the resultant vector (R) is obtained. The first point of the resultant vector (R) was arbitrarily defined according to what wants to be analyzed in the structure, for example: selecting the extreme outer point of the base in a buttress to find a thrust line in the maximum width edge.

Fourth, using graphic statics a force polygon is constructed for the sum of the principal vectors (H, P, R) and the corresponding funicular polygon is drawn over the structure to observe if it lies within the boundaries.

### **2.4.2 Kinematic approach**

Skeletal systems (structures composed of arches and linear elements) allow large deformations by the rearrangement of the load paths when hinges are produced. The objective is finding an ultimate equilibrium condition generated by a sufficient additional number of hinges provoking a collapse mechanism. (Roca, Damage and Collapse Mechanisms - Part 1., 2009-2010)

The kinematic approach is applied to systems composed of rigid blocks and involves the following procedure:

The parameters of evaluation of the structure to be analyzed are defined. For example: horizontal forces (earthquakes or wind), a distributed overload (extra material being added through different periods), a critical live load (a contemporary vehicle passing over a bridge), among others.

The geometry is simplified neglecting minor imperfections, decorations and the like. If the structure has been heavily deteriorated, then the section considered for the analysis is the most critical one (the reduced section).

Considering that the objective is finding an *upper bound of the maximum load* taken into account, the position and direction of the vector representing this force must be defined in the geometry of the structure with the criterion considering where the most critical effect will be. For example: For evaluating a predominantly vertical structure (a tower) against the effect of an earthquake, the direction of the unknown force vector is horizontal, and the most critical position will be on the top. For the case of evaluating the live load (a vehicle passing over a bridge), the direction of the unknown force vector is vertical and the most critical position will be in  $\frac{1}{4}$  of the span.

The magnitude of the unknown load will be obtained from the expression of Total Work (W) which establishes the equilibrium between internal and external forces, relating forces with displacements and rotations. To solve this system, three main steps are identified:

First, a mechanism is defined with a sufficient number of hinges to make the structure unstable. The location of these hinges is done after several tryouts, and the final position will be the one with the minimum value of the unknown load evaluated (the closest one to the real solution). To determine the type of mechanism will also require several tryouts if there is no previous experience in the structural typology or load conditions, in order to select which one will give the lowest value for the unknown variable. For example: in the analysis of a semicircular barrel vault over buttresses, the mechanism

can be defined for the isolated arch or can include the buttresses for a specific load condition. The one which gives as a result the lower value will be the most critical one<sup>1</sup>. Defining the mechanism implies a subdivision of the structure in blocks which is determined by the location of the hinges, and a relative movement between the blocks (angles and displacements are interdependent).

Second, the internal forces of the blocks are calculated and scaled to a distance unit in order to be able to integrate the values in the graphical procedure.

Third, the upper bound of the unknown external load is calculated by solving the Total Work expression (equilibrium). Because the internal forces have been previously calculated, a load factor  $\lambda$  (or multiplier) affecting the unknown external force is to be found when defining a reference value of 1 to the unknown load.

The kinematic approach will provide an upper bound of the real ultimate load for the unknown force being evaluated; in order to obtain the real ultimate load, a series of trials combining both static and kinematic approaches should be done, which can be tedious (apart from the trials mentioned for defining the location of hinges and determining the mechanism).

Another important use of limit analysis arose in Italy to assess more complex and articulated masonry structures that needed another method for evaluating the behavior of historical structures subjected to earthquakes, and that did not comply with techniques considering a box behavior. A set of abacus (O.P.C.M. 3431, 2005) was developed by classifying several cases of collapsing configurations within similar typologies. Local failures (loss of equilibrium) were considered for diverse types of buildings such as out-of-plane rotation of a load-bearing masonry wall. (Roca, Damage and Collapse Mechanisms - Part 2, 2009-2010). Two examples have been included (a tower and an aqueduct) applying one of the local failure modes typical of vertical predominant structural elements with little or lack of orthogonal connections.

## 2.5 Computational limit analysis

Considering the tedious process involved in the tryouts needed for determining the ultimate collapse load through the static and kinematic approaches, *“hand based limit analysis techniques have been largely superseded by computer based methods”* (Gilbert, Limit analysis applied to masonry arch bridges: state-of-the-art and recent developments, 2007). These methods constitute optimization processes for the use of limit analysis in the assessment of masonry structures.

---

<sup>1</sup> When trials are needed, this means that the result will only be obtained after doing all the process that is being described.

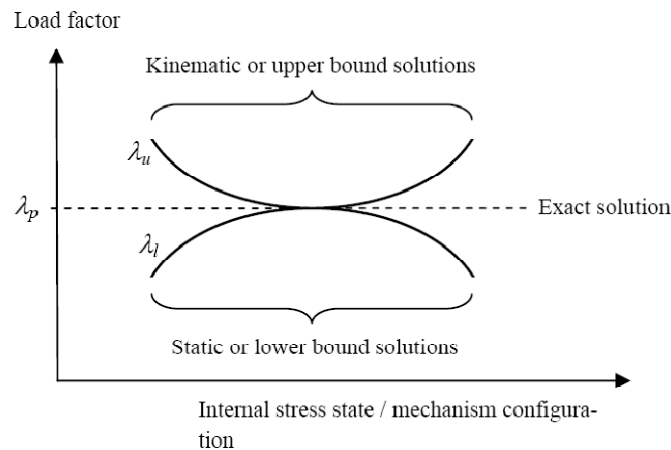


Fig. 9 - The relationship between upper and lower bound solutions (Gilbert, Limit analysis applied to masonry arch bridges: state-of-the-art and recent developments, 2007)

The following are examples of computational (mathematical) optimization methods that have been developed.

*RING© software* in its version 1.5 for windows has been developed by Matthew Gilbert of the Computational Limit Analysis and Design Unit of the University of Sheffield in 2005, but it has been available for public use since 2001. The application is oriented to the assessment of masonry arch bridges; *“it is a computer software designed to compute the ultimate load carrying capacities of masonry arch bridges”* (Gilbert, 2005). It can be applied for single and multi-span masonry arch bridges. In this thesis *RING© software* was used to verify some of the results being obtained through the graphical procedure (the analysis performed for the cases where it was used is included in the annexes).

*Interactive Thrust* is a project developed in the Massachusetts Institute of Technology with the objective of *“creating structural analysis tools based on limit state analysis for vaulted masonry buildings”*; *“The models developed are interactive and parametric to explore the relationships between building geometry and possible equilibrium conditions in real time”*. *“Collapse analysis due to applied displacements is determined by combining kinematics and statics”*. (Massachusetts Institute of Technology - MIT)

*Thrust-Network Analysis* is a three-dimensional computational method developed in the Massachusetts Institute of Technology to obtain lower-bound solutions for masonry vaults with complex geometries. (Block & Ochsendorf)



### **3. EXAMPLES OF APPLICATION OF LIMIT ANALYSIS METHODS**

The application of Static and Kinematic approaches was performed for the following case studies:

- A single span arch bridge: Bridgemill Bridge (UK)
- A barrel vault with buttresses: Cuernavaca Church (México)
- A one level multiple span arch façade: Plaza Reial (Spain)
- A two level multiple span arch bridge: Roman Aqueduct of Tarragona (Spain)
- A wall in a tower: Quintela Tower (Portugal)

The solutions for the case studies include: Kinematic analysis were performed using computer-aided design software for the graphic schemes and a spreadsheet for the step-by-step calculations. Static analysis were performed using computer-aided design software in order to obtain the thrust line corresponding for the specific objectives defined in each case (for example obtaining the corresponding thrust line for the collapse mechanism and applied load defined in the kinematic approach). When it was appropriate, an analysis was performed using the analysis software for masonry arch bridges RING© 1.5 version, in order to verify the results obtained for the behavior of the structure (location of hinges and shape of the thrust line) with the assumptions considered (geometry, material properties and loading cases).



### 3.1 Arch Bridge (Bridgemill Bridge in UK)

The Bridgemill Bridge (Girvan, UK) was selected considering the available experimental and analytical results obtained when it was tested to failure in 1984. The arch bridge had a single flat segmental span of 18.29 meters and a width of 8.3 meters, and was built with sandstone voussoirs joined with lime mortar. The test performed on the structure consisted in applying an increasing vertical load at a distance of a quarter of the span until the expected four-hinge collapse mechanism was obtained. The maximum value obtained for the incrementally increased load was 3.0 MN. Further numerical analyses for this case were performed by other researchers obtaining values for the collapsing load of 2.7, 2.8 and 2.93 MN (Molins, June 1998).

The geometric characteristics of the arch bridge are:

- Equation of the parabola to define the intrados of the arch:  $Z(X) = -0.033958X^2 + 0.621104X$  with the origin of coordinates at the abutment (Molins, June 1998).

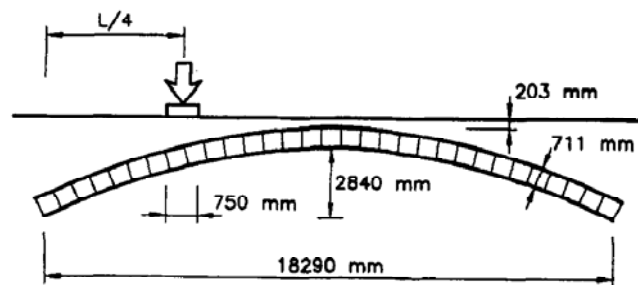


Fig. 10 – Geometry of Bridgemill Bridge (Molins, June 1998)

The mechanical characteristics of the structural masonry, a compressive strength of 15 MPa and a deformation modulus of 4000 MPa, were neglected for the analysis of this example considering the initial assumption (compressive strength is infinite). The material properties considered were 20 KN/m<sup>3</sup> for the unit weight of the masonry arch and 18 KN/m<sup>3</sup> for the unit weight of the infill.

### 3.1.1 Kinematic Approach

The objective of this approach is determining the upper bound of the applied load that will cause a defined collapse mechanism. Therefore, the first aspect to be established is what is to be evaluated in the structure analyzed in order to define the parameters for the kinematic evaluation.

The Bridgemill Bridge was analyzed for the most critical live load condition considering that for its width (8.3 meters) it would have been capable of allowing the passing of modern vehicle transportation. The most critical live load condition would be defined by a point load. The location of this vertical load representing the most critical live load condition was also demonstrated using RING© (see annex) to be in the  $\frac{1}{4}$  of the span.

In the case of the Bridgemill bridge, some of the parameters have already been defined as this is an example that has available data from experimental results (the value of the experimental collapse load is known as well as other values for this obtained from other numerical analysis). For the case of another example of the same typology (single span arch bridge with infill) the collapse load should be found using an iterative procedure and starting from a hypothetical value for this load in order to see the behavior of the structure. This value (collapse vertical load) was used as a reference of verification in order to perform the kinematic analysis with a graphic procedure. The value for the collapse vertical load obtained from the kinematic analysis, as well as the value verified from RING© were used as a starting reference for performing the static approach. However, considering that the value obtained in the kinematic approach is an upper bound of the real value, a reduction of this value was expected for the static approach as it is a lower bound.

Another point of start parameter that was defined after several trials, is the exact location of the four hinges which was verified with the RING© software as it is shown in the annex.

#### PROCEDURE:

Case: Single span arch with non-symmetrical applied vertical force; typical collapse mechanism involves four hinges.

Objective: To calculate the entity of the force causing the collapse (upper bound of the maximum vertical load  $V$ ).

A vertical load is applied in  $\frac{1}{4}$  of the span. A mechanism of four hinges was defined. The location of the hinges was found through an iterative procedure and the result was verified using RING©.



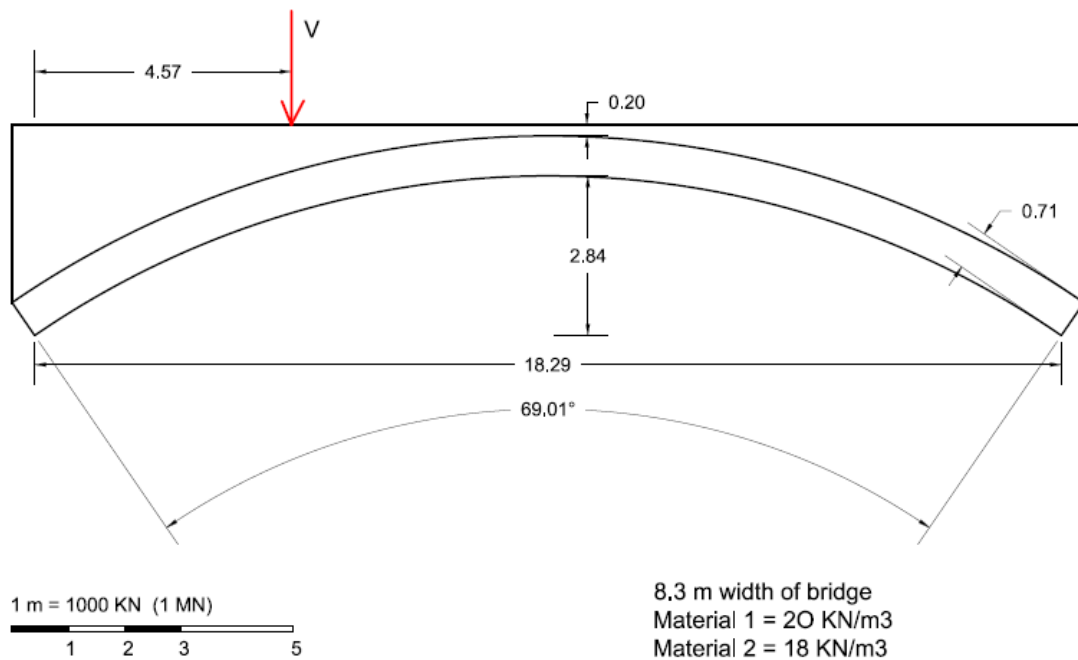


Fig. 11 – Scaled geometry of Bridgemill Bridge with position of the vertical load V at ¼ of the span.

The objective is finding the *upper bound of the maximum vertical load* for the mechanism analyzed. The vertical load (V in MN), is obtained by solving the system given by the following expression:

$$W = \sum_{k=1}^N V_{kg} * X_{kg}^c * K_k^\theta \theta + \lambda \sum_{j=1}^{n_f} V_j * X_{k(j)}^c * K_{k(j)}^\theta \theta = 0$$

$$\lambda = - \frac{\sum_{k=1}^N V_{kg} * X_{kg}^c * K_k^\theta}{\sum_{j=1}^{n_f} V_j * X_{k(j)}^c * K_{k(j)}^\theta}$$

Fig. 12 - Expressions for TOTAL WORK (Roca, Ancient Rules and Classical Approaches- Part 1-4. SA1 Lectures., 2009-2010)

Where:

W = Total work

W = Sum of the internal forces + Sum of the external forces.

Sum of the internal forces:

$V_{kg}$  = Weight force resultant in block k applied at the centroid g.

$X_{kg}^c$  = Horizontal component of the distance between the center of rotation to the centroid g of block k.

$K_k^\theta$  = Angle of rotation of block k.

Sum of the external forces:

$V_j$  = External vertical load applied (this is the unknown of the system)

$X_{ck(j)}$  = Horizontal component of the distance between the center of rotation of the block where the external vertical load  $V_j$  is applied, to the point of application of the force.

$K_{k(j)}^\theta$  = Angle of rotation of the block where the external force is being applied.

According to this, the procedure involves three main steps:

PART I: Determining the rotations and displacements of the mechanism.

PART II: Calculating the internal forces

PART III: With the expression of total work, calculating the *upper bound of the maximum vertical load*.

#### PART I – DETERMINING ROTATIONS AND DISPLACEMENTS OF THE MECHANISM

- 1) Establish the mechanism to be analyzed by defining a sufficient number of hinges to make the structure unstable; Determine, by several tryouts, the exact location of the hinges that will require the lowest value of collapse load. In this case as it was explained before, this location was verified by the use of RING©. “Fixed” and “moving” hinges must be identified. For this case the hinges in each support and the hinge on the position of application of the vertical force  $V$  correspond to the “fixed” hinges (A, B, D), and the third hinge (C) would have been the one to be determined by several tryouts. Notice that each consequent hinge is located in the opposite side of the thickness of the arch (A in intrados, B in extrados).

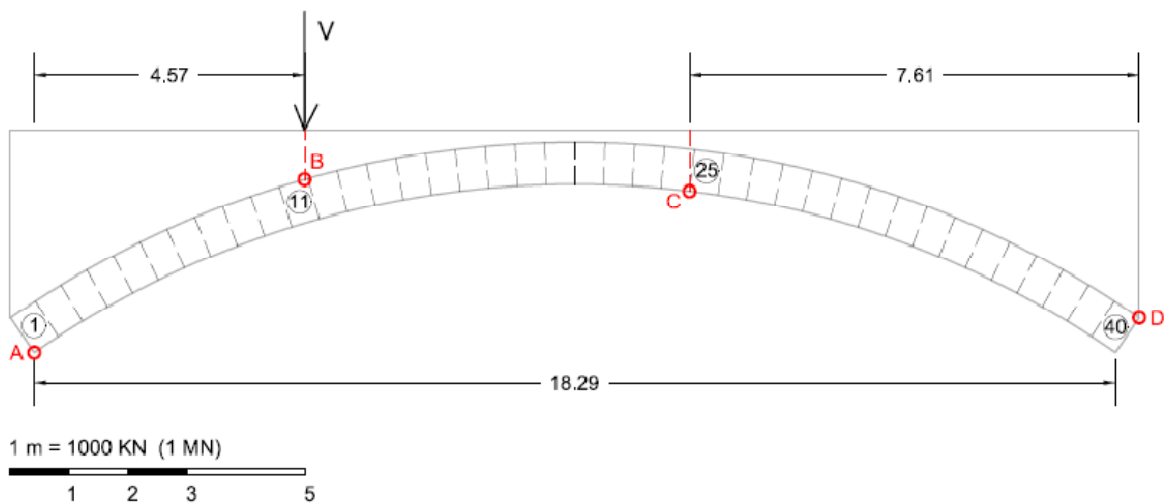


Fig. 13 – Bridgemill Bridge with location of the four hinges.

The mechanism to be analyzed is defined. For a vertical load applied in  $\frac{1}{4}$  of the span a four-hinge mechanism is selected. The hinges are located in the arch dividing the arch in three blocks. The hinges in the support of the arch will not have displacements and the hinge in  $\frac{1}{4}$  of the span, where the load is applied, will have both vertical and horizontal displacements. The other hinge will have horizontal and vertical displacements as well.

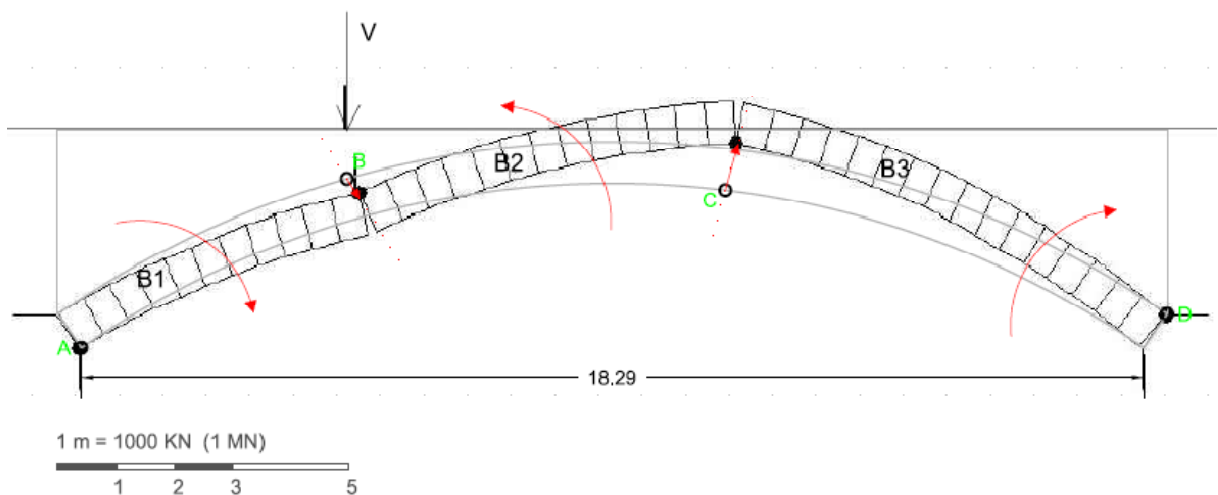


Fig. 14 - Overlapped mechanism from RING© in order to identify the movement of each block.

2) The sign criteria are defined for displacements and forces.

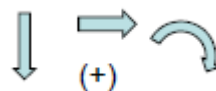


Fig. 15 – Sign criteria.

3) Each block will have a corresponding center of rotation. Lines are drawn connecting the hinges without displacements (A and D), which correspond to the center of rotations  $C_1$  and  $C_3$ , with the consequent hinges (B and C). These lines are perpendicular to the directions defined by the displacements of the extreme hinges that define each block ( $B_1$  and  $B_3$ ). The center of rotation  $C_2$  corresponding for the block B is found in the intersection of the rays AB and DC.

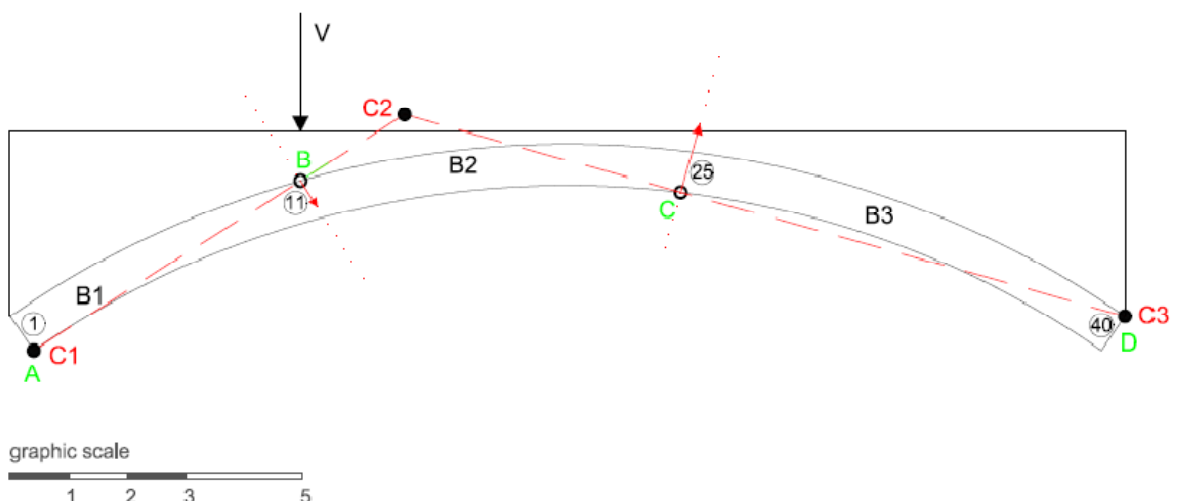


Fig. 16 - Location of rotation centers for the three blocks in a four-hinge collapse mechanism in arch

4) The rotations and displacements are identified in the mechanism and correlated with the hinges and centers of rotation.

$\delta_B$  = perpendicular displacement of hinge B to the line connecting centers of rotation  $C_1-C_2$ .

$\delta_C$  = perpendicular displacement of hinge C to the line connecting centers of rotation  $C_2-C_3$ .

$L_{1B}$  = Distance between center of rotation  $C_1$  and hinge B.

$L_{2B}$  = Distance between center of rotation  $C_2$  and hinge B.

$L_{2C}$  = Distance between center of rotation  $C_2$  and hinge C.

$L_{3C}$  = Distance between center of rotation  $C_3$  and hinge C.

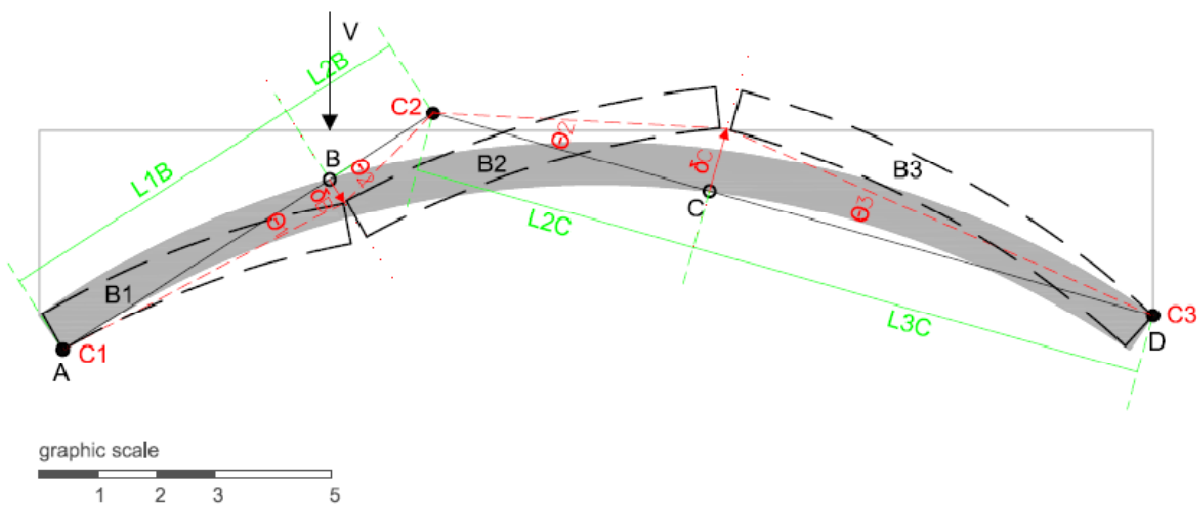


Fig. 17 - Identification of the rotations, displacements and correlations with the hinges and centers of rotation.

5) The angles according to the sign criteria will be as following:

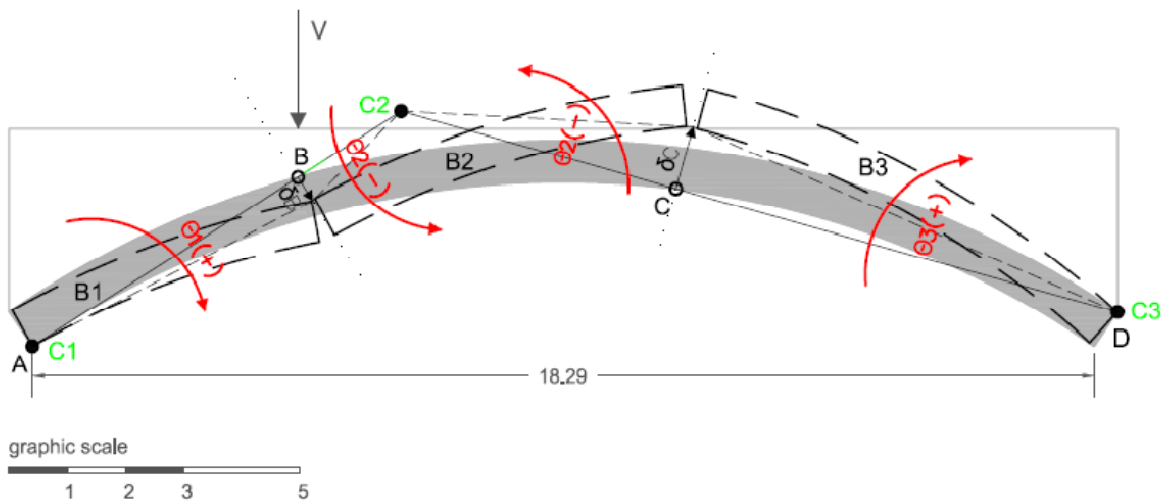


Fig. 18 - Identification of the signs of the angles of rotation of the blocks.

Once the mechanism has been established, the first step is defining the first angle of rotation. This value is decided arbitrarily ( $\theta_1$ ) and all the displacements and rotations will depend on it.

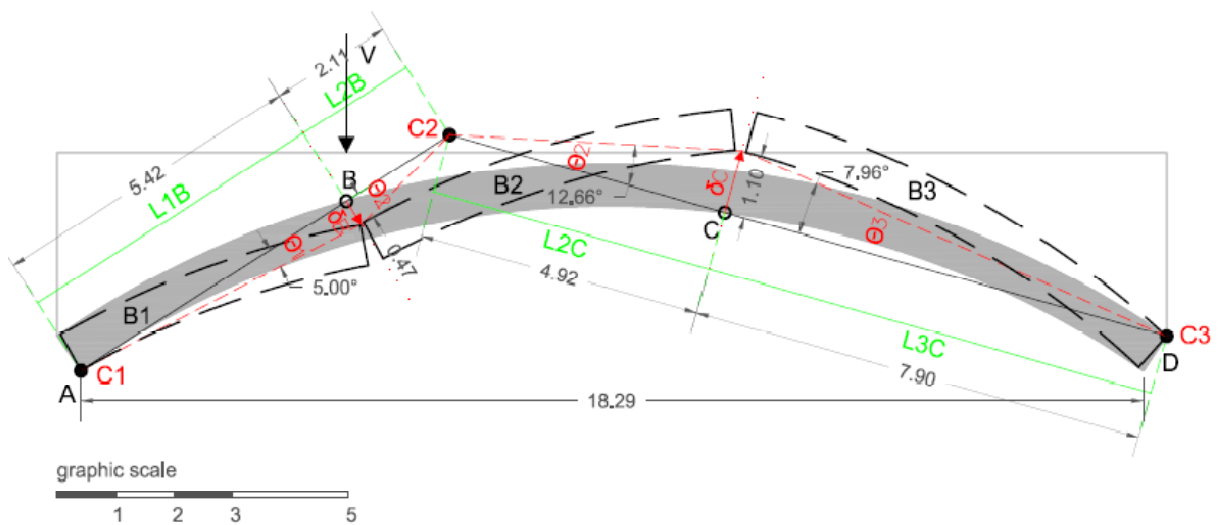


Fig. 19 - Displacements and rotations determined in sequence.

In order to perform the calculations, the relationships between rotations, displacements are established in a sequence from defining  $\Theta_1$ , and according to the sign criteria previously defined:

$$\begin{aligned} \delta_B &= \Theta_1 * L_{1B} = -\Theta_2 * L_{2B} & \longrightarrow & \quad -\Theta_1 * L_{1B} / L_{2B} = \Theta_2 \\ \delta_C &= -\Theta_2 * L_{2C} = \Theta_3 * L_{3C} & \longrightarrow & \quad -\Theta_2 * L_{2C} / L_{3C} = \Theta_3 \end{aligned}$$

The procedure was as following:

- 6) Define an angle of rotation ( $\Theta_1$ ) from the first hinge-A (first point of rotation- $C_1$ ). Draw a perpendicular line from the second hinge-B to the new rotated line. This line segment corresponds to the displacement of hinge-B ( $\delta_B$ ) which is the new location of the second hinge.

This value ( $\delta_B$ ) is also verified analytically by:  $\delta_B = \Theta_1 * L_{1B}$ , where  $L_{1B}$  is the distance between the first point of rotation- $C_1$  and hinge-B.

**Assume  $\Theta_1$  (in radians):**

**$\Theta_1$  (degrees)     $\Theta_1$  (radians)**

5                      0.09

**Determine  $\delta_B$  (displacement of point B) from  $\Theta_1$**

$$\delta_B = \Theta_1 * L_{1B}$$

**$\Theta_1$  (rad)             $L_{1B}$  (meters)     $\delta_B$  (meters)**

0.09                    5.42                    0.47                    *0.47(verification in autocad)*

- 7) The angle  $\Theta_2$  is found by connecting the new point of displacement of hinge-B given by  $\delta_B$ . Analytically this value is obtained (therefore verified) from the expression:

$\Theta_2 = (-L_{1B}/L_{2B}) * \Theta_1$ . Where  $L_{2B}$  is the distance between hinge-B and the second point of rotation- $C_2$ . This expression is obtained from the following equivalence:

$$\delta_B = \Theta_1 * L_{1B} = -\Theta_2 * L_{2B}$$

**Determine  $\Theta_2$  (rad) from  $\Theta_1$**

$$\Theta_2 = (-L_{1B}/L_{2B}) * \Theta_1$$

$\Theta_1$ (rad)	$L_{1B}$ (meters)	$L_{2B}$ (meters)	$\Theta_2$ (rad)	$\Theta_2$ (degrees)
0.09	5.42	2.11	-0.22	-12.87

- 8) The displacement of the hinge-C is found with the expression  $\delta_C = -\Theta_2 * L_{2C}$  where  $L_{2C}$  is the distance between the second point of rotation- $C_2$  and hinge-C.

**Determine  $\delta_C$  (displacement of point C) from  $\Theta_2$**

$$\delta_C = -\Theta_2 * L_{2C}$$

$\Theta_2$ (rad)	$L_{2C}$ (meters)	$\delta_C$ (meters)
-0.22	4.92	1.10

- 9) The angle  $\Theta_3$  is obtained from the expression  $\Theta_3 = -\Theta_2 * (L_{2C}/L_{3C})$

**Determine  $\Theta_3$  (rad) from  $\Theta_2$**

$$\Theta_3 = -\Theta_2 * (L_{2C}/L_{3C})$$

$L_{2C}$ (meters)	$L_{3C}$ (meters)	$\Theta_2$ (rad)	$\Theta_3$ (rad)	$\Theta_3$ (degrees)
4.92	7.90	-0.22	0.14	8.01

Considering that for calculating the work performed by the weight-force of each block a displacement has to be defined.

$$\text{Work} = \text{Force} * \text{Displacement}$$

Work (block-i) = Weight-force resultant located in the centroid of block ( $V_i$ ) \* angle of rotation of block ( $\Theta_i$ ) \* horizontal component of the distance between the center of rotation of the block and the centroid of the initial block ( $X_{ci}$ ),

Or,

Work (block-i) = Weight-force resultant located in the centroid of block ( $V_i$ ) \* vertical component of the distance between the centroids of the initial and rotated blocks ( $\delta_{iy}$ ).

- 10) For the work of internal vertical forces, measure the horizontal component ( $X_{ci}$ ) of the distance between the center of rotation of the block and the centroid of the initial block. Take into account the signs taking as reference the location of the center of rotation (starting point).

11) Multiply  $X_{ci}$  with the angle of rotation of the block to obtain the VERTICAL component ( $\delta_{iy}$ ) of the distance between the centroids of the initial and the rotated blocks.  $\delta_{iy}$  will be the “arm” that multiplied by the weight-force (vertical internal resultant force) gives the value of the WORK for the block.

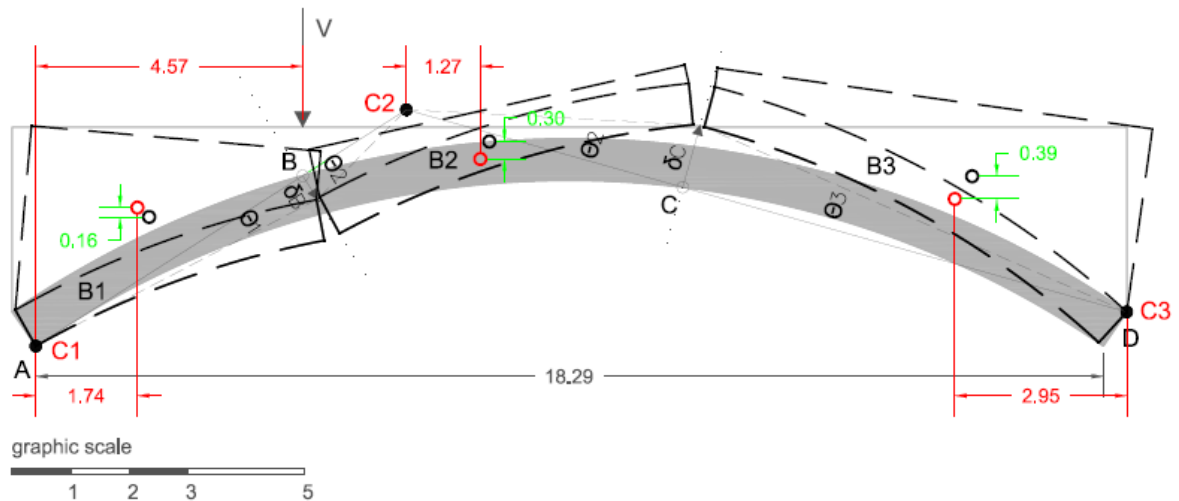


Fig. 20 - Measuring the horizontal component distance from centroid of initial block to rotation center (in red). Verification of vertical displacement between centroids of initial blocks and rotated blocks (in green).

**BLOCK 1**

$\Theta_1$ (rad)	$X_{c1}$	$\delta_{1y}$	
0.09	1.74	0.15	0.16 (verification of $\delta_{1y}$ measuring from drawing)

**BLOCK 2**

$\Theta_2$ (rad)	$X_{c2}$	$\delta_{2y}$	
-0.22	1.27	-0.28	0.30 (verification of $\delta_{1y}$ measuring from drawing)

**BLOCK 3**

$\Theta_3$ (rad)	$X_{c3}$	$\delta_{3y}$	
0.14	-2.95	-0.41	0.39 (verification of $\delta_{1y}$ measuring from drawing)

**PART II – CALCULATING THE INTERNAL FORCES**

The resultant weight-force is calculated for each block summing the partial forces of the corresponding part of the arch (Material-1) and the filling material (Material-2).

	<b>density</b> <b>(kN/m<sup>3</sup>)</b>	<b>Width</b> <b>(meters)</b>	<b>Area</b> <b>(m<sup>2</sup>)</b>	<b>Weight</b> <b>(kN)</b>	<b>scaled force</b> <b>(1m=1MN)</b>
Forces in blocks for the arch:					
A <sub>1</sub> (M <sub>1</sub> )	20	8.3	3.84	637.74	0.64
A <sub>2</sub> (M <sub>1</sub> )	20	8.3	4.64	769.54	0.77
A <sub>3</sub> (M <sub>1</sub> )	20	8.3	5.65	938.18	0.94
Forces in blocks for the infill:					
A <sub>1</sub> (M <sub>2</sub> )	18	8.3	9.13	1364.23	1.36
A <sub>2</sub> (M <sub>2</sub> )	18	8.3	2.38	355.23	0.36
A <sub>3</sub> (M <sub>2</sub> )	18	8.3	10.52	1572.02	1.57
<b>Total per block (arch and infill):</b>					
w <sub>1</sub> (A <sub>1</sub> )	= A <sub>1</sub> (M <sub>1</sub> ) + A <sub>1</sub> (M <sub>2</sub> )			2001.97	2.00
w <sub>2</sub> (A <sub>2</sub> )	= A <sub>2</sub> (M <sub>1</sub> ) + A <sub>2</sub> (M <sub>2</sub> )			1124.77	1.12
w <sub>3</sub> (A <sub>3</sub> )	= A <sub>3</sub> (M <sub>1</sub> ) + A <sub>3</sub> (M <sub>2</sub> )			2510.20	2.51

## PART III - CALCULATING THE UPPER BOUND OF THE MAXIMUM VERTICAL LOAD.

W (work)

w (weight force)

P (force applied in 1/4 of span)

$$W_i + W_e = 0 \quad (\text{Internal work} + \text{External work in equilibrium})$$

$W = F \cdot \delta$  (Work can be expressed as a force \* displacement/rotation)

$$W_i = (w_1 \cdot \delta_{1y} + w_2 \cdot \delta_{2y} + w_3 \cdot \delta_{3y} + w_4 \cdot \delta_{4y})$$

$$W_e = P \cdot \delta_{py}$$

$$(w_1 \cdot \delta_{1y} + w_2 \cdot \delta_{2y} + w_3 \cdot \delta_{3y} + w_4 \cdot \delta_{4y}) + (P \cdot \delta_{py}) = 0$$

$$P = -(w_1 \cdot \delta_{1y} + w_2 \cdot \delta_{2y} + w_3 \cdot \delta_{3y} + w_4 \cdot \delta_{4y}) / \delta_{py}$$

P can be expressed as:

$$\lambda P = -(w_1 \cdot \delta_{1y} + w_2 \cdot \delta_{2y} + w_3 \cdot \delta_{3y} + w_4 \cdot \delta_{4y}) / \delta_{py}$$

$$\delta_{py} = \theta \cdot X_p$$



Determine  $\bar{\delta}_{py}$ : vertical displacement point of application of force P due to rotation of the block where the force is applied: in this example is  $\Theta_1$ .

$\bar{\delta}_{py} = \Theta_1 * X_p$       $X_p$ : Horizontal distance from rotation center to external vertical load applied

$\Theta_1$ (rad)	$X_p$ (meters)	$\bar{\delta}_{py}$ (meters)	
0.09	4.57	0.40	0.41 (verification measured in drawing)

Determine  $\lambda$  (Factor load) for a given P (assumed)

$\lambda = -(w_1 * \bar{\delta}_{1y} + w_2 * \bar{\delta}_{2y} + w_3 * \bar{\delta}_{3y} + w_4 * \bar{\delta}_{4y}) / P * \bar{\delta}_{py}$

w1 (KN)	$\delta_{1y}$ (M)	w2 (KN)	$\delta_{2y}$ (M)	w3 (KN)	$\delta_{3y}$ (M)	$\delta_{py}$ (M)	<b>P (KN)</b>	<b><math>\lambda</math></b>
2001.97	0.15	1124.77	-0.28	2510.20	-0.41	0.40	<b>1</b>	<b>2630.38</b>

Table 1 - Load Factor table from Excel©

Comparing the results obtained with the use of graphic statics, with the verification in RING©:

FAILURE LOAD FACTOR

<b>RING©</b>	<b>Spreadsheet-<math>\lambda</math></b>
<b>2740</b>	<b>2630.38</b>

### 3.1.2 Static Approach

The objective was finding a thrust line that passes through the hinges for the mechanism previously defined, using the value obtained from the upper bound approach. Therefore the value to be considered for the static approach will be a reduced value from **2630.38 Kn (2551.5 kN; 3% reduction)**.

#### GENERAL ASPECTS

The structure to be analyzed is evaluated considering the equilibrium equations.

The number of available equations is three:

- 1- Sum of the vertical forces equal to zero
- 2- Sum of the horizontal forces equal to zero
- 3- Sum of the moments equal to zero

To define the VECTOR, three properties must be defined:

- 1- Entity (magnitude)
- 2 - Direction
- 3 - Position

#### PROCEDURE USING CAD

- 1) Draw the geometry of the structure.
- 2) The structure is discretized into segments (voussoirs in arches). The more amount of segments the structure is divided in, the "smoother" the thrust-line obtained will be. However, doing graphic statics "by hand" can be tedious with too many divisions. An intermediate consideration is then taken into account. Recommendation: Put a number to identify each segment in order to have a guide when constructing the force polygon.
- 3) Find and locate force-weight vector for each segment, taking into account the existence of two different materials (therefore different densities).
  - Find the area of each part of the segment for each material
    - From <DRAW> use the command <BOUNDARY> to create an "object" (polyline).
    - Use the command <area> to obtain the value in m<sup>2</sup>
  - Find the volume of each part of the segment by multiplying the obtained areas with the width/thickness of the structural element.

- To obtain the weight for each part of each segment, multiply the given density value of each material ( $\text{kN/m}^3$ ) to the corresponding volume.
- Find the centroid coordinates for each material in each segment:
  - From <DRAW> use the command <REGION> by selecting the created "object" previously.
  - Use the command <MASSPROP> to obtain the x,y coordinates of the centroid for each part of the segment.
- Find the total centroid for each segment.
  - To find the coordinates for the total centroid of each segment with two different material densities, apply the formula:

$$x = \frac{(x_1 * P_1) + (x_2 * P_2)}{P_1 + P_2}$$

$x_1$ : x coordinate centroid material 1

$x_2$ : x coordinate centroid material 2

$y_1$ : y coordinate centroid material 1

$y_2$ : y coordinate centroid material 2

$$y = \frac{(y_1 * P_1) + (y_2 * P_2)}{P_1 + P_2}$$

$P_1$ : weight material 1

$P_2$ : weight material 2

- Find the total weight-force (kN) for each segment.
  - Sum each of the weights from the different materials for each segment.
- Locate each centroid of each segment:
  - Use <POINT> to draw a reference in each segment by giving the coordinates obtained before.
- Locate the weight-force (kN)
  - Define a scale for drawing the weight-force values (kN) represented as a dimension value (M). For example: 1 M = 250 kN.
  - Draw the <LINE> with the scaled magnitude in meters representing the weight-force (kN) with the starting point in the centroid of each corresponding segment.

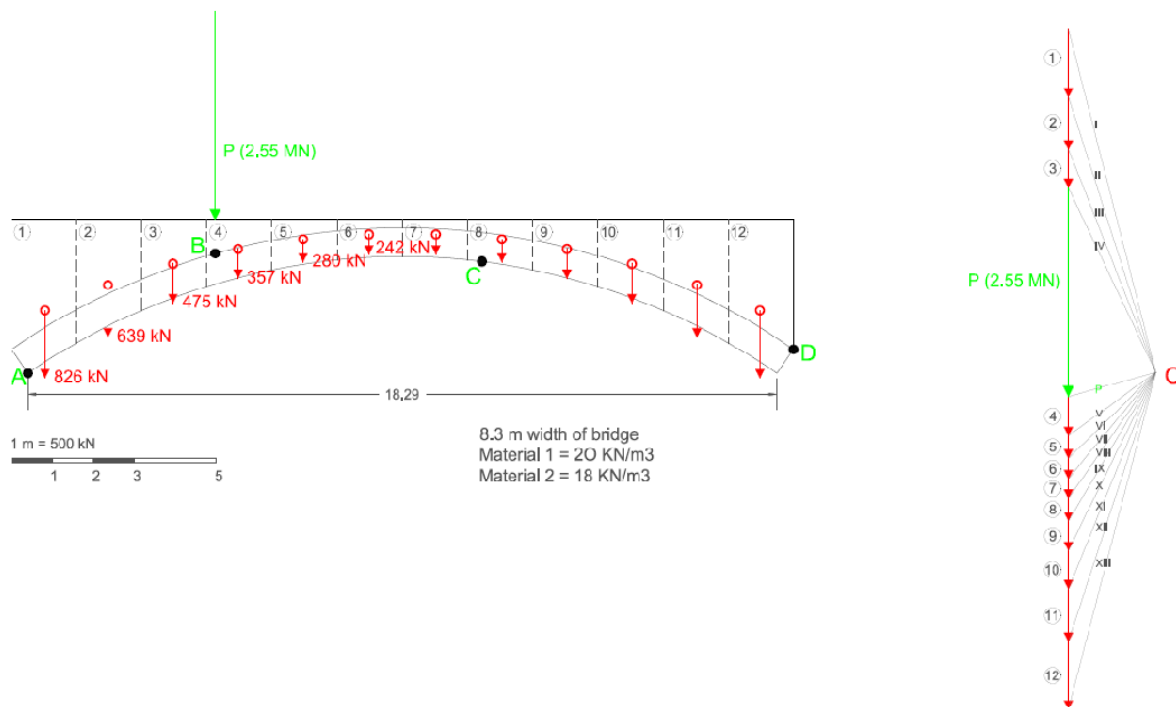


Fig. 21 - Discretization of arch, Location of centroids and vertical forces.

#### 4) Define the live weight

- Determine the location of the resultant live weight to be considered.

For this example the vertical load applied in 1/4 of the span has been obtained from the kinematic analysis.

#### 5) Apply STATIC GRAPHIC to calculate de <RESULTANT FORCE>

- To find the **magnitude** and **direction** of the <RESULTANT FORCE>: Sum in order of appearance the weight-forces (sum as vectors).
- To find the **position** of the <RESULTANT FORCE>:
  - Define an "origin" next to the summed force vectors
  - Draw ray-lines from the start and end of each individual force vectors: This will form a FORCE POLYGON
  - Take each ray-line (keeping its direction) and locate one of its ends intersecting the reference line of each corresponding weight-force vector in the analyzed structure: This will form a FUNICULAR POLYGON
  - Sum the two ray-line vectors of each extreme in the FUNICULAR POLYGON (sum of vectors): The position of the RESULTANT FORCE (with magnitude and direction that was found before), is achieved.

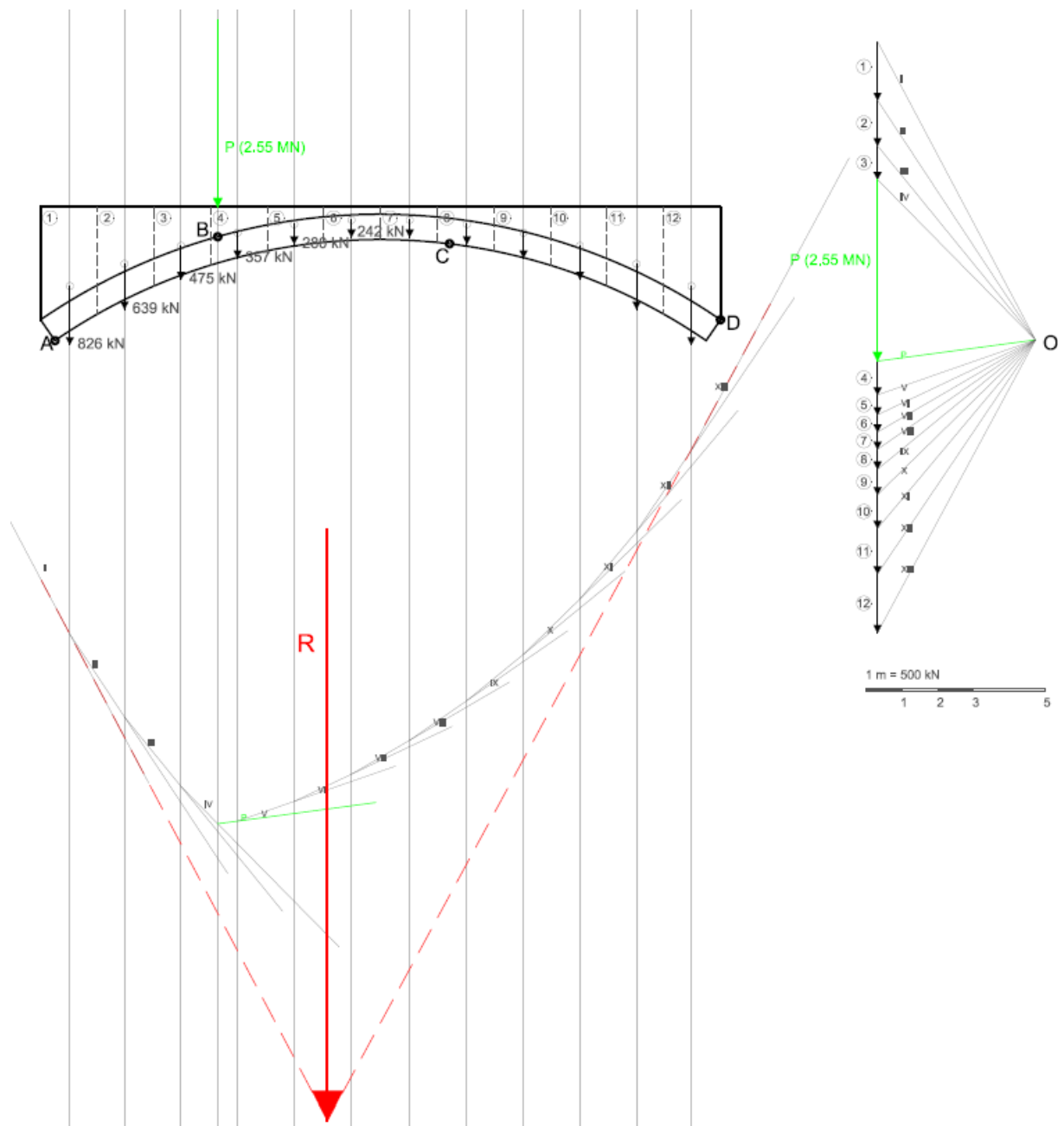


Fig. 22 - Funicular polygon and resultant force.

- 6) Considering that this case of application of the STATIC APPROACH has been defined with the objective of finding a thrust line for the evaluated mechanism in the KINEMATIC APPROACH, three hinges are selected as the fixed points.
- Three fixed points (hinges) are selected and referenced to the funicular polygon.
    - Reference lines are drawn ( $A'$  and  $B'$ ) connecting the hinges and projected over the funicular polygon.
    - Reference lines are drawn ( $A$  and  $B$ ) connecting the three points projected from the location of the hinges on the funicular polygon.

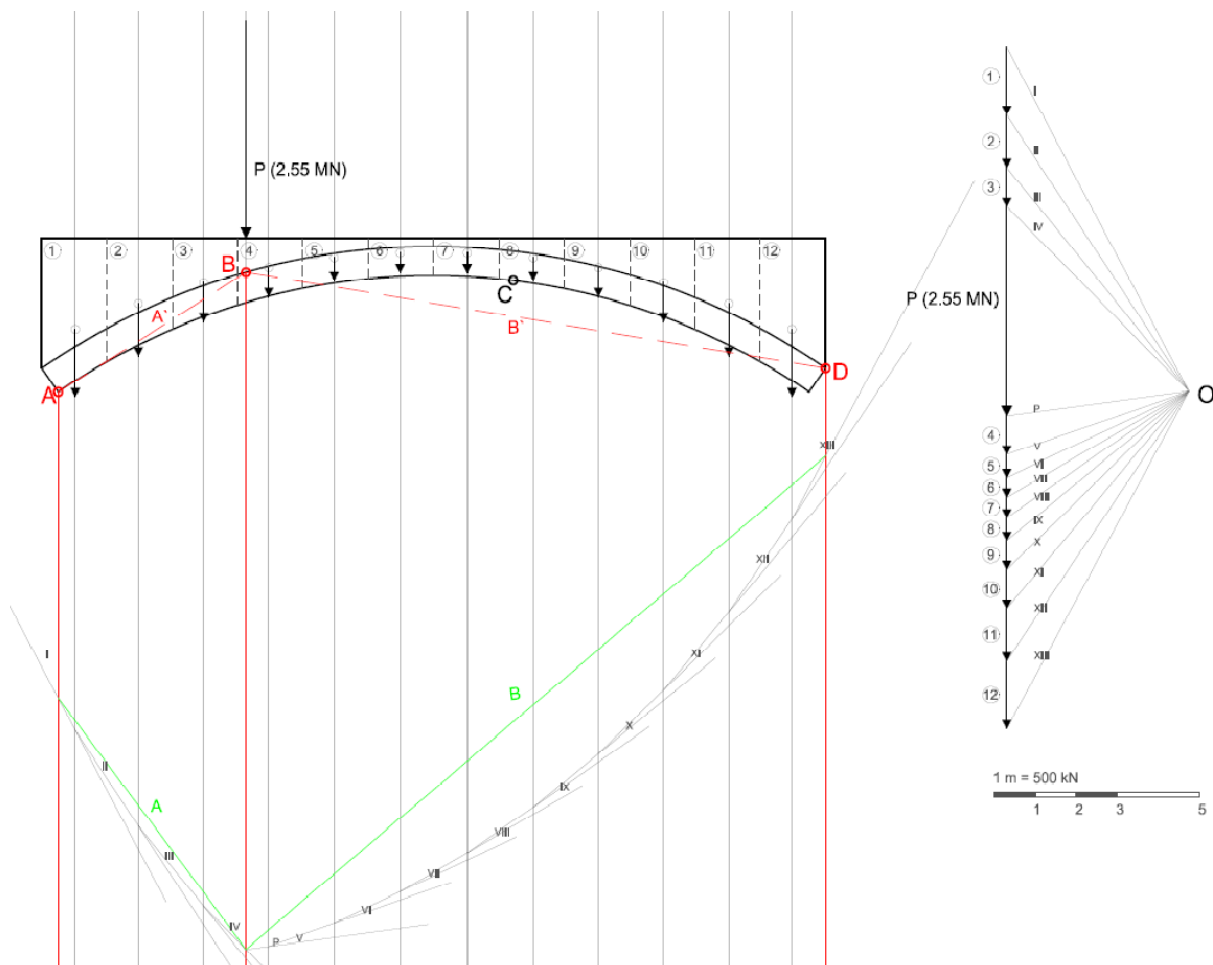


Fig. 23 - Selection of three hinges for the thrust line to pass through and projection on the funicular polygon.

- 7) Reference lines are used to define the location of a new origin ( $O'$ ) defining the rays to build the force polygon.
- 8) Draw the THRUST LINE. With the "new origin" ( $O'$ ) defined, the force polygon is constructed over the arch. Each line from origin -  $O'$  to each force, is relocated to cross the reference lines of the centroids of each segment of the arch. A sum of vectors occurs as each resultant force is summed with the vertical force located in each centroid, defining the new location of the consequent resultant.

For this example a thrust line has been found passing through ALL the four hinges of the defined mechanism. With the analysis in RING© software, the true solution was verified, therefore the location of the hinges was exact and the Critical Load Factor obtained. With the kinematic approach performed, the upper bound of the vertical load was verified.

In conclusion, for this example the UNIQUENESS THEOREM has been verified as *"a thrust line has been found causing as many hinges as needed to develop a mechanism"*. Therefore, for this example, the load evaluated *"is the true ultimate load, the mechanism is the true ultimate"*

*mechanism, and the thrust line is the only possible one". (Roca, Ancient Rules and Classical Approaches- Part 1-4. SA1 Lectures., 2009-2010)*

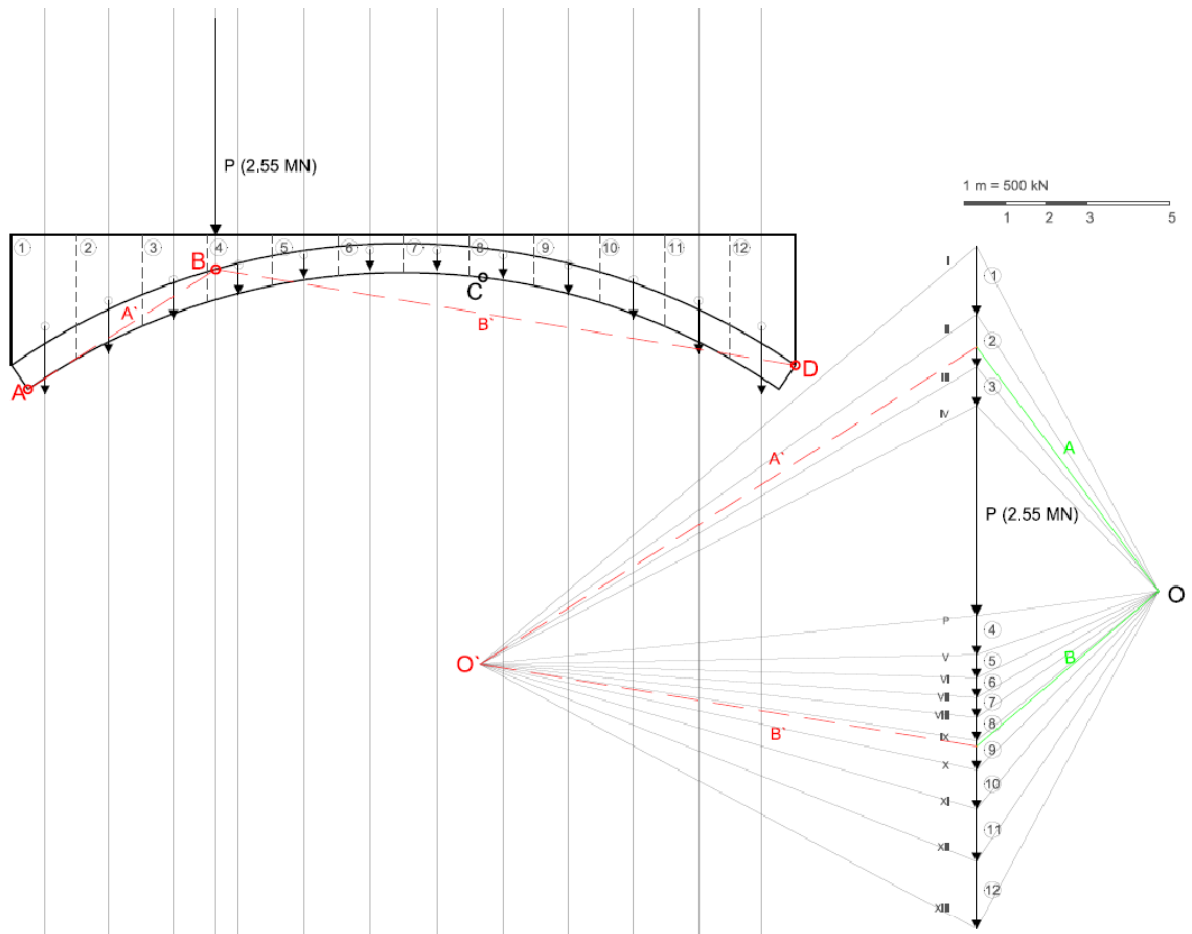


Fig. 24 - Defining the new origin for the force polygon.

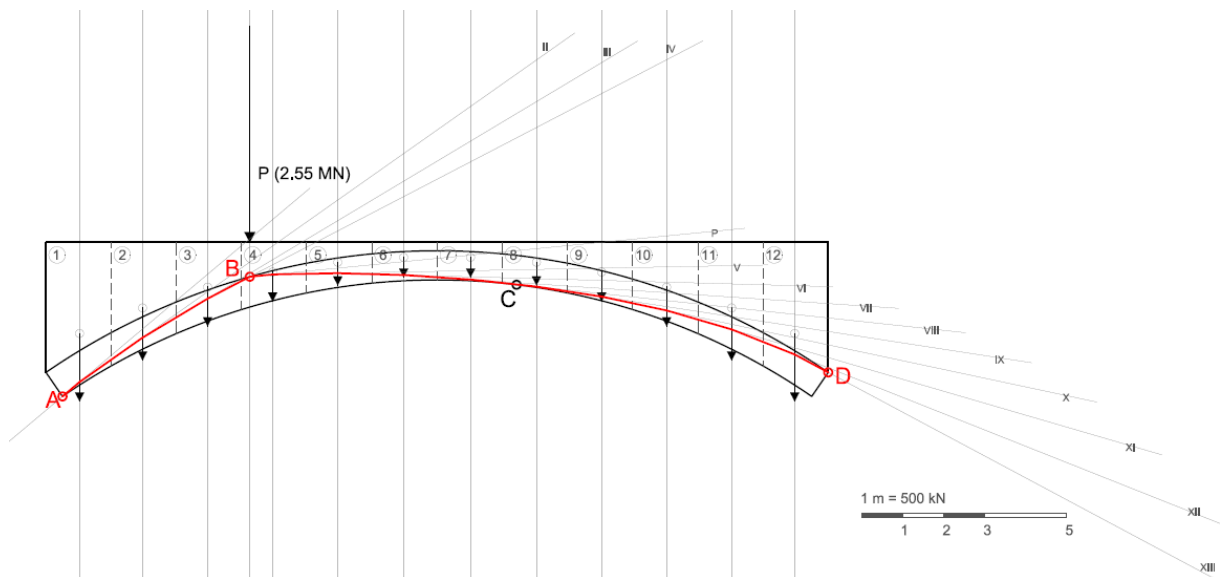


Fig. 25 - A thrust line passing through ALL hinges is found inside the arch.





### 3.2 Continuous barrel vault with buttresses (Cuernavaca Church in Mexico)

The building selected for this example is a Convent Church in Cuernavaca, located in the state of Morelos in Mexico.

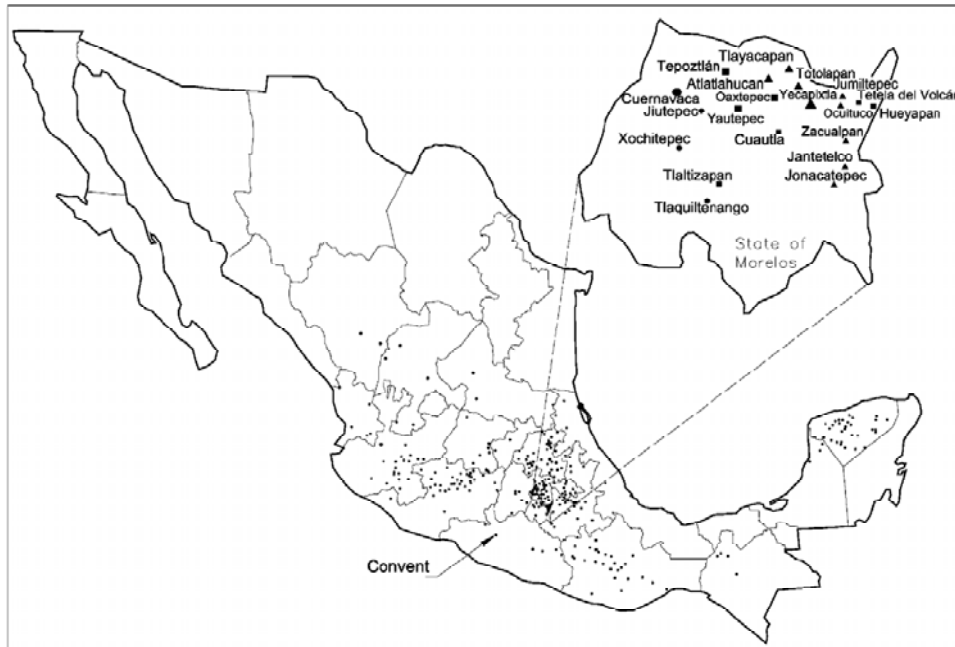


Fig. 26 - Map of the distribution of convent compounds in Mexico and in the State of Morelos (Meli, 2009)

The Cuernavaca Church was selected considering that it is the most distinguished as the most representative type of Mexican sixteenth century convents. (Meli, 2009)



Fig. 27 – Continuous barrel vault of Cuernavaca convent church (Meli, 2009)

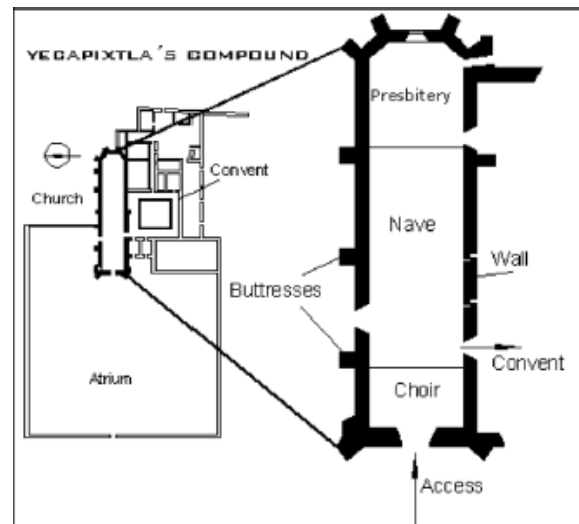


Fig. 28 – Typical ground plan of a convent compound and its church (Meli, 2009)

The Cuernavaca convent church has an arch buttress that was added later, maybe due to the fact of a change from wooden roofing to masonry vault or to other kind of structural problems. The study performed by Meli did not consider the effect of safety to lateral forces (earthquake), considering that this issue was not taken into account by the original builders in this zone. Furthermore, the conclusion

about structural modifications in colonial times are said to be done in order to “provide additional capacity for vertical loads” (Meli, 2009).

In the following table, the geometric parameters are described. The main properties that will influence the load capacity of the analyzed structure will be the buttress depth, the height of the nave, and the thickness and span of the vault.

Probable building date	Convent	Length (nave, choir, presbytery)			Vault		Buttress depth (includes wall thickness)		Wall		
		Span	Height	thickness	thickness	Span/ Length	Height/ Span	Buttress / Wall			
<b>Continuous barrel vault</b>											
1525-1570	Cuernavaca (F)	68.50	13.50	20.40	1.00	4.25 (a)	12.50 (*b)	2.00	1:5.0	1.50	2.13

(A) Augustinian; (D) Dominicans; (F) Franciscan; (a) attached buttress; (b) arch buttress; (\*a) attached buttress built on later; (\*b) arch buttress built on later; (\*aa) increase of original buttress section.

Table 2 – Geometric characteristics of the Cuernavaca Convent Church (Meli, 2009)

Considering the initial buttress depth (disregarding the arch buttress built on later), an example was performed to observe if Blondel’s Rule was applied and it was observed that this was not the parameter used. However, in (Meli, 2009) other rules were evaluated which take into account the buttress height “leading to similar load capacity of the nave under vertical loads”.

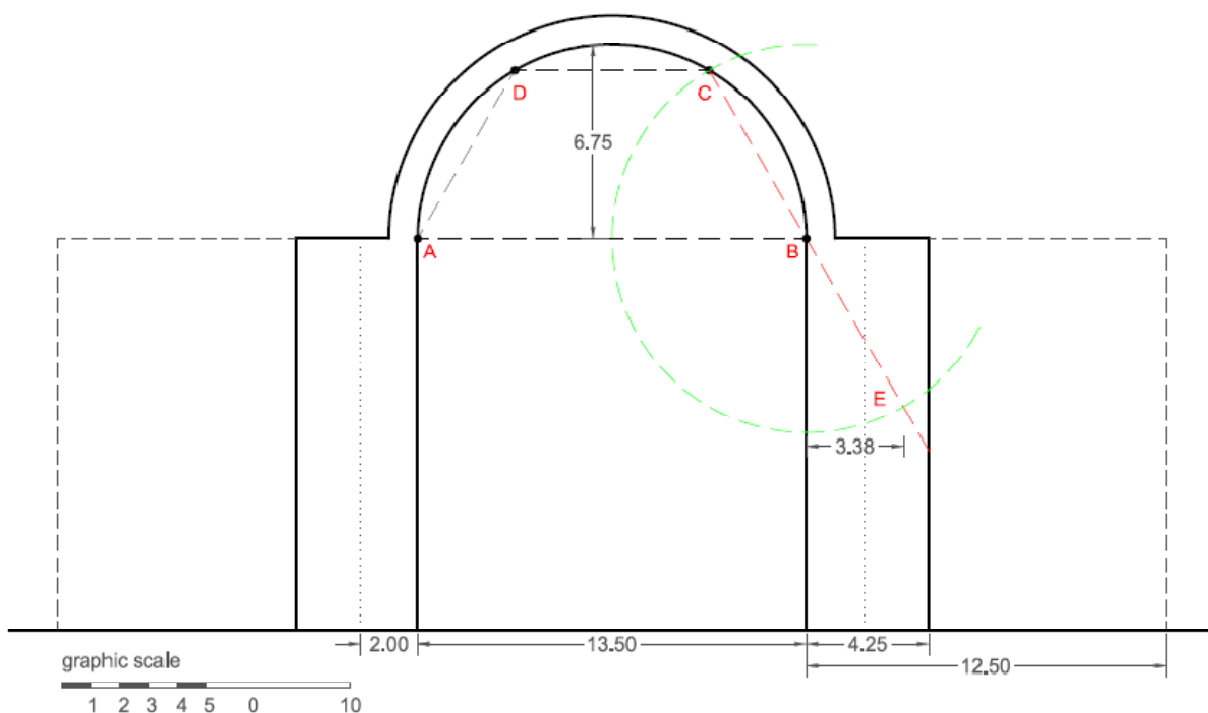


Fig. 29 – Buttress depth verification with Blondel’s Rule to Cuernavaca church.

The structural typology is a semicircular vault supported directly on thick-buttressed masonry walls. The structural material is a heterogeneous masonry composed by stones of different size and shape, agglutinated by lime-sand mortar. For the mechanical properties of the masonry used in Cuernavaca Convent Church, it was used the value of  $15.69 \text{ kN/m}^3$  for the volumetric weight based on the

information about the wall of a colonial building in Mexico City which is normally made of *tezontle*, a porous volcanic rock. (Meli, 2009)

Type	Volumetric weight (kN/m <sup>3</sup> )	Young modulus (MPa)	Compression strength (MPa)	Reference
I	15.69	1961	2.94	(Sánchez and Meli, 1991)

Table 3 - Mechanical properties of stone masonries.

The examples of application of Limit Analysis performed for the Cuernavaca Church were the following:

- Kinematic Approach:
  - o Kinematic isolated arch mechanism-1 (point load in the key of the arch for 5 hinges in the arch)
  - o Kinematic arch-buttress mechanism-2 (point load in the key of the arch with 3 hinges in the arch and 2 hinges in the base of the buttresses).
- Static Approach:
  - o Static (thrust line) for Kinematic mechanism (with minimum upper bound – vertical load- between mechanisms 1-2)

A verification using RING© software was also performed for the Isolated arch - mechanism-1 (point load in the key of the arch with 5 hinges in the arch). See annex.

The geometrical properties used for all the examples were obtained from (Meli, 2009), but two aspects were assumed based on the typical geometrical properties for the twelve meter span church available in the reference document. Therefore, a distance of ten meters was considered between the structural axes of the buttresses and a thickness of two meters was defined for each buttress. The other dimensions correspond to the dimensions in the table of geometrical characteristics previously presented.

The scale used for the value of forces and distances has been specified in each drawing.

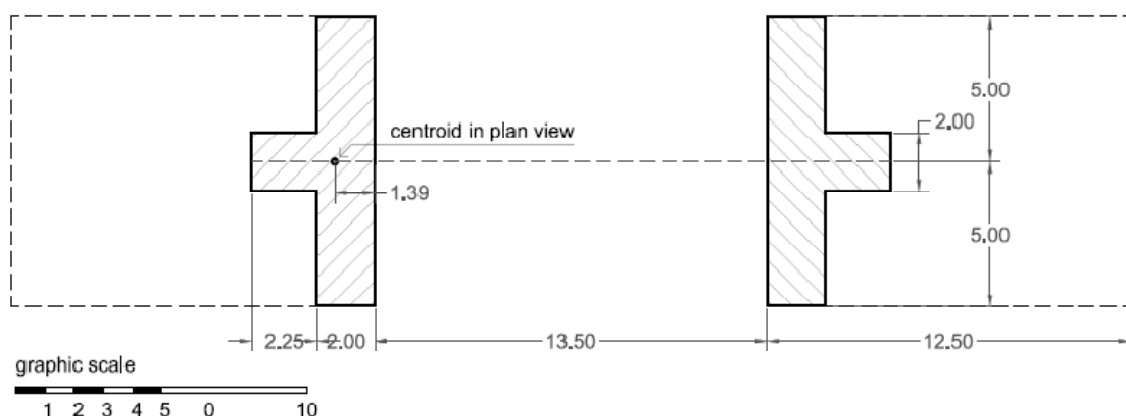


Fig. 30 – Geometrical properties for the plan view of Cuernavaca Church. The thickness of the buttress was assumed.

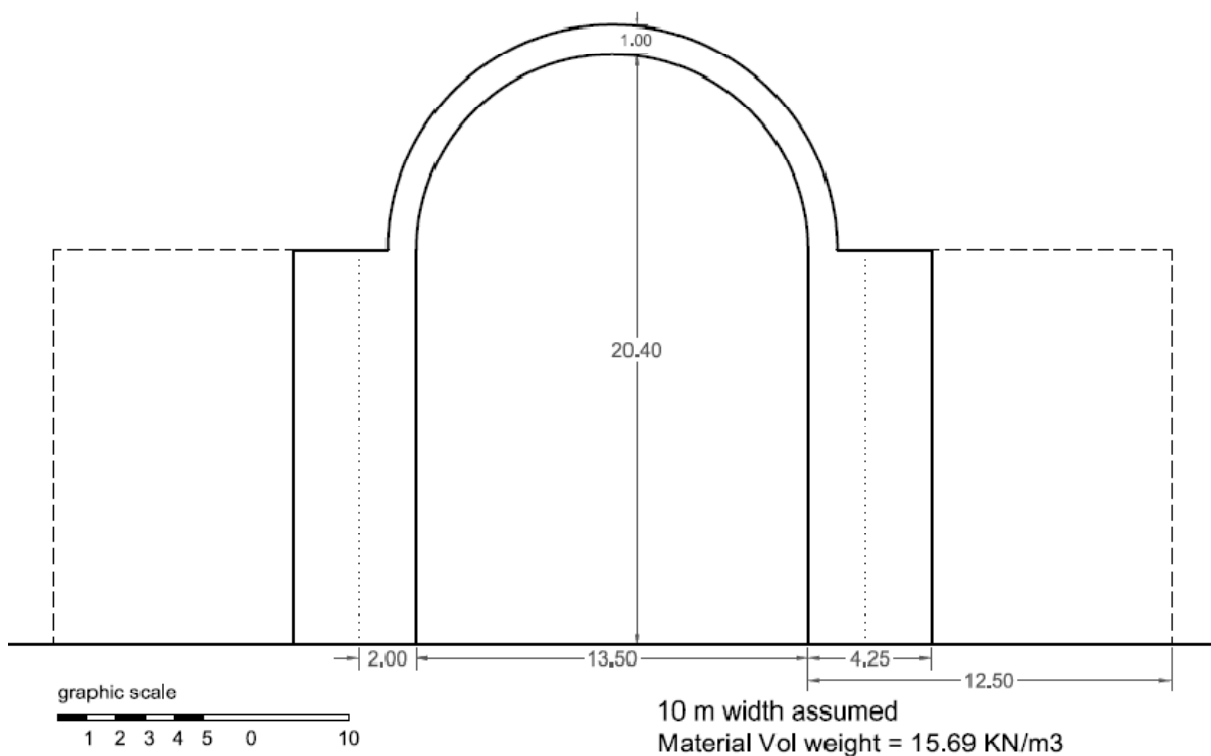


Fig. 31 – Geometrical properties for the vertical section of Cuernavaca Church

In the plan view image the location of the centroid for the “T” section of the wall and buttress considered as the contributing area has been determined. This will be considered in the mechanism that involves the participation of the buttresses.

For calculating each weight-force applied in the centroid of each segment in which the buttress will be divided in, the area considered is the plan view, and the thickness will be the height of the segment. For the case of the arch, for calculating each weight-force applied in the centroid of each voussior, the area considered will be the voussior in section and the thickness will be 10 meters which correspond to the depth of the vault taken into account.

### 3.2.1 Kinematic Approach

Two mechanisms were evaluated:

- Mechanism-1: Five hinges in isolated arch (the buttresses make no contribution)
- Mechanism-2: Three hinges in arch and two hinges in buttresses.

#### 3.2.1.1 Mechanism – 1: Five hinges in isolated arch.

A vertical load is applied in the key of the arch. A mechanism of five hinges was defined. The location of the hinges was based on the result obtained from the analysis performed in RING© that has previously been described.

The objective is finding the *upper bound of the maximum vertical load* for the mechanism analyzed. The vertical load (V in MN), is obtained by solving the system given by the following expression:

$$W = \sum_{k=1}^N V_{kg} * X_{kg}^c * K_k^\theta + \lambda \sum_{j=1}^{n_f} V_j * X_{k(j)}^c * K_{k(j)}^\theta \quad \theta = 0 \quad \lambda = - \frac{\sum_{k=1}^N V_{kg} * X_{kg}^c * K_k^\theta}{\sum_{j=1}^{n_f} V_j * X_{k(j)}^c * K_{k(j)}^\theta}$$

Fig. 32 - Expressions for TOTAL WORK (Roca, Ancient Rules and Classical Approaches- Part 1-4. SA1 Lectures., 2009-2010)

Where:

W = Total work

W = Sum of the internal forces + Sum of the external forces.

Sum of the internal forces:

$V_{kg}$  = Weight force resultant in block k applied at the centroid g.

$X_{kg}^c$  = Horizontal component of the distance between the center of rotation to the centroid g of block k.

$K_k^\theta$  = Angle of rotation of block k.

Sum of the external forces:

$V_j$  = External vertical load applied (this is the unknown of the system)

$X_{ck(j)}$  = Horizontal component of the distance between the center of rotation of the block where the external vertical load  $V_j$  is applied, to the point of application of the force.

$K_{k(j)}^\theta$  = Angle of rotation of the block where the external force is being applied.

According to this, the procedure involves three main steps:

PART I: Determining the rotations and displacements of the mechanism.

PART II: Calculating the internal forces

PART III: With the expression of total work, calculating the *upper bound of the maximum vertical load*.

PART I – DETERMINING ROTATIONS AND DISPLACEMENTS OF THE MECHANISM

- 1) The mechanism to be analyzed is defined. For a vertical load applied in the center of the arch a five-hinge mechanism is selected. The hinges are located in the arch dividing the arch in four blocks. The hinges in the support of the arch will not have displacements and the hinge in the center of the arch, where the load is applied, will only have a vertical displacement. The other two hinges will have horizontal and vertical displacements.

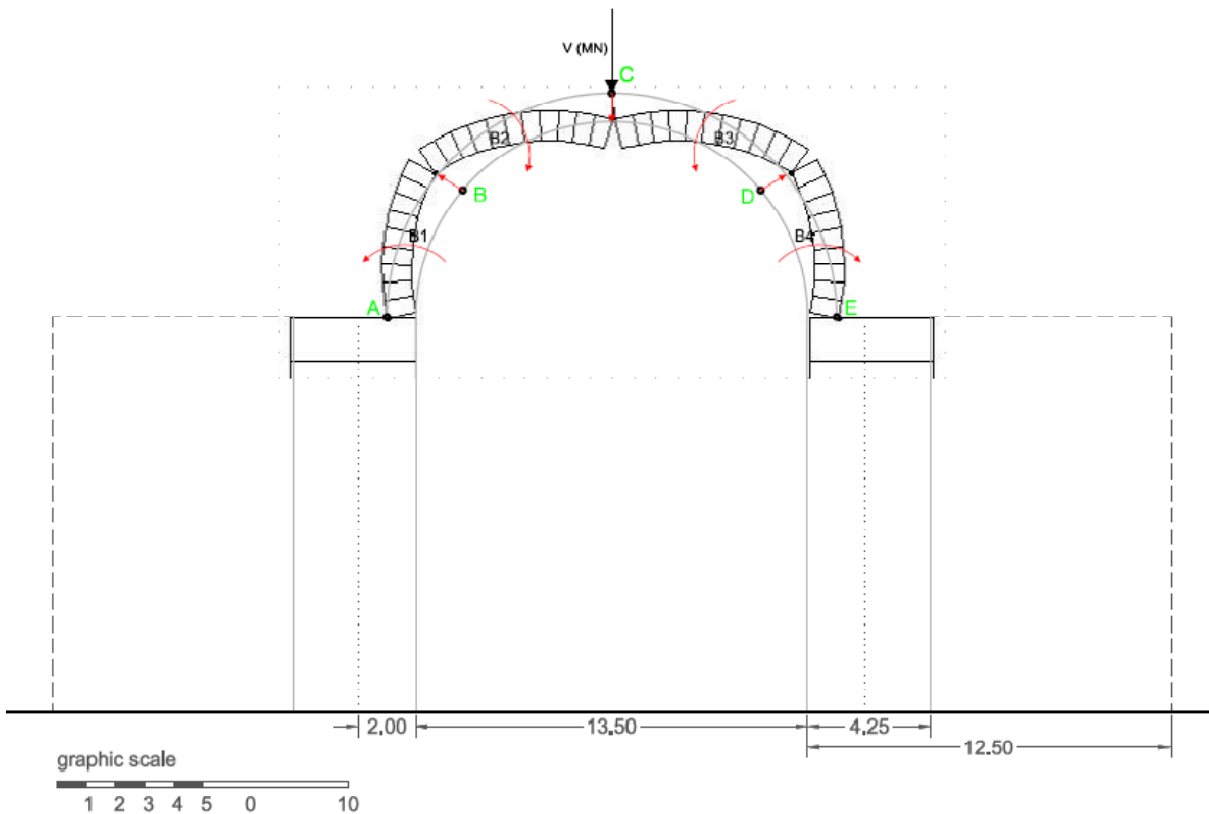


Fig. 33 – Overlapped mechanism from RING© in order to identify the movement of each block.

- 2) The sign criteria are defined for displacements and forces.

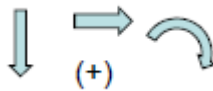


Fig. 34 – Sign criteria.

- 3) Each block will have a corresponding center of rotation. Lines are drawn connecting the hinges without displacements ( $A$  and  $E$ ), which correspond to the center of rotations  $C_1$  and  $C_4$ , with the consequent hinges ( $B$  and  $D$ ). These lines are perpendicular to the directions defined by the displacements of the extreme hinges that define each block ( $B_1$  and  $B_4$ ). With the same criteria, knowing that the displacement of the central blocks ( $B_2$  and  $B_3$ ) in the hinge  $C$  will have only a vertical component, a line is drawn perpendicular to this direction passing through hinge  $C$ . The intersection between this line and the line connecting hinges  $A$  and  $B$  will be the center

of rotation  $C_2$ . By symmetry, the intersection of the line connecting hinges E and D, with the perpendicular line to the displacement of hinge C, will correspond to the center of rotation  $C_3$ .

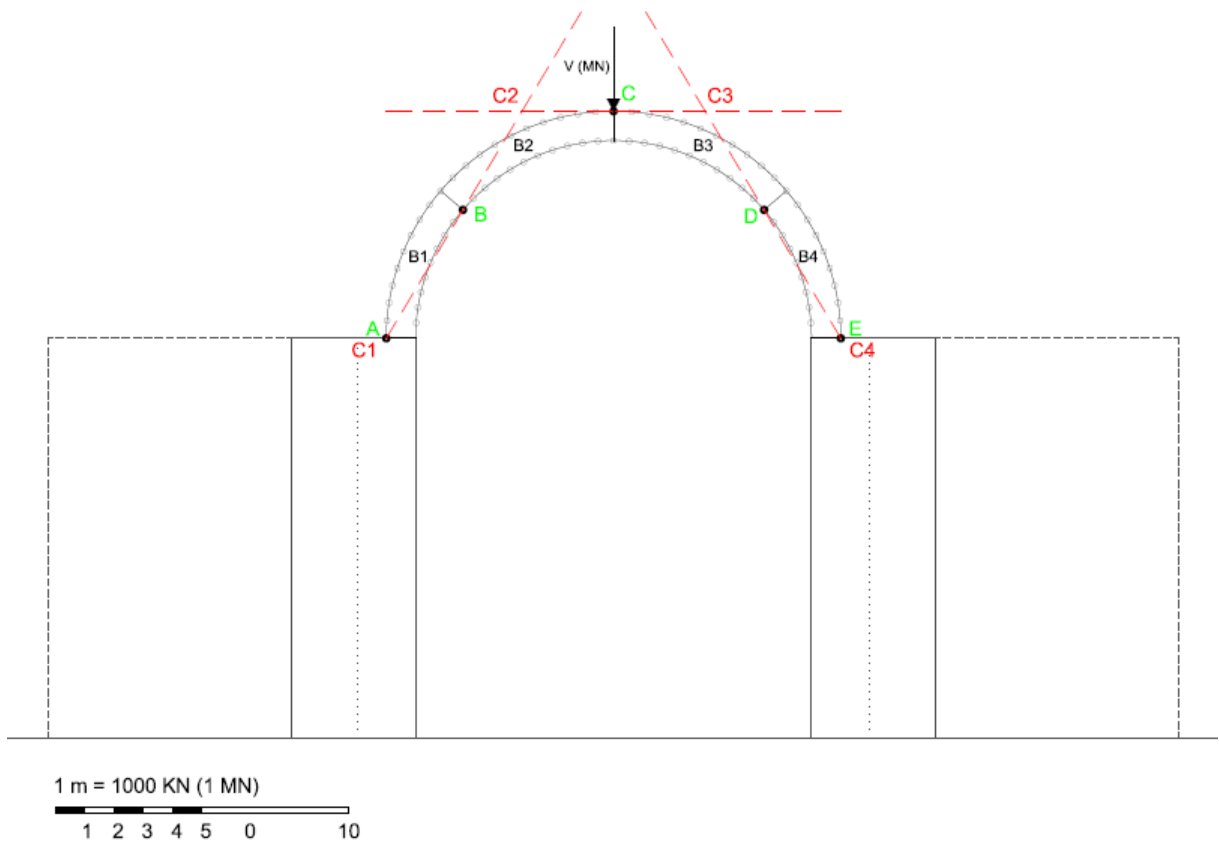


Fig. 35 - Location of rotation centers for the four blocks in a symmetrical five-hinge collapse mechanism in arch  
Considering that for this mechanism the buttresses are not being considered, the following images will only show the arch.

- 4) The rotations and displacements are identified in the mechanism and correlated with the hinges and centers of rotation.

$\delta_B$  = perpendicular displacement of hinge B to the line connecting centers of rotation  $C_1 - C_2$ .

$\delta_C$  = vertical displacement of hinge C. The perpendicular line to this vector connects centers of rotation  $C_2 - C_3$ .

$\delta_D$  = perpendicular displacement of hinge D to the line connecting centers of rotation  $C_3 - C_4$ .

$L_{1B}$  = Distance between center of rotation  $C_1$  and hinge B.

$L_{2B}$  = Distance between center of rotation  $C_2$  and hinge B.

$L_{2C}$  = Distance between center of rotation  $C_2$  and hinge C.

$L_{3C}$  = Distance between center of rotation  $C_3$  and hinge C.

$L_{3D}$  = Distance between center of rotation  $C_3$  and hinge D.

$L_{4D}$  = Distance between center of rotation  $C_4$  and hinge D.

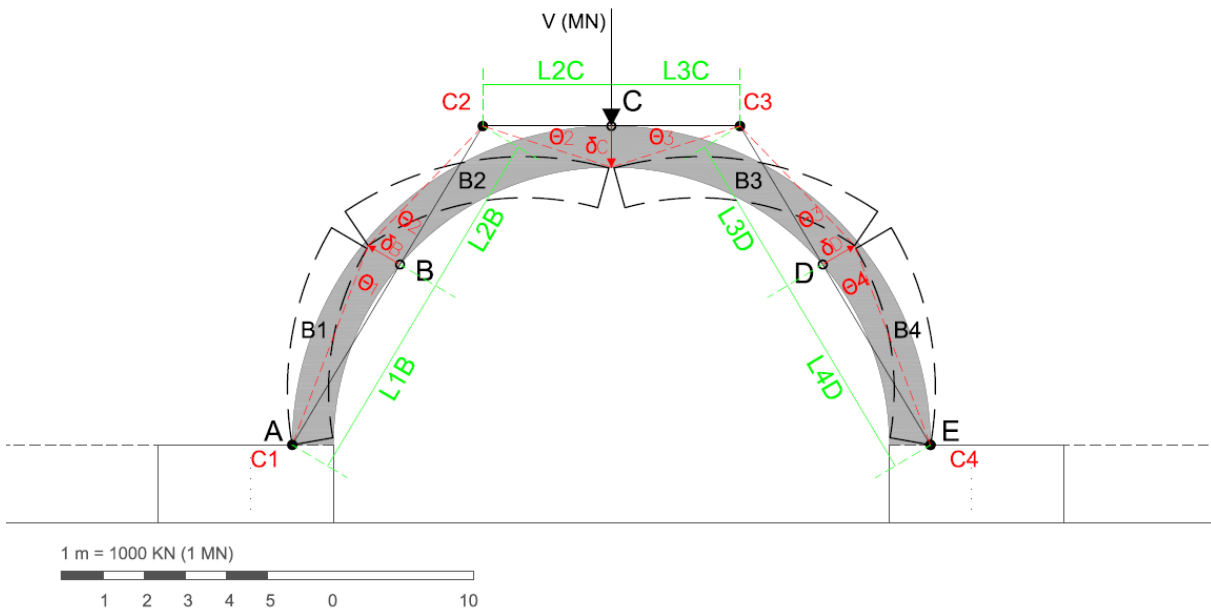


Fig. 36 - Identification of the rotations, displacements and correlations with the hinges and centers of rotation.

5) The angles according to the sign criteria will be as following:

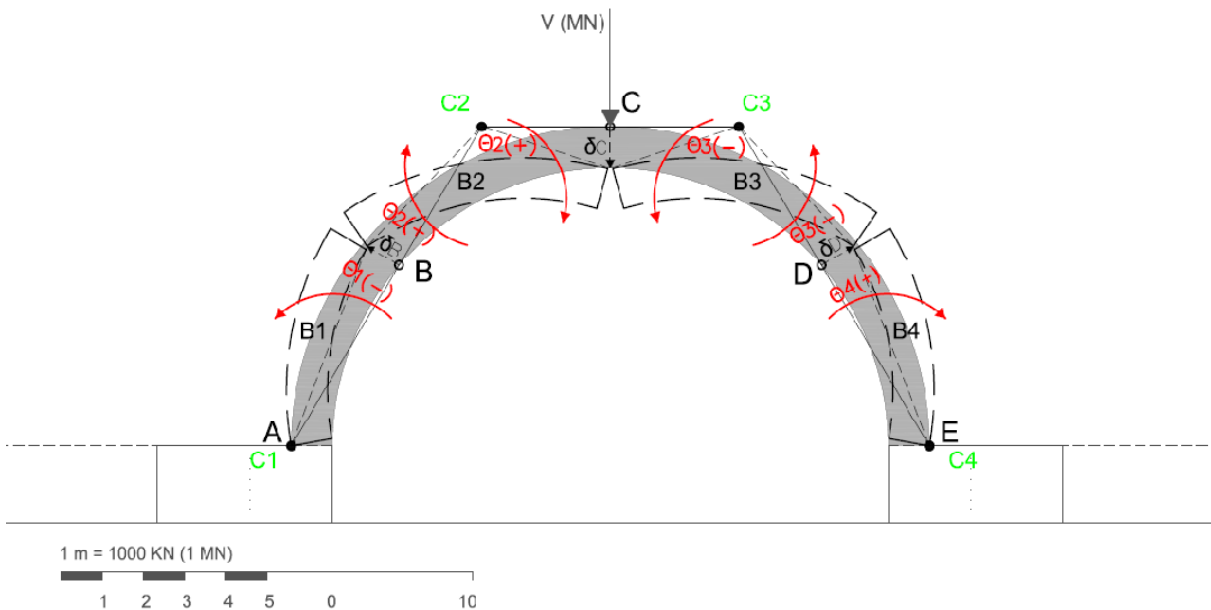


Fig. 37 - Identification of the signs of the angles of rotation of the blocks.

Once the mechanism has been established, the first step is defining the first angle of rotation. This value is decided arbitrarily ( $\theta_1$ ) and all the displacements and rotations will depend on it.



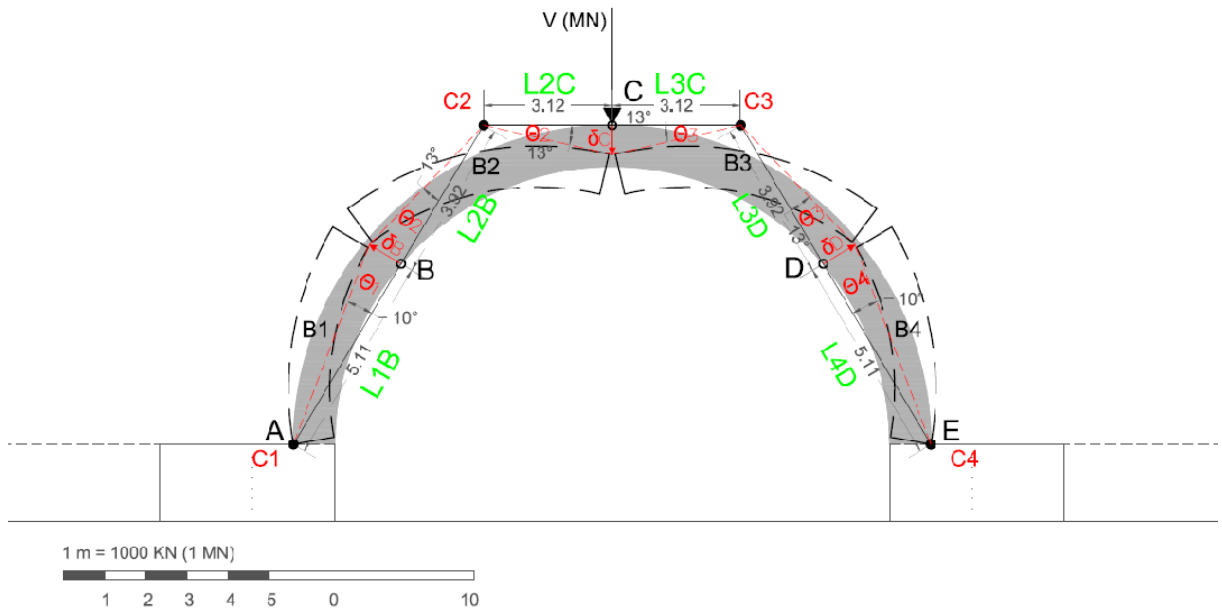


Fig. 38 – Displacements and rotations determined in sequence.

In order to perform the calculations, the relationships between rotations, displacements are established in a sequence from defining  $\Theta_1$ , and according to the sign criteria previously defined:

$$\begin{aligned} \delta_B &= \Theta_1 * L_{1B} = -\Theta_2 * L_{2B} & \longrightarrow & \longrightarrow & -\Theta_1 * L_{1B} / L_{2B} & = \Theta_2 \\ \delta_C &= -\Theta_2 * L_{2C} = \Theta_3 * L_{3C} & \longrightarrow & \longrightarrow & -\Theta_2 * L_{2C} / L_{3C} & = \Theta_3 \\ \delta_D &= \Theta_3 * L_{3D} = -\Theta_4 * L_{4D} & \longrightarrow & \longrightarrow & \Theta_3 * L_{3D} / L_{4D} & = \Theta_4 \end{aligned}$$

The procedure was as following:

- 6) Define an angle of rotation ( $\Theta_1$ ) from the first hinge - A (first point of rotation -  $C_1$ ). Draw a perpendicular line from the second hinge-B to the new rotated line. This line segment corresponds to the displacement of hinge-B ( $\delta_B$ ) which is the new location of the second hinge.

This value ( $\delta_B$ ) is also verified analytically by:  $\delta_B = \Theta_1 * L_{1B}$ , where  $L_{1B}$  is the distance between the first point of rotation- $C_1$  and hinge-B.

**Assume  $\Theta_1$  (in radians):**

**$\Theta_1$  (degrees)     $\Theta_1$  (radians)**

-10                      -0.17

**Determine  $\delta_B$  (displacement of point B) from  $\Theta_1$**

$$\delta_B = \Theta_1 * L_{1B}$$

**$\Theta_1$  (rad)               $L_{1B}$  (meters)       $\delta_B$  (meters)**

-0.17                      5.11                      -0.89                      0.90(verification in autocad)

- 7) The angle  $\Theta_2$  is found by connecting the new point of displacement of hinge-B given by  $\delta_B$ . Analytically this value is obtained (therefore verified) from the expression

$$\Theta_2 = (-L_{1B}/L_{2B}) * \Theta_1$$

Where  $L_{2B}$  is the distance between hinge-B and the second point of rotation- $C_2$ . This expression is obtained from the following equivalence:

$$\delta_B = \Theta_1 * L_{1B} = -\Theta_2 * L_{2B}$$

**Determine  $\Theta_2$  (rad) from  $\Theta_1$**

$$\Theta_2 = (-L_{1B}/L_{2B}) * \Theta_1 \text{ this formula comes from } \delta_B = \Theta_1 * L_{1B} = -\Theta_2 * L_{2B}$$

$\Theta_1$ (rad)	$L_{1B}$ (meters)	$L_{2B}$ (meters)	$\Theta_2$ (rad)	$\Theta_2$ (degrees)
-0.17	5.11	3.92	0.23	13.02

- 8) The displacement of the hinge-C is found with the expression  $\delta_C = -\Theta_2 * L_{2C}$  where  $L_{2C}$  is the distance between the second point of rotation -  $C_2$  and hinge-C.

**Determine  $\delta_C$  (displacement of point C) from  $\Theta_2$**

$$\delta_C = -\Theta_2 * L_{2C}$$

$\Theta_2$ (rad)	$L_{2C}$ (meters)	$\delta_C$ (meters)
0.23	3.12	-0.71

- 9) The angle  $\Theta_3$  is obtained from the expression  $\Theta_3 = -\Theta_2 * (L_{2C}/L_{3C})$

**Determine  $\Theta_3$  (rad) from  $\Theta_2$**

$$\Theta_3 = -\Theta_2 * (L_{2C}/L_{3C}) \text{ in this example } L_{2C} = L_{3C}$$

$L_{2C}$ (meters)	$L_{3C}$ (meters)	$\Theta_2$ (rad)	$\Theta_3$ (rad)	$\Theta_3$ (degrees)
3.12	3.12	0.23	-0.23	-13.02

- 10) The displacement of the hinge-D is found with the expression  $\delta_D = \Theta_3 * L_{3D}$  where  $L_{3D}$  is the distance between the third point of rotation -  $C_3$  and hinge-D.

**Determine  $\delta_D$  (displacement of point D) from  $\Theta_3$**

$$\delta_D = \Theta_3 * L_{3D}$$

$\Theta_3$ (rad)	$L_{3D}$ (meters)	$\delta_D$ (meters)
-0.23	3.92	-0.89
		<i>0.90(verification in autocad)</i>

- 11) The angle  $\Theta_4$  is obtained from the expression  $\Theta_4 = -\Theta_3 * (L_{3D}/L_{4D})$

**Determine  $\Theta_4$  (rad) from  $\Theta_3$**

$$\Theta_4 = -\Theta_3 * (L_{3D}/L_{4D}) \text{ in this example } L_{4D} = L_{1B}$$

$L_{3D}$ (meters)	$L_{4D}$ (meters)	$\Theta_3$ (rad)	$\Theta_4$ (rad)	$\Theta_4$ (degrees)
3.92	5.11	-0.23	0.17	10.00

The following equivalences have been verified graphically and analytically:  $\Theta_1 = -\Theta_4$ ;  $\Theta_2 = -\Theta_3$ .

Considering that for calculating the work performed by the weight-force of each block a displacement has to be defined.

$$\text{Work} = \text{Force} * \text{Displacement}$$

Work (block-i) = Weight-force resultant located in the centroid of block ( $V_i$ ) \* angle of rotation of block ( $\Theta_i$ ) \* horizontal component of the distance between the center of rotation of the block and the centroid of the initial block ( $X_{ci}$ ),

Or,

Work (block-i) = Weight-force resultant located in the centroid of block ( $V_i$ ) \* vertical component of the distance between the centroids of the initial and rotated blocks ( $\delta_{iy}$ ).

12) For the work of internal vertical forces, measure the horizontal component ( $X_{ci}$ ) of the distance between the center of rotation of the block and the centroid of the initial block. Take into account the signs taking as reference the location of the center of rotation (starting point).

13) Multiply  $X_{ci}$  with the angle of rotation of the block to obtain the VERTICAL component ( $\delta_{iy}$ ) of the distance between the centroids of the initial and the rotated blocks.  $\delta_{iy}$  will be the “arm” that multiplied by the weight-force (vertical internal resultant force) gives the value of the WORK for the block.

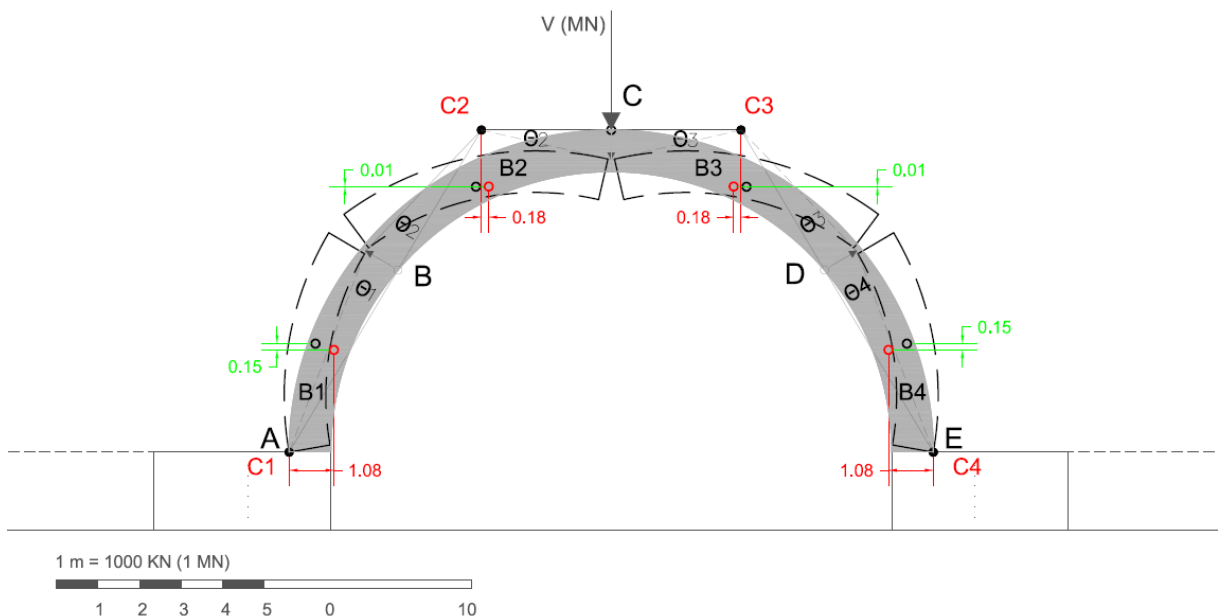


Fig. 39 – Measuring the horizontal component distance from centroid of initial block to rotation center (in red).

**BLOCK 1**

$\Theta_1$ (rad)	$X_{c1}$	$\delta_{1y}$	
-0.17	1.08	-0.19	0.15(verification of $\delta_{1y}$ measuring from drawing)

**BLOCK 2**

$\Theta_2$ (rad)	$X_{c2}$	$\delta_{2y}$	
0.23	0.18	0.04	0.01(verification of $\delta_{1y}$ measuring from drawing)

**BLOCK 3**

$\Theta_3$ (rad)	$X_{c3}$	$\delta_{3y}$	
-0.23	-0.18	0.04	0.01(verification of $\delta_{1y}$ measuring from drawing)

**BLOCK 4**

$\Theta_4$ (rad)	$X_{c4}$	$\delta_{4y}$	
0.17	-1.08	-0.19	0.15(verification of $\delta_{1y}$ measuring from drawing)

## PART II – CALCULATING THE INTERNAL FORCES

	density (kN/m <sup>3</sup> )	Width (meters)	Area (m <sup>2</sup> )	Weight (kN)	scaled force (1m=1MN)
A <sub>1</sub>	15.69	10	5.1247	804.07	0.80
A <sub>2</sub>	15.69	10	6.2636	982.76	0.98
A <sub>3</sub>	15.69	10	6.2636	982.76	0.98
A <sub>4</sub>	15.69	10	5.1247	804.07	0.80

## PART III - CALCULATING THE UPPER BOUND OF THE MAXIMUM VERTICAL LOAD.

W (work)

w (weight force)

P (force applied in 1/4 of span)

$W_i + W_e = 0$  (Internal work + External work in equilibrium)

$W = F \cdot \delta$  (Work can be expressed as a force \* displacement/rotation)

$W_i = (w_1 \cdot \delta_{1y} + w_2 \cdot \delta_{2y} + w_3 \cdot \delta_{3y} + w_4 \cdot \delta_{4y})$

$$W_e = P \cdot \delta_{py}$$

$$(w_1 \cdot \delta_{1y} + w_2 \cdot \delta_{2y} + w_3 \cdot \delta_{3y} + w_4 \cdot \delta_{4y}) + (P \cdot \delta_{py}) = 0$$

$$P = -(w_1 \cdot \delta_{1y} + w_2 \cdot \delta_{2y} + w_3 \cdot \delta_{3y} + w_4 \cdot \delta_{4y}) / \delta_{py}$$

P can be expressed as:

$$\lambda P = -(w_1 \cdot \delta_{1y} + w_2 \cdot \delta_{2y} + w_3 \cdot \delta_{3y} + w_4 \cdot \delta_{4y}) / \delta_{py}$$

$$\delta_{py} = \theta \cdot X_p$$

Determine  $\delta_{py}$ : vertical displacement point of application of force P due to rotation of the block where the force is applied: in this example is  $\Theta_2$ .

$$\delta_{py} = \Theta_2 \cdot X_p \quad X_p: \text{Horizontal distance from rotation center to external vertical load applied}$$

$\Theta_2$ (rad)	$X_p$ (meters)	$\delta_{py}$ (meters)	
0.23	3.12	0.71	0.71 (verification measured in drawing)

Determine  $\lambda$  (Factor load) for a given P (assumed)

$$\lambda = -(w_1 \cdot \delta_{1y} + w_2 \cdot \delta_{2y} + w_3 \cdot \delta_{3y} + w_4 \cdot \delta_{4y}) / P \cdot \delta_{py}$$

w1 (KN)	$\delta_{1y}$ (M)	w2 (KN)	$\delta_{2y}$ (M)	w3 (KN)	$\delta_{3y}$ (M)	w4 (KN)	$\delta_{4y}$ (M)	$\delta_{py}$ (M)	P (KN)	$\lambda$
804.07	-0.19	982.76	0.04	982.76	0.04	804.07	-0.19	0.71	1	315.22

Table 4 - Load Factor table from Excel©

Comparing the results obtained with the use of CAD and a spreadsheet, with the one obtained in RING©:

FAILURE LOAD FACTOR (Mechanism-1)

RING©	Spreadsheet- $\lambda$
315.38	315.22

### 3.2.1.2 Mechanism – 2: Three hinges in arch and two hinges in buttresses.

A vertical load is applied in the key of the arch. A mechanism of three hinges in the arch and two hinges in the buttresses was defined.

The objective is finding the *upper bound of the maximum vertical load* for the mechanism analyzed. The vertical load (V in MN), is obtained by solving the system given by the following expression:

$$W = \sum_{k=1}^N V_{kg} * X_{kg}^c * K_k^\theta \theta + \lambda \sum_{f=1}^{n_f} V_j * X_{k(j)}^c * K_{k(j)}^\theta \theta = 0 \quad \lambda = - \frac{\sum_{k=1}^N V_{kg} * X_{kg}^c * K_k^\theta}{\sum_{f=1}^{n_f} V_j * X_{k(j)}^c * K_{k(j)}^\theta}$$

Fig. 40 - Expressions for TOTAL WORK (Roca, Ancient Rules and Classical Approaches- Part 1-4. SA1 Lectures., 2009-2010)

Where:

W = Total work

W = Sum of the internal forces + Sum of the external forces.

Sum of the internal forces:

$V_{kg}$  = Weight force resultant in block k applied at the centroid g.

$X_{kg}^c$  = Horizontal component of the distance between the center of rotation to the centroid g of block k.

$K_k^\theta$  = Angle of rotation of block k.

Sum of the external forces:

$V_j$  = External vertical load applied (this is the unknown of the system)

$X_{k(j)}^c$  = Horizontal component of the distance between the center of rotation of the block where the external vertical load  $V_j$  is applied, to the point of application of the force.

$K_{k(j)}^\theta$  = Angle of rotation of the block where the external force is being applied.

According to this, the procedure involves three main steps:

PART I: Determining the rotations and displacements of the mechanism.

PART II: Calculating the internal forces

PART III: With the expression of total work, calculating the *upper bound of the maximum vertical load*.

#### PART I – DETERMINING ROTATIONS AND DISPLACEMENTS OF THE MECHANISM

- 1) The mechanism to be analyzed is defined. For a vertical load applied in the center of the arch a three-hinges in arch and two-hinges in buttresses mechanism is selected. The hinges are located in the arch and buttresses dividing the structure in four blocks. The hinges in the support of the buttresses will not have displacements and the hinge in the center of the arch, where the load is applied, will only have a vertical displacement. The other two hinges will have horizontal and vertical displacements.

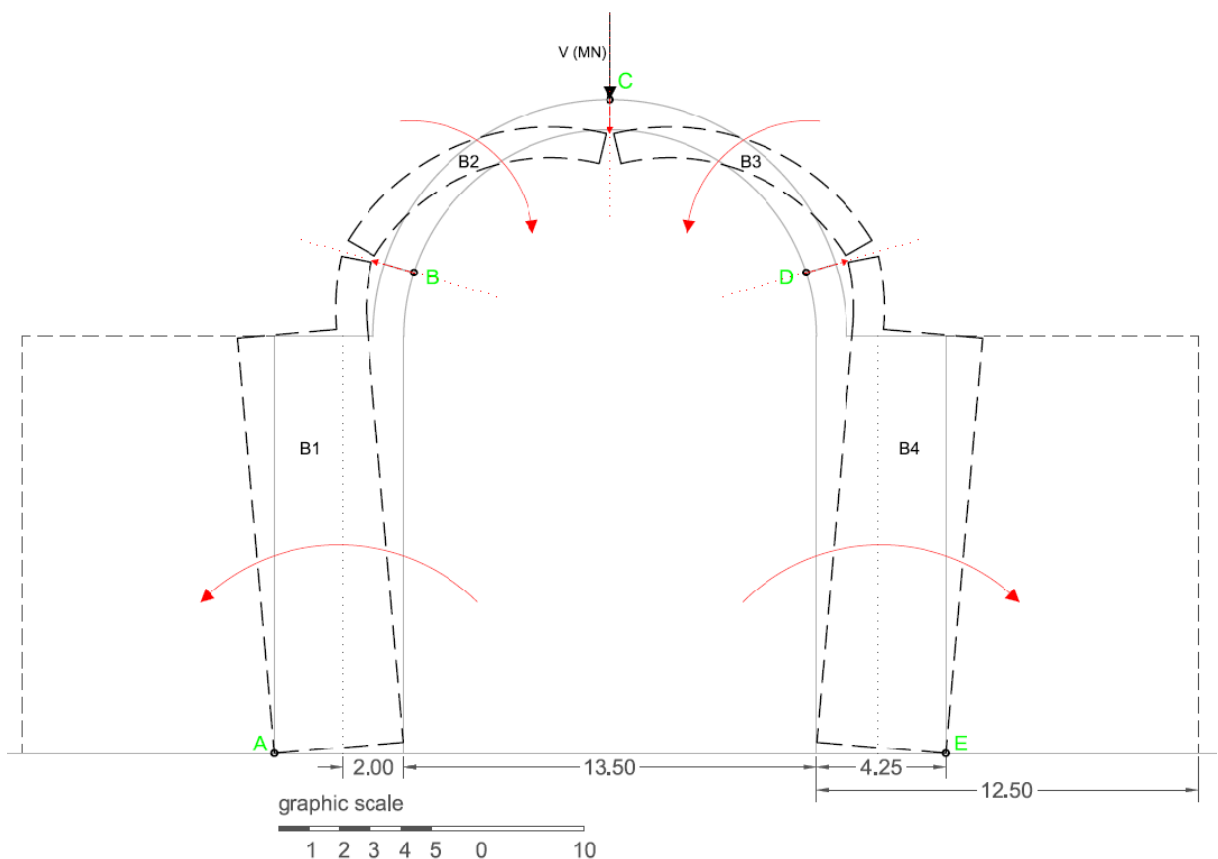


Fig. 41 - Identification of the movement of each block for the defined mechanism

2) The sign criterion is defined for displacements and forces.

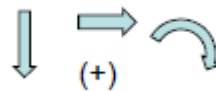


Fig. 42 – Sign criteria.

3) Each block will have a corresponding center of rotation. Lines are drawn connecting the hinges without displacements (A and E), which correspond to the center of rotations  $C_1$  and  $C_4$ , with the consequent hinges (B and D). The location of hinges B and D was defined arbitrarily (B in voussior N°4 and D in voussior N°37, with the arch divided in 40 voussiors). These lines are perpendicular to the directions defined by the displacements of the extreme hinges that define each block ( $B_1$  and  $B_4$ ). With the same criteria, knowing that the displacement of the central blocks ( $B_2$  and  $B_3$ ) in the hinge C will have only a vertical component, a line is drawn perpendicular to this direction passing through hinge C. The intersection between this line and the line connecting hinges A and B will be the center of rotation  $C_2$ . By symmetry, the intersection of the line connecting hinges E and D, with the perpendicular line to the displacement of hinge C, will correspond to the center of rotation  $C_3$ .

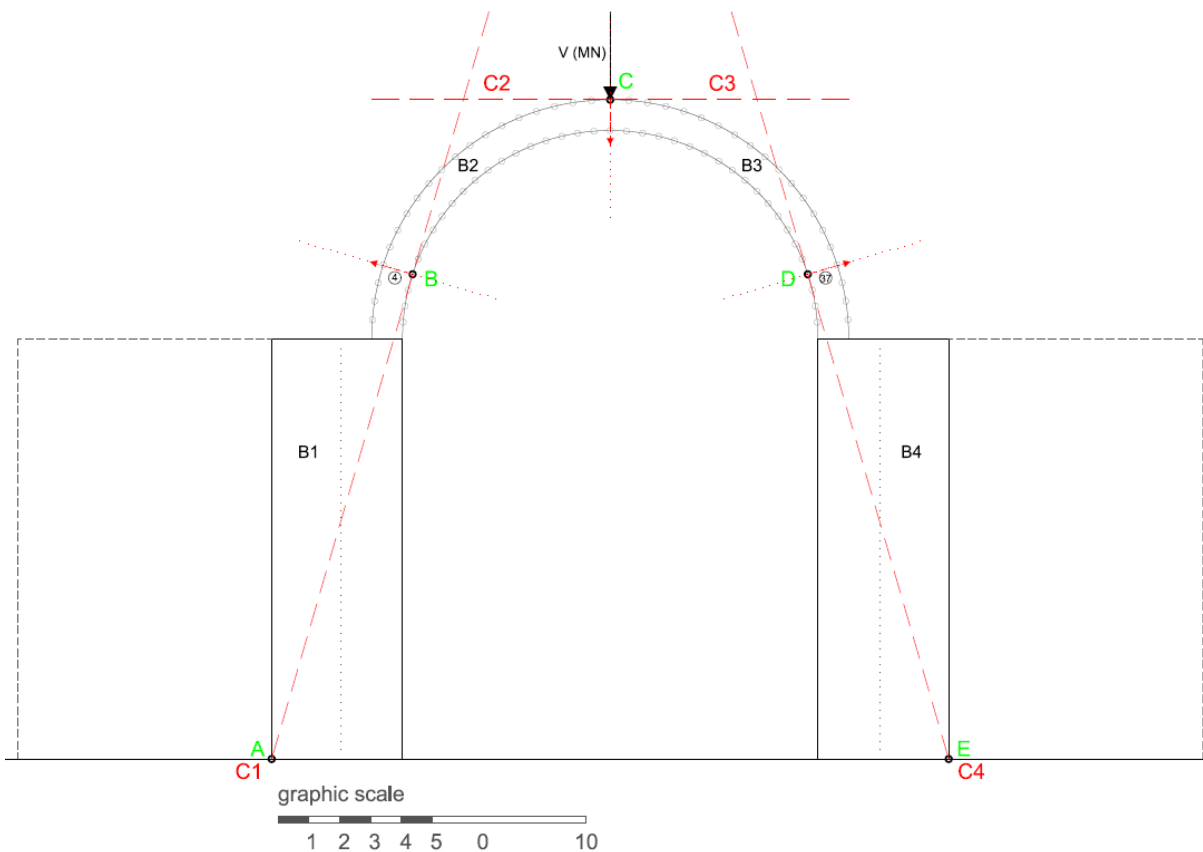


Fig. 43 - Location of rotation centers for the four blocks in a symmetrical five-hinge collapse mechanism in arch  
 For this mechanism only the original buttresses have been considered (a width of 4.25), not the additions. Therefore the following images will only show the original structure.

- 4) The rotations and displacements are identified in the mechanism and correlated with the hinges and centers of rotation.

$\delta_B$  = perpendicular displacement of hinge B to the line connecting centers of rotation  $C_1 - C_2$ .

$\delta_C$  = vertical displacement of hinge C. The perpendicular line to this vector connects centers of rotation  $C_2 - C_3$ .

$\delta_D$  = perpendicular displacement of hinge D to the line connecting centers of rotation  $C_3 - C_4$ .

$L_{1B}$  = Distance between center of rotation  $C_1$  and hinge B.

$L_{2B}$  = Distance between center of rotation  $C_2$  and hinge B.

$L_{2C}$  = Distance between center of rotation  $C_2$  and hinge C.

$L_{3C}$  = Distance between center of rotation  $C_3$  and hinge C.

$L_{3D}$  = Distance between center of rotation  $C_3$  and hinge D.

$L_{4D}$  = Distance between center of rotation  $C_4$  and hinge D.



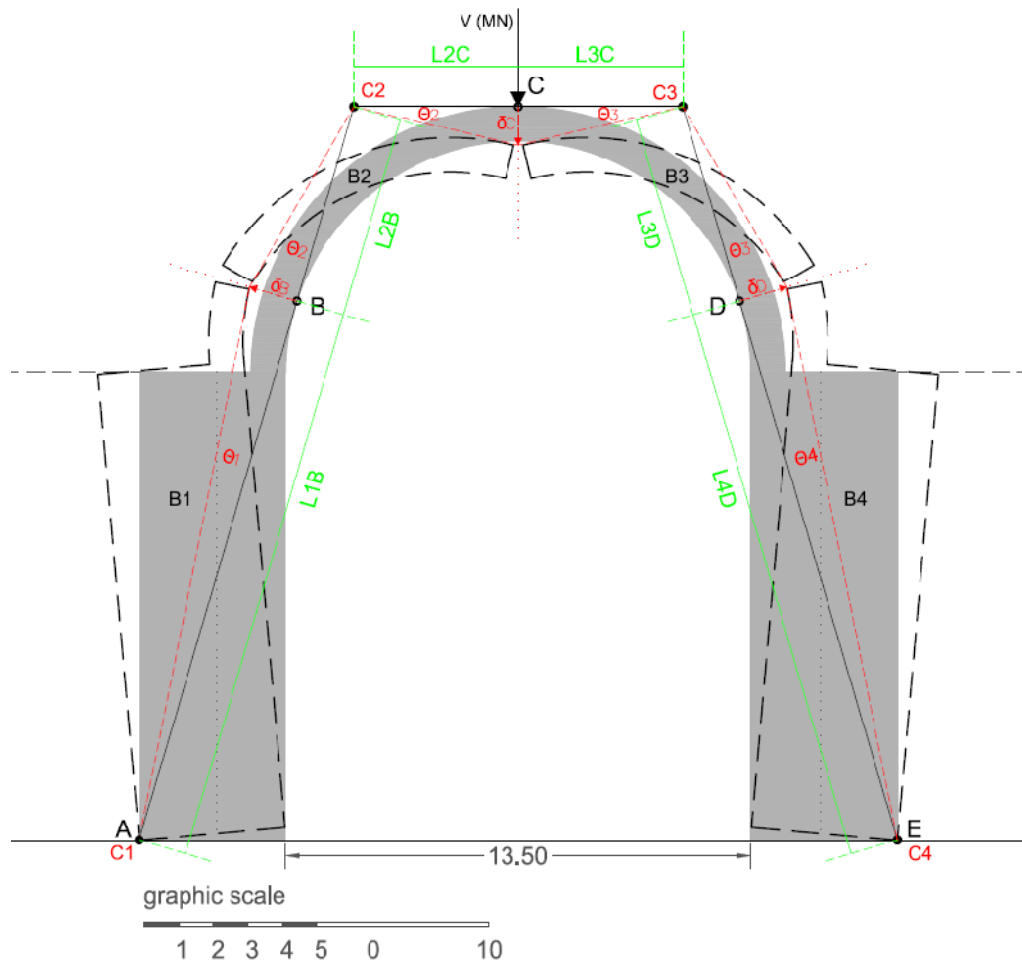


Fig. 44 - Identification of the rotations, displacements and correlations with the hinges and centers of rotation.

5) The angles according to the sign criteria will be as following:

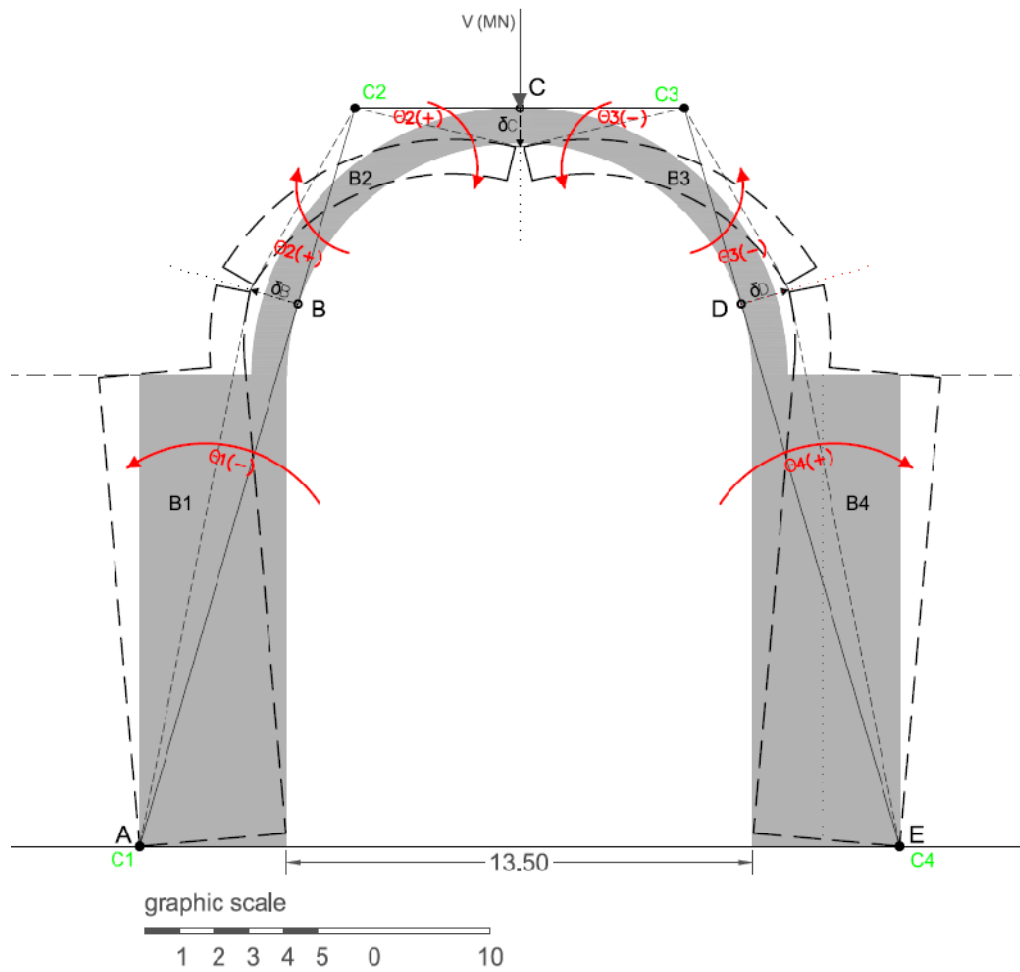


Fig. 45 - Identification of the signs of the angles of rotation of the blocks.

Once the mechanism has been established, the first step is defining the first angle of rotation. This value is decided arbitrarily ( $\theta_1$ ) and all the displacements and rotations will depend on it.

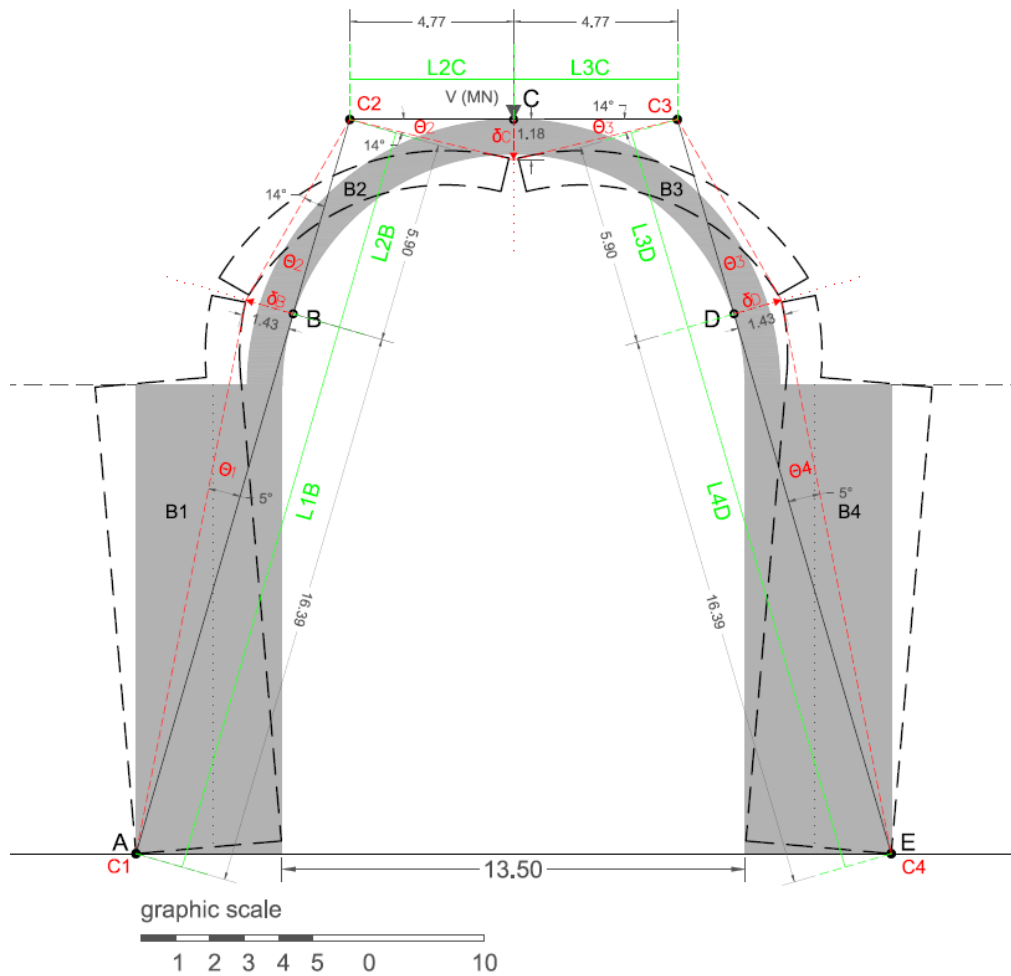


Fig. 46 - Displacements and rotations determined in sequence according to the following procedure.

In order to perform the calculations, the relationships between rotations, displacements are established in a sequence from defining  $\Theta_1$ , and according to the sign criteria previously defined:

$$\delta_B = \Theta_1 * L_{1B} = -\Theta_2 * L_{2B} \quad \longrightarrow \quad -\Theta_1 * L_{1B} / L_{2B} = \Theta_2$$

$$\delta_C = -\Theta_2 * L_{2C} = \Theta_3 * L_{3C} \quad \longrightarrow \quad -\Theta_2 * L_{2C} / L_{3C} = \Theta_3$$

$$\delta_D = \Theta_3 * L_{3D} = -\Theta_4 * L_{4D} \quad \longrightarrow \quad \Theta_3 * L_{3D} / L_{4D} = \Theta_4$$

The procedure was as following:

- 1) Define an angle of rotation ( $\Theta_1$ ) from the first hinge - A (first point of rotation -  $C_1$ ). Draw a perpendicular line from the second hinge-B to the new rotated line. This line segment corresponds to the displacement of hinge-B ( $\delta_B$ ) which is the new location of the second hinge.

This value ( $\delta_B$ ) is also verified analytically by:  $\delta_B = \Theta_1 * L_{1B}$ , where  $L_{1B}$  is the distance between the first point of rotation- $C_1$  and hinge-B.

**Assume  $\Theta_1$  (in radians):** **$\Theta_1$  (degrees)     $\Theta_1$  (radians)**

-5                    -0.09

**Determine  $\delta_B$  (displacement of point B) from  $\Theta_1$** 

$$\delta_B = \Theta_1 * L_{1B}$$

 **$\Theta_1$  (rad)             $L_{1B}$  (meters)     $\delta_B$  (meters)**

-0.09                16.39                -1.43                1.43 (verification in autocad)

- 2) The angle  $\Theta_2$  is found by connecting the new point of displacement of hinge-B given by  $\delta_B$ . Analytically this value is obtained (therefore verified) from the expression

$\Theta_2 = (-L_{1B}/L_{2B}) * \Theta_1$ . Where  $L_{2B}$  is the distance between hinge-B and the second point of rotation -  $C_2$ . This expression is obtained from the following equivalence:

$$\delta_B = \Theta_1 * L_{1B} = -\Theta_2 * L_{2B}$$

**Determine  $\Theta_2$  (rad) from  $\Theta_1$** 

$\Theta_2 = (-L_{1B}/L_{2B}) * \Theta_1$  this formula comes from  $\delta_B = \Theta_1 * L_{1B} = -\Theta_2 * L_{2B}$

 **$\Theta_1$  (rad)             $L_{1B}$  (meters)     $L_{2B}$  (meters)     $\Theta_2$  (rad)             $\Theta_2$  (degrees)**

-0.09                16.39                5.90                0.24                13.89

- 3) The displacement of the hinge-C is found with the expression  $\delta_C = -\Theta_2 * L_{2C}$  where  $L_{2C}$  is the distance between the second point of rotation -  $C_2$  and hinge-C.

**Determine  $\delta_C$  (displacement of point C) from  $\Theta_2$** 

$$\delta_C = -\Theta_2 * L_{2C}$$

 **$\Theta_2$  (rad)             $L_{2C}$  (meters)     $\delta_C$  (meters)**

0.24                4.77                -1.16                1.18 (verification in autocad)

- 4) The angle  $\Theta_3$  is obtained from the expression  $\Theta_3 = -\Theta_2 * (L_{2C}/L_{3C})$

**Determine  $\Theta_3$  (rad) from  $\Theta_2$** 

$\Theta_3 = -\Theta_2 * (L_{2C}/L_{3C})$  in this example  $L_{2C} = L_{3C}$

 **$L_{2C}$  (meters)     $L_{3C}$  (meters)     $\Theta_2$  (rad)             $\Theta_3$  (rad)             $\Theta_3$  (degrees)**

4.77                4.77                0.24                -0.24                -13.89

- 5) The displacement of the hinge-D is found with the expression  $\delta_D = \Theta_3 * L_{3D}$  where  $L_{3D}$  is the distance between the third point of rotation -  $C_3$  and hinge-D.

**Determine  $\delta_D$  (displacement of point D) from  $\Theta_3$**

$$\delta_D = \Theta_3 * L_{3D}$$

$\Theta_3$ (rad)	$L_{3D}$ (meters)	$\delta_D$ (meters)	
-0.24	5.90	-1.43	1.43(verification in autocad)

- 6) The angle  $\Theta_4$  is obtained from the expression  $\Theta_4 = -\Theta_3 * (L_{3D}/L_{4D})$

**Determine  $\Theta_4$  (rad) from  $\Theta_3$**

$$\Theta_4 = -\Theta_3 * (L_{3D}/L_{4D}) \text{ in this example } L_{4D} = L_{1B}$$

$L_{3D}$ (meters)	$L_{4D}$ (meters)	$\Theta_3$ (rad)	$\Theta_4$ (rad)	$\Theta_4$ (degrees)
5.90	16.39	-0.24	0.09	5.00

The following equivalences have been verified graphically and analytically:  $\Theta_1 = -\Theta_4$ ;  $\Theta_2 = -\Theta_3$ .

Considering that for calculating the work performed by the weight-force of each block a displacement has to be defined.

$$\text{Work} = \text{Force} * \text{Displacement}$$

Work (block-i) = Weight-force resultant located in the centroid of block ( $V_i$ ) \* angle of rotation of block ( $\Theta_i$ ) \* horizontal component of the distance between the center of rotation of the block and the centroid of the initial block ( $X_{ci}$ ),

Or,

Work (block-i) = Weight-force resultant located in the centroid of block ( $V_i$ ) \* vertical component of the distance between the centroids of the initial and rotated blocks ( $\delta_{iy}$ ).

- 7) For the work of internal vertical forces, measure the horizontal component ( $X_{ci}$ ) of the distance between the center of rotation of the block and the centroid of the initial block. Take into account the signs taking as reference the location of the center of rotation (starting point).
- 8) Multiply  $X_{ci}$  with the angle of rotation of the block to obtain the VERTICAL component ( $\delta_{iy}$ ) of the distance between the centroids of the initial and the rotated blocks.  $\delta_{iy}$  will be the "arm" that multiplied by the weight-force (vertical internal resultant force) gives the value of the WORK for the block.

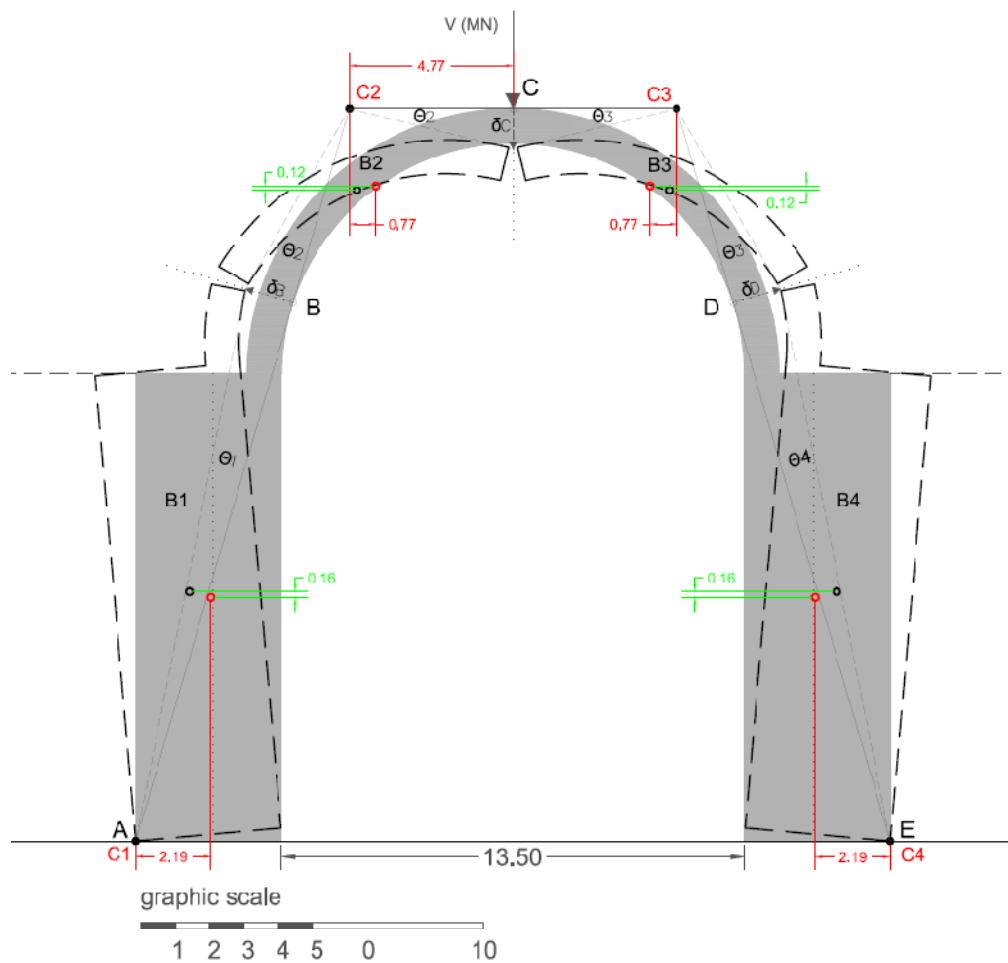


Fig. 47 - Measuring the horizontal component distance from centroid of initial block to rotation center, and distance from point of application of the external vertical force  $V$  to the nearest centroid (in red). Measuring the vertical component distance between the centroids of the initial and the rotated blocks (in green).

#### BLOCK 1

$\Theta_1$ (rad)	$X_{c1}$	$\delta_{1y}$	
-0.09	2.19	-0.19	0.16 (verification of $\delta_{1y}$ measuring from drawing)

#### BLOCK 2

$\Theta_2$ (rad)	$X_{c2}$	$\delta_{2y}$	
0.24	0.77	0.19	0.12 (verification of $\delta_{1y}$ measuring from drawing)

#### BLOCK 3

$\Theta_3$ (rad)	$X_{c3}$	$\delta_{3y}$	
-0.24	-0.77	0.19	0.12 (verification of $\delta_{1y}$ measuring from drawing)

#### BLOCK 4

$\Theta_4$ (rad)	$X_{c4}$	$\delta_{4y}$	
0.09	-2.19	-0.19	0.16 (verification of $\delta_{1y}$ measuring from drawing)

PART II – CALCULATING THE INTERNAL FORCES

Considering that the buttresses and walls supporting the arch have a “T” section in plan view, this will be the area considered for part corresponding to the buttresses in blocks 1 and 4. Therefore the width considered to calculate the volume will be the height of the buttresses and walls. For calculating volume of the arches (or the part of arch belonging to blocks 1 and 4), the area considered is taken from the section view and the width corresponds to the length of the vault assumed (10 meters in this case).

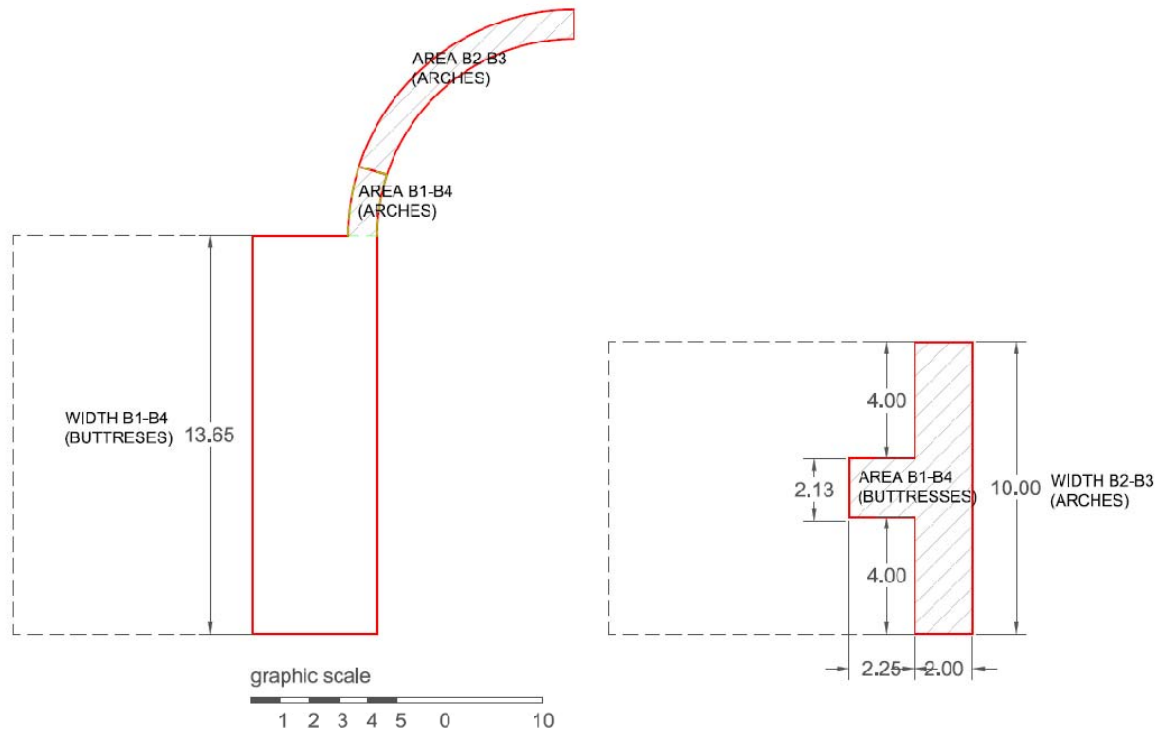


Fig. 48 – Areas and widths considered for calculating the volume of arches and buttresses.

	Density (kN/m <sup>3</sup> )	Width (meters)	Area (m <sup>2</sup> )	Weight (kN)	Scaled force (1m=1MN)
<b>B1</b>		10	2.26		
<b>(arch – butt)</b>	15.69	13.65	24.50	5602.07	5.60
<b>B2 (arch)</b>	15.69	10	9.13	1431.89	1.43
<b>B3 (arch)</b>	15.69	10	9.13	1431.89	1.43
<b>B4</b>		10	2.26		
<b>(arch – butt)</b>	15.69	13.65	24.50	5602.07	5.60

PART III - CALCULATING THE UPPER BOUND OF THE MAXIMUM VERTICAL LOAD.

W (work)

w (weight force)

P (force applied in 1/4 of span)

$W_i + W_e = 0$  (Internal work + External work in equilibrium)

$W = F \cdot \delta$  (Work can be expressed as a force \* displacement/rotation)

$$W_i = (w_1 \cdot \delta_{1y} + w_2 \cdot \delta_{2y} + w_3 \cdot \delta_{3y} + w_4 \cdot \delta_{4y})$$

$$W_e = P \cdot \delta_{py}$$

$$(w_1 \cdot \delta_{1y} + w_2 \cdot \delta_{2y} + w_3 \cdot \delta_{3y} + w_4 \cdot \delta_{4y}) + (P \cdot \delta_{py}) = 0$$

$$P = -(w_1 \cdot \delta_{1y} + w_2 \cdot \delta_{2y} + w_3 \cdot \delta_{3y} + w_4 \cdot \delta_{4y}) / \delta_{py}$$

P can be expressed as:

$$\lambda P = -(w_1 \cdot \delta_{1y} + w_2 \cdot \delta_{2y} + w_3 \cdot \delta_{3y} + w_4 \cdot \delta_{4y}) / \delta_{py}$$

$$\delta_{py} = \theta \cdot X_p$$

Determine  $\delta_{py}$ : vertical displacement point of application of force P due to rotation of the block where the force is applied: in this example is  $\Theta_2$ .

$$\delta_{py} = \Theta_2 \cdot X_p \quad X_p: \text{Horizontal distance from rotation center to external vertical load applied}$$

**$\Theta_2$  (rad)  $X_p$  (meters)  $\delta_{py}$  (meters)**

0.24            4.77            1.16    1.18 (verification measured in drawing)

Determine  $\lambda$  (Factor load) for a given P (assumed)

$$\lambda = -(w_1 \cdot \delta_{1y} + w_2 \cdot \delta_{2y} + w_3 \cdot \delta_{3y} + w_4 \cdot \delta_{4y}) / P \cdot \delta_{py}$$

w1 (KN)	$\delta_{1y}$ (M)	w2 (KN)	$\delta_{2y}$ (M)	w3 (KN)	$\delta_{3y}$ (M)	w4 (KN)	$\delta_{4y}$ (M)	$\delta_{py}$ (M)	<b>P (KN)</b>	<b><math>\lambda</math></b>
5602.07	-0.19	1431.89	0.19	1431.89	0.19	5602.07	-0.19	1.16	1	1387.31

Table 5 - Load Factor table from Excel©

Comparing the results obtained from the mechanism-1 (five-hinges in arch) with mechanism-2 (three-hinges in arch and two-hinges in buttresses):

#### FAILURE LOAD FACTOR

<b>Mechanism-1</b>	<b>Mechanism-2</b>
<b>315.22</b>	<b>1387.31</b>

From the upper bound values obtained, the minimum is selected in order to do the static approach:  
**315.22 (mechanism-1).**



### 3.2.2 Static Approach

The objective was finding a thrust line that passes through the hinges for the mechanism that gave the lower Load Value. Therefore the value to be considered for the static approach will be a reduced value from 315.22 kN.

#### 3.2.2.1 5 hinges in arch (no contribution of buttresses)

A reduction of 3% is proposed for the maximum load value obtained for the mechanism of five-hinges in arch without contribution of the buttresses. Therefore the vertical load applied in the center of the arch will be: **305.76 kN**.

#### GENERAL ASPECTS

The objective is verifying if a thrust line can be found that passes through the five hinges defined for the mechanism in isolated arch previously for the specified vertical load.

The structure to be analyzed is evaluated considering the equilibrium equations.

The number of available equations is three:

- 1- Sum of the vertical forces equal to zero
- 2- Sum of the horizontal forces equal to zero
- 3- Sum of the moments equal to zero

To define the VECTOR, three properties must be defined:

- 1- Entity (magnitude)
- 2 - Direction
- 3 - Position

#### PROCEDURE USING CAD

- 9) Draw the geometry of the structure.
- 10) The structure is discretized into segments segments (voussoirs in arches). The more amount of segments the structure is divided in, the “smoother” the thrust-line obtained will be. However, doing graphic statics “by hand” can be tedious with too many divisions. An intermediate consideration is then taken into account. Recommendation: Put a number to identify each segment in order to have a guide when constructing the force polygon.
- 11) Find and locate force-weight vector for each segment. This example has only one material (this is one of the differences with the Bridgemill Bridge example).
  - Find the area of each part of the segment.

- From <DRAW> use the command <BOUNDARY> to create an "object" (polyline).
- Use the command <area> to obtain the value in  $m^2$
- Find the volume of each part of the segment by multiplying the obtained areas with the width/thickness of the structural element.
- To obtain the weight for each part of each segment, multiply the given density value ( $kN/m^3$ ) to the corresponding volume.
- Find centroid coordinates for each segment
  - From <DRAW> use the command <REGION> by selecting the created "object" previously.
  - Use the command <MASSPROP> to obtain the x,y coordinates of the centroid for each part of the segment.
- Locate each centroid of segment:
  - Use <POINT> to draw a reference in each segment by giving the coordinates obtained before.
- Locate the weight-force (kN)
  - Define a scale for drawing the weight-force values (kN) represented as a dimension value (m). For example: 1 M = 250 kN.
  - Draw the <LINE> with the scaled magnitude in meters representing the weight-force (kN) with the starting point in the centroid of each corresponding segment.

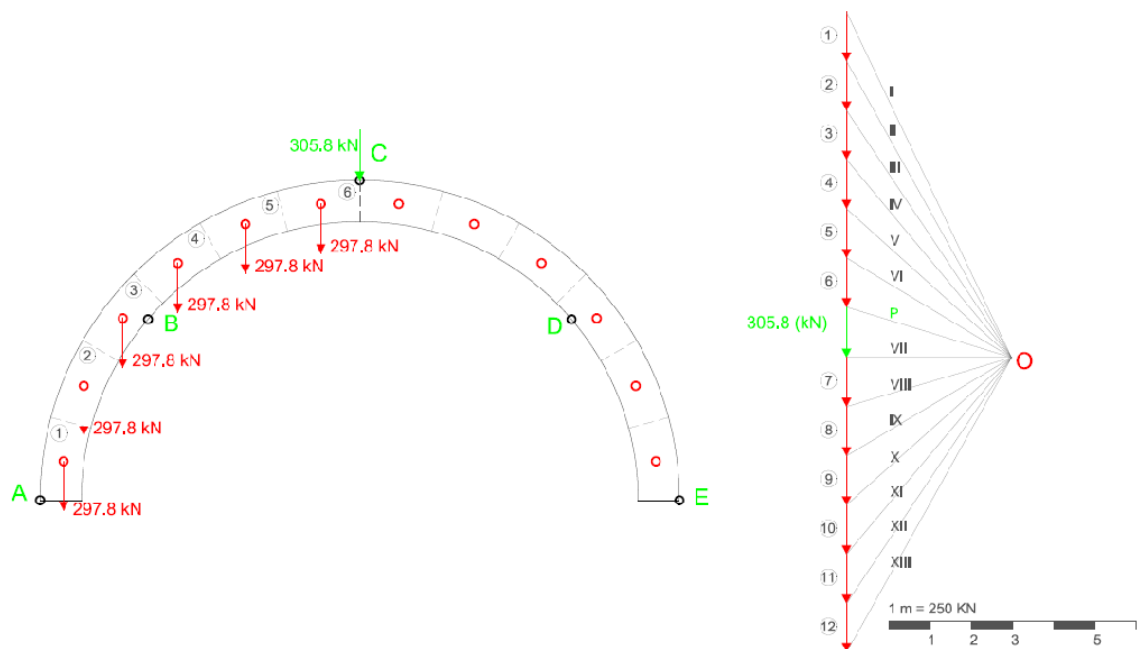


Fig. 49 – Discretization of arch, location of centroids and vertical forces.

12) Define the live weight

- Determine the location of the resultant live weight to be considered.

For this example the vertical load applied in the center of the span has been obtained from the kinematic analysis.

13) Apply STATIC GRAPHIC to calculate de <RESULTANT FORCE>

- To find the **magnitud** and **direction** of the <RESULTANT FORCE>: Sum in order of appearance the weight-forces (sum as vectors).
- To find the **position** of the <RESULTANT FORCE>:
  - Define an "origin" next to the summed force vectors
  - Draw ray-lines from the start and end of each individual force vectors: This will form a FORCE POLYGON
  - Take each ray-line (keeping its direction) and locate one of its ends intersecting the reference line of each corresponding weight-force vector in the analyzed structure: This will form a FUNICULAR POLYGON
  - Sum the two ray-line vectors of each extreme in the FUNICULAR POLYGON (sum of vectors): The position of the RESULTANT FORCE (with magnitude and direction that was found before), is achieved.

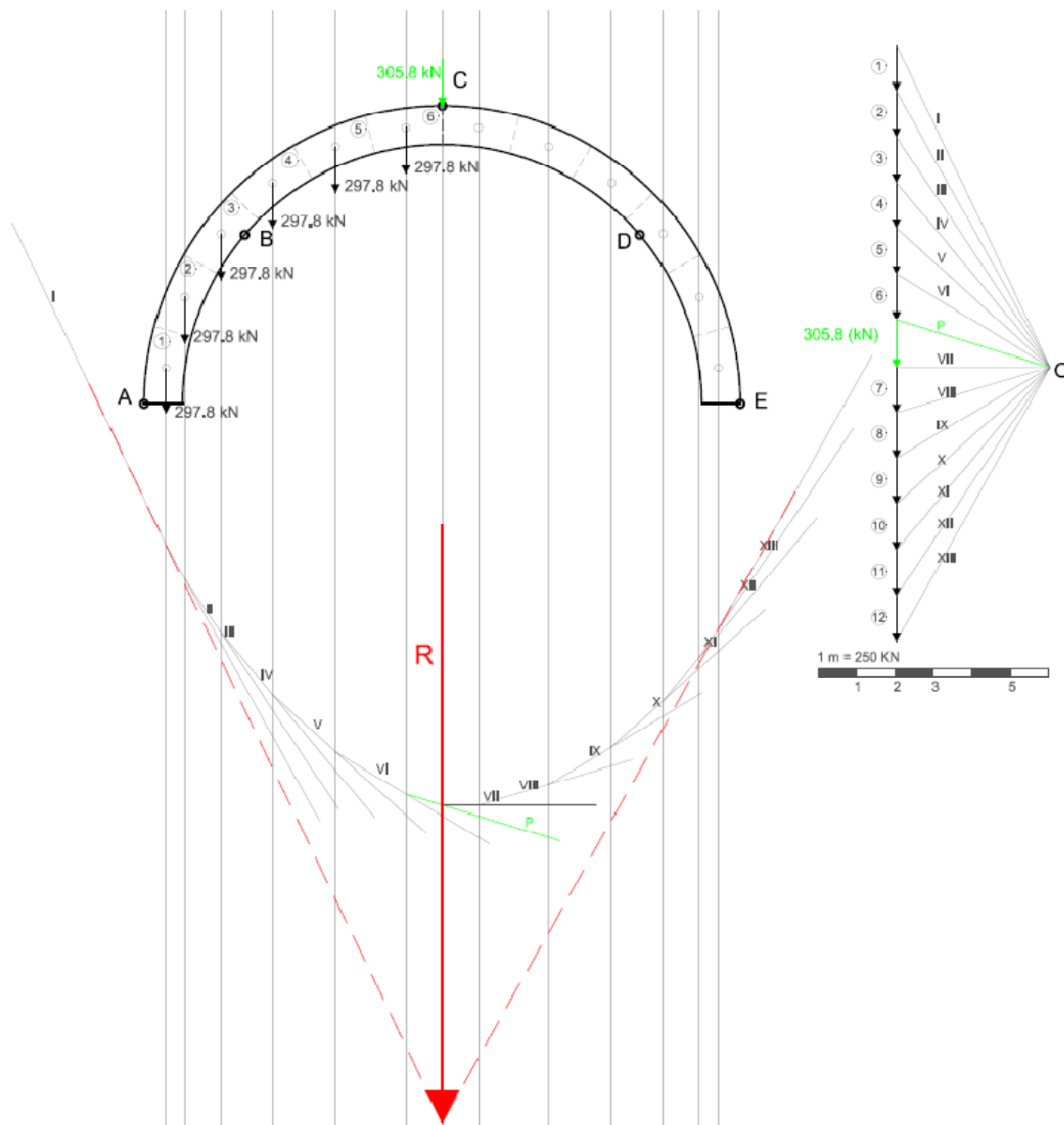


Fig. 50 - Funicular polygon and resultant force

14) Considering that this case has of application of the STATIC APPROACH has been defined with the objective of finding a thrust line for the evaluated mechanism in the KINEMATIC APPROACH, three hinges are selected as the fixed points.

- Three fixed points (hinges) are selected and referenced to the funicular polygon.
  - Reference lines are draw (A` and B`= connecting the hinges and projected over the funicular polygon.
  - Reference lines are draw (A and B) connecting the three points projected from the location of the hinges on the funicular polygon.

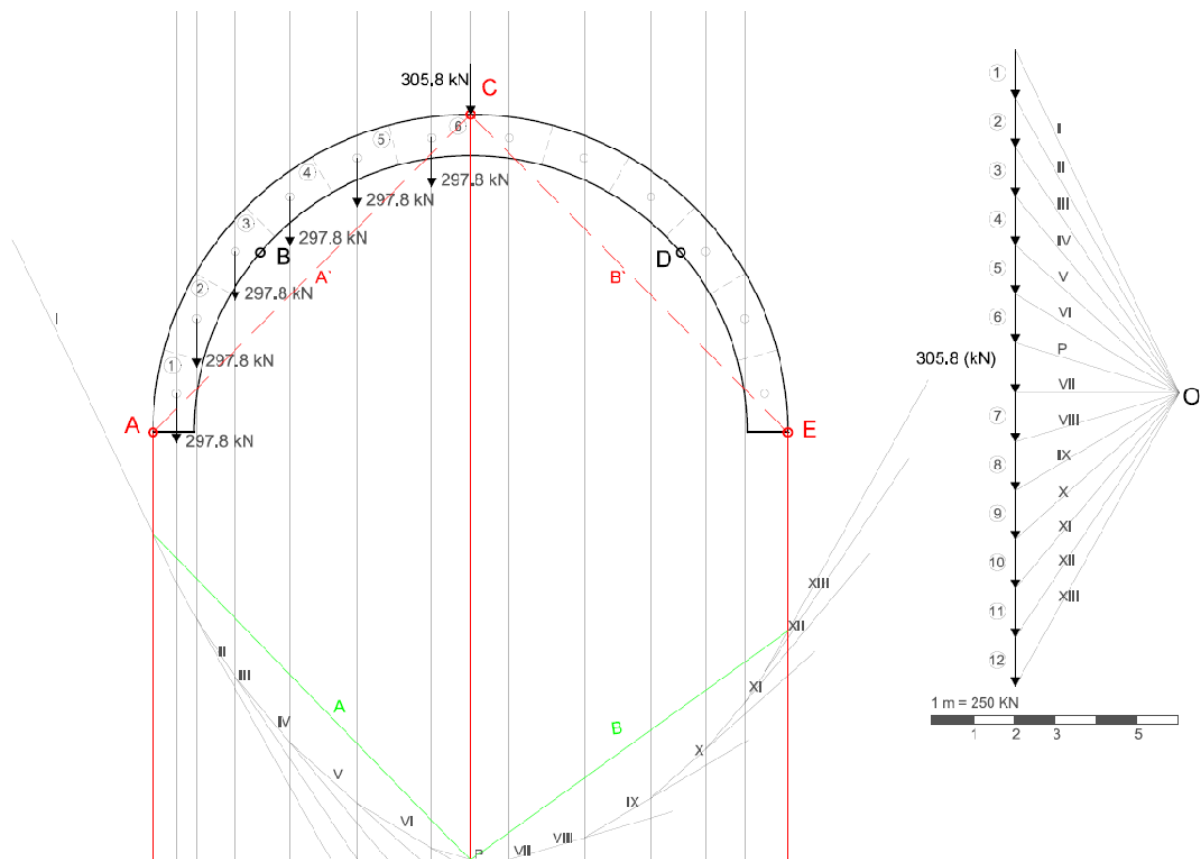


Fig. 51 - Selection of three hinges for the thrust line to pass through and projection on the funicular polygon.

- 15) Reference lines are used to define the location of a new origin ( $O'$ ) defining the rays to build the force polygon.
- 16) Draw the THRUST LINE. With the "new origin" ( $O'$ ) defined, the force polygon is constructed over the arch. Each line from origin -  $O'$  to each force, is relocated to cross the reference lines of the centroids of each segment of the arch. A sum is vector occurs as each resultant force is summed with the vertical force located in each centroid, defining the new location of the consequent resultant.

For this example a thrust line has been found passing through ALL (5) the hinges of the defined mechanism. With the kinematic approach performed, the upper bound of the vertical load was verified.

In conclusion, for this example the UNIQUENESS THEOREM has been verified as *"a thrust line has been found causing as many hinges as needed to develop a mechanism"*. Therefore, for this example, the load evaluated *"is the true ultimate load, the mechanism is the true ultimate mechanism, and the thrust line is the only possible one"*. (Roca, Ancient Rules and Classical Approaches- Part 1-4. SA1 Lectures., 2009-2010)

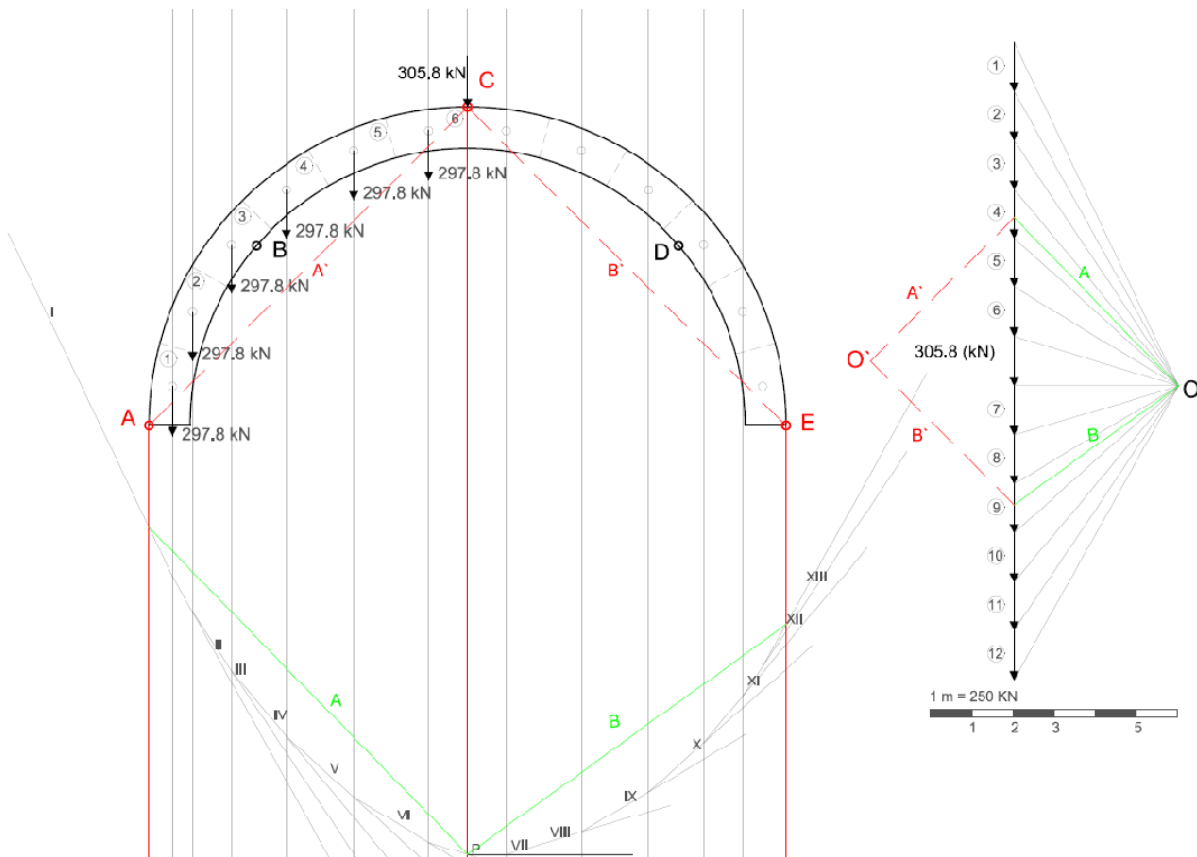


Fig. 52 - Defining the new origin for the force polygon.

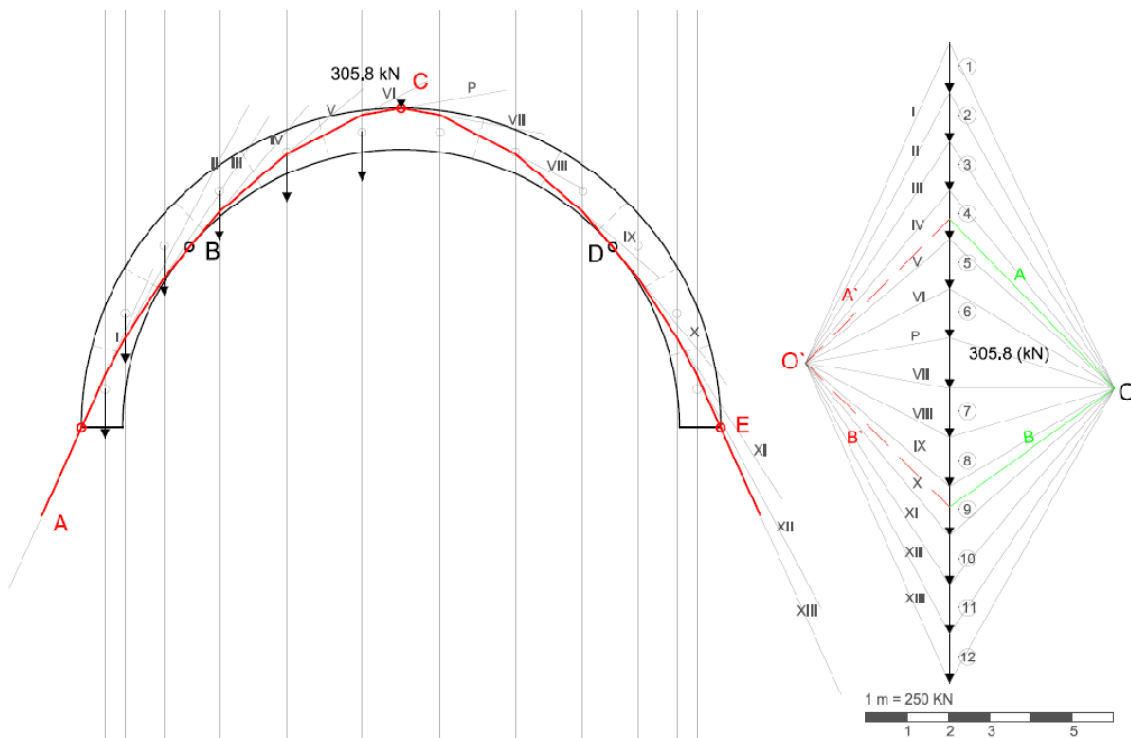


Fig. 53 – A thrust line passing through ALL hinges is found inside the arch.

### 3.3 Multiple span one level arch façade (Plaça Reial in Spain)

The Plaça Reial (“Royal Plaza” in English) is a square located in the Gothic neighborhood of the city of Barcelona in Spain, designed by the catalan architect Francesc Daniel Molina i Casamajó (1812 – 1867). The project was developed during the years 1848 – 1859 and constitutes an example of a traditional Spanish *plaza mayor* (principal square) with a ground floor façade with a sequence of arches. (archINFORM)



Fig. 54 – Façade with series of arches in the Plaça Reial. (La Plaça Reial)



Fig. 55 – Aerial view Plaça Reial. (Aero-plano)



Fig. 56 – View of the arches. (Alcolea Antigüedades)

In this example, the objective was analyzing the stability of one of the arches located at the end of one of the buildings of the Plaça Reial. Two arches were initially observed as target, one inside the square and the other one at the end of the carrer de Colom (street connecting the Ramblas with the Plaça Reial).



Fig. 57 – Arch in corner of Plaça Reial.



Fig. 58 – Arch in corner of Carrer de Colom



The arch located in the corner of the Ramblas with the Carrer de Colom was selected taking into account it had a less dimension in the width of the external buttress for the same height of building.

Width of external buttress of arch inside Plaça Reial: 2.50 meters

Width of external buttress of arch in Carrer de Colom: 1.20 meters

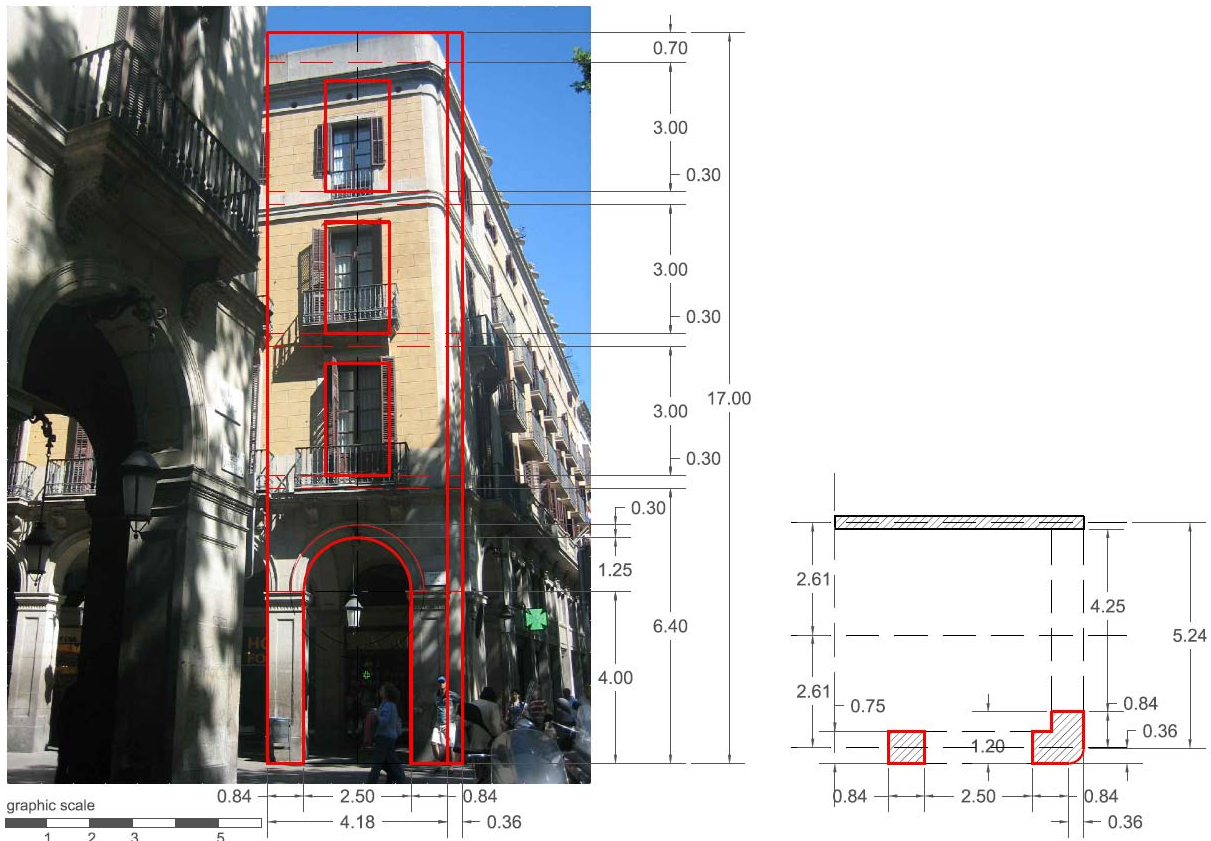


Fig. 59 - Geometry of last arch in carrer de Colom.

Considering the buttress depth of the selected external arch, an example was performed to observe if Blondel's Rule was applied and the result obtained was less than the real dimension.

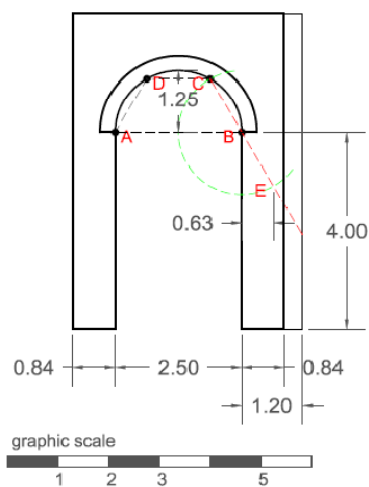


Fig. 60 – Blondel rule applied to the external buttress of the last arch.



### 3.3.1 Static Approach

The application of Limit Analysis to this case study consists in the evaluation of the stability of the external buttress of the last arch in a series of multiple arch façade. The Static Approach was used. The main differences with the Roman Aqueduct of Tarragona (Devil's Bridge) will consist in the fact that the buttress in this case must withstand the horizontal thrust generated by the arch. In Devil's Bridge the buttress analyzed was in a middle section, therefore the horizontal thrusts generated by the arches in each side were equilibrated. In the arch in Plaça Reial the width of the buttress must be enough. Other differences rely in the type of loads considered, as in Plaça Reial the contribution of the slabs and a use overload were taken into account.

The case is the last arch and buttress in a series of arches façade. Using the static approach, a thrust line is found for the permanent and live loads the arch and external buttress are supporting.

#### GENERAL ASPECTS

The objective is verifying if a thrust line can be found that passes through three defined hinges for the calculated vertical load.

The structure to be analyzed is evaluated considering the equilibrium equations.

The number of available equations is three:

- 1- Sum of the vertical forces equal to zero
- 2- Sum of the horizontal forces equal to zero

To define the VECTOR, three properties must be defined:

- 1- Entity (magnitude)
- 2 - Direction
- 3 - Position

#### PROCEDURE USING CAD

- 1) Draw the geometry of the structure.
- 2) Considering that the structure to be evaluated (last arch and external buttress in ground level) is supporting three stories, the weight forces for permanent and live loads are calculated. The permanent loads considered are the façade walls and the slabs. A horizontal slab is considered for all the floors including the first level even though in reality, for this level, it corresponds to vaults. This is done taking into account no information was available concerning the geometry (rise of the vault) or for determining if the vault is structural or not. In order to simplify the analysis, all the slabs were assumed equal.

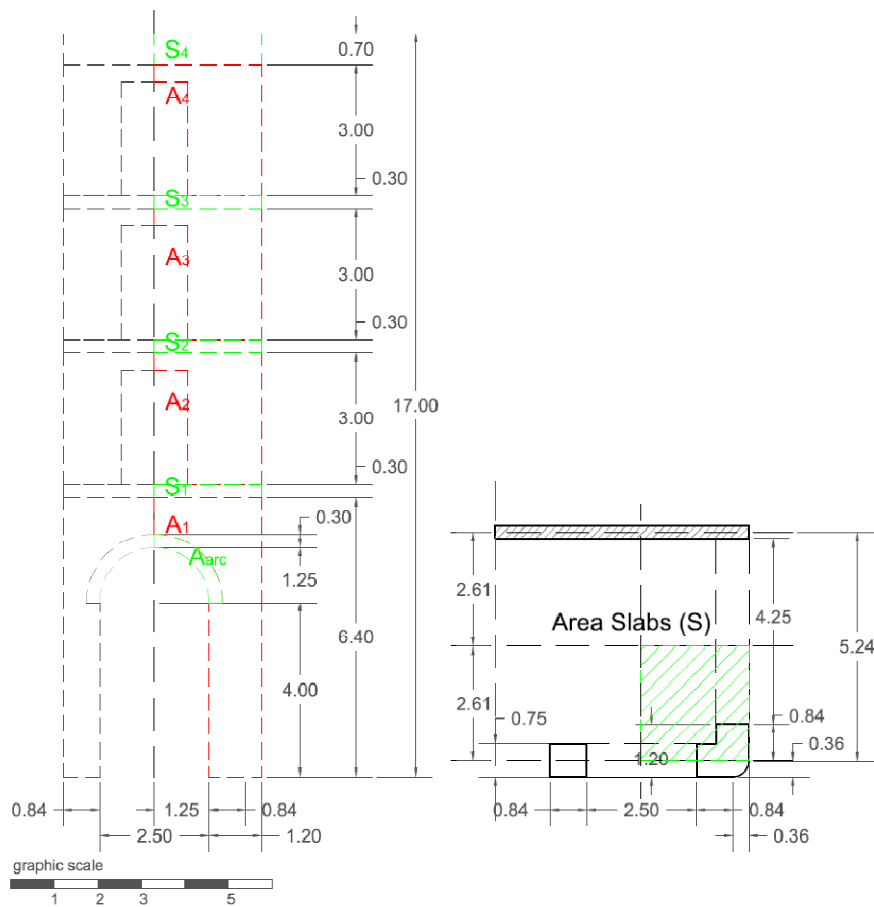


Fig. 61 - Vertical and horizontal areas for calculating the permanent and live loads.

**Material (structural)  
walls upper levels**

 Unit weight ( $\text{kN/m}^3$ ): 18

Thickness (M): 0.3

**Material (Structural)  
slabs**

 Unit weight ( $\text{kN/m}^2$ ): 3.5

**Live loads (on slabs)**

 Unit weight ( $\text{kN/m}^2$ ): 2

**Sum of the loads calculated for each level**

	Area ( $\text{m}^2$ )	weight (kN)	
$S_4$	6.40	22.40	
$L_{S4}$	6.40	12.80	live load
$A_4$	5.40	29.16	
$S_3$	6.40	22.40	
$L_{S3}$	6.40	12.80	live load
$A_3$	5.40	29.16	
$S_2$	6.40	22.40	
$L_{S2}$	6.40	12.80	live load
$A_2$	5.40	29.16	
$S_1$	6.40	22.40	

**Total weight applied on half of the structure**
**Distributed load on half of the structure:**

Length structure: 2.45 m  
 Distributed load: 93.18  $\text{kN/m}$

**Point load per segments type-1 ( $V_1$ ):**

Length per segment: 0.42 m  
 Point load per segment: 38.83 kN

**Point load per segment type-2 ( $V_2$ ):**

Length per segment: 1.20 m  
 Point load per segment: 111.82 kN

$L_{S1}$	6.40	12.80	live load
<b>Total weight:</b>		<b>228.29</b>	<b>kN</b>

Table 6 – Loads above the half of the arch and buttress analyzed.

- 3) The structure is discretized into segments. The more amount of segments the structure is divided in, the “smoother” the thrust-line obtained will be. However, doing graphic statics “by hand” can be tedious with too many divisions. An intermediate consideration is then taken into account. Recommendation: Put a number to identify each segment in order to have a guide when constructing the force polygon. The total weight over the level of the arch and buttress being analyzed that was calculated is located as point loads on the centroid axis of each of the segments in which the structure has been divided.

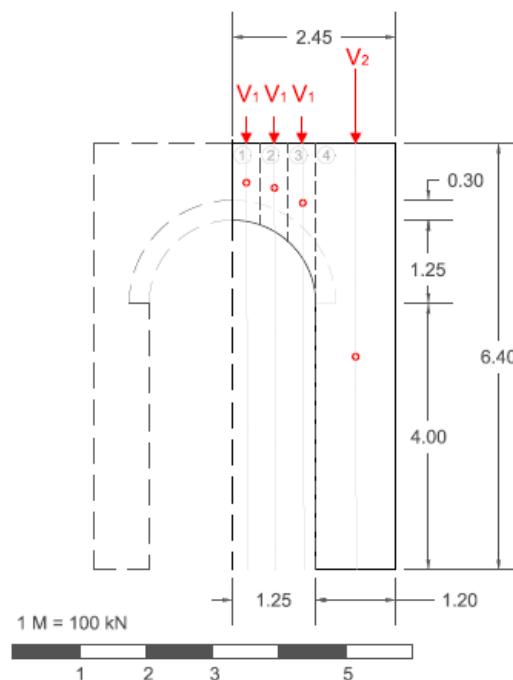


Fig. 62 - Permanent and live loads applied on each segment as point loads.

- 4) Find and locate force-weight vector for each segment. Considering that the arch and the infill over it are from the same material, the loads are calculated together. The results for each segment that are obtained are summed with the corresponding weight vector calculated before for each segment.
- Find the area of each part of the segment.
    - From <DRAW> use the command <BOUNDARY> to create an "object" (polyline).
    - Use the command <area> to obtain the value in  $m^2$
  - Find the volume of each part of the segment by multiplying the obtained areas with the width/thickness of the structural element.

- To obtain the weight for each part of each segment, multiply the given density value ( $\text{kN/m}^3$ ) to the corresponding volume.
- Find the centroid coordinates for each segment.
  - From <DRAW> use the command <REGION> by selecting the created "object" previously.
  - Use the command <MASSPROP> to obtain the x,y coordinates of the centroid for each part of the segment.
- Locate each centroid of segment:
  - Use <POINT> to draw a reference in each segment by giving the coordinates obtained before.
- Locate the weight-force (kN)
  - Define a scale for drawing the weight-force values (kN) represented as a dimension value (m). For this example: 1 m = 100 kN.
  - Draw the <LINE> with the scaled magnitud in meters representing the weight-force (kN) with the starting point in the centroid of each corresponding segment. For this example the vector that appears in the image corresponds to the scaled sum of the weight vector of the segment and the corresponding vector of the weight from the superior levels.

MATERIAL (STRUCTURAL)	Length per segment (m): 0.42	Length per segment (m): 1.20
UNIT WEIGHT ( $\text{kN/m}^3$ ): 18	Point load segment (kN): 38.83	Point load segment (kN):111.82
THICKNESS (m): 0.75		

N°	GROUND LEVEL			ALL LEVELS	
	Area ( $\text{m}^2$ )	Weight (kN)	Scaled weight (kN)	Total Weight (kN)	Scaled Total Weight (m)
1	0.49	6.60	0.07	45.43	0.45
2	0.55	7.46	0.08	46.29	0.46
3	0.73	9.87	0.10	48.70	0.49
4	7.68	103.68	1.04	215.50	2.16

Table 7 – Total weights in structure

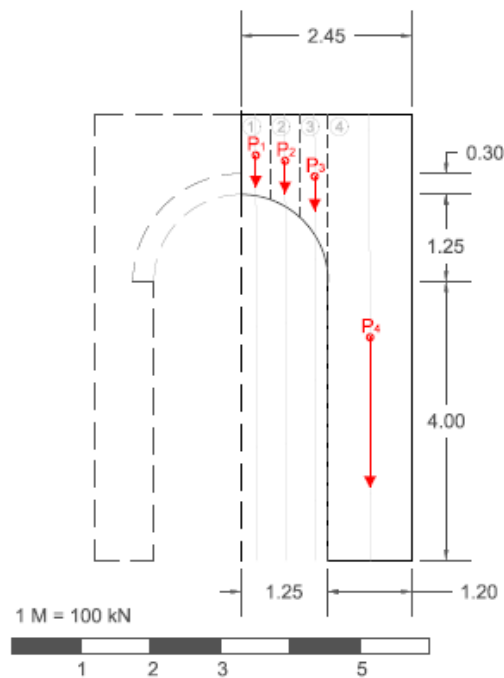


Fig. 63 - Discretization of arch, location of centroids and vertical forces.

5) Apply STATIC GRAPHIC to calculate de <RESULTANT FORCE>

- To find the **magnitud** and **direction** of the <RESULTANT FORCE>: Sum in order of appearance the weight-forces (sum as vectors).
- To find the **position** of the <RESULTANT FORCE>:
  - Define an "origin" next to the summed force vectors
  - Draw ray-lines from the start and end of each individual force vectors: This will form a FORCE POLYGON
  - Take each ray-line (keeping its direction) and locate one of its ends intersecting the reference line of each corresponding weight-force vector in the analyzed structure: This will form a FUNICULAR POLYGON
  - Sum the two ray-line vectors of each extreme in the FUNICULAR POLYGON (sum of vectors): The position of the RESULTANT FORCE (with magnitude and direction that was found before), is obtained.

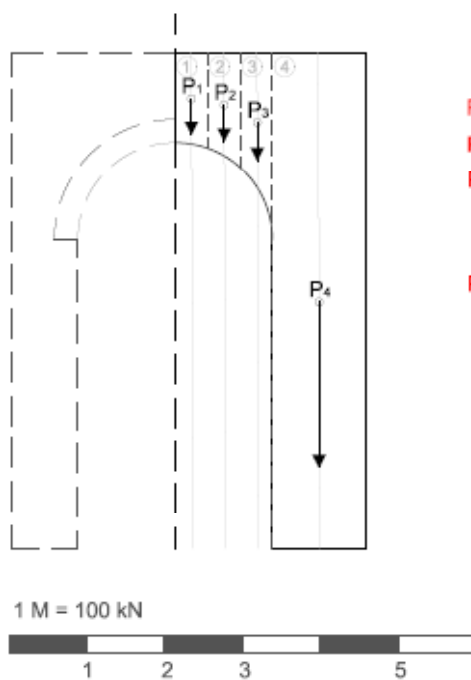


Fig. 64 - Sum of the weight vectors.

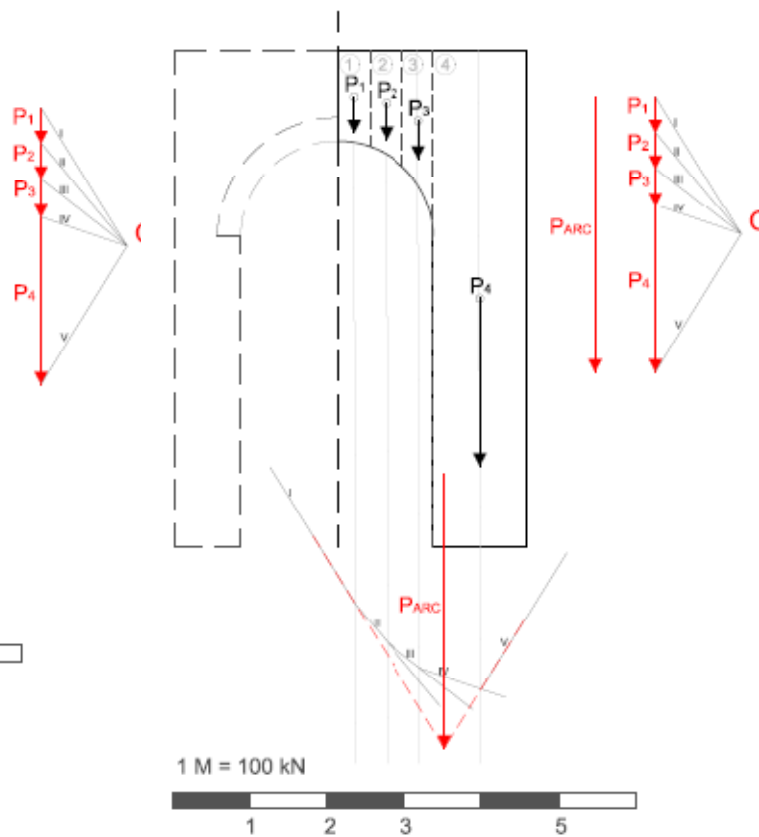


Fig. 65 - Position of the resultant force.

- 6) For this exercise, the objective of finding a safe condition for the structure is obtaining a thrust line within the boundaries of the arch wall with buttress. A value of thrust is searched using both analytical and graphical procedures.  $H$  will be obtained by defining two points where the thrust line should pass. The target in this specific case is to obtain a value of thrust; the horizontal force applied in the middle of the arch is defined as located in the upper boundary of the wall. The point of location the resultant force to be obtained is defined in the outer boundary of the base.
- 7) For the procedure performed analytically, in order to estimate the  $H$ , the equilibrium equation regarding the action of the moments in the point specified as the location of the resultant force is defined (point A in red).

The sum of the moments acting in point A is zero for the structure to be in equilibrium.

$$\sum M = 0$$

The signs of the moments are defined as negative when the direction is clockwise and positive when counterclockwise. Therefore the sum of the acting moments in point for each of the forces and corresponding distances is expressed as:

$$(-H_{min} * bH) + (P_1 * b_1) + (P_2 * b_2) + (P_3 * b_3) + (P_4 * b_4) = 0$$

$b_H$  is the vertical distance between the horizontal force  $H$  and point  $A$ .

$b_1, b_2, b_3$  and  $b_4$  are the horizontal distances between the vertical weight forces  $P_i$  and point  $A$ .

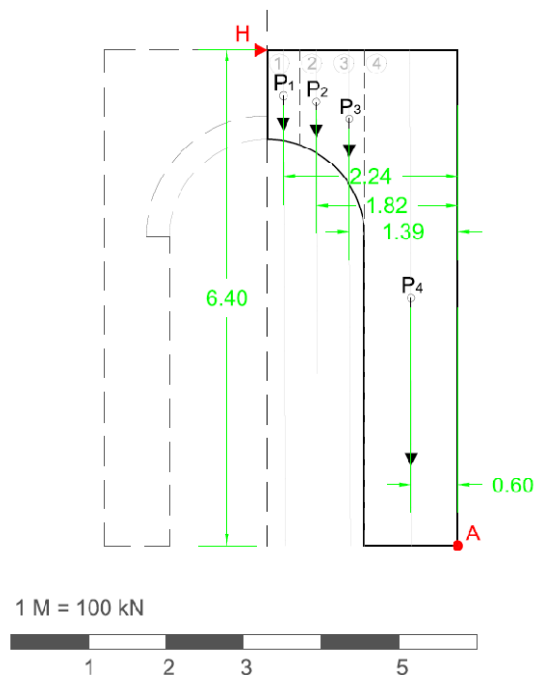


Fig. 66 – Location of forces and distances from centroids to point  $A$  from where the moments are evaluated.

The equivalence between negative and positive moments is expressed as:

$$(P_1 * b_1) + (P_2 * b_2) + (P_3 * b_3) + (P_4 * b_4) = (H * b_H)$$

All values are known except  $H$  which is the objective. The expression isolating  $H$  is expressed as:

$$\frac{(P_1 * b_1) + (P_2 * b_2) + (P_3 * b_3) + (P_4 * b_4)}{b_H} = H$$

$P_1$	$b_1$	$P_2$	$b_2$	$P_3$	$b_3$	$P_4$	$b_4$	$b_H$	<b>H</b>	scaled H
45.43	2.24	46.29	1.82	48.70	1.39	215.50	0.60	6.40	<b>59.86</b>	0.60 m

8) For the procedure performed graphically, in order to find a thrust line and a resultant for the analyzed segments of the structure, parameters for two vectors are defined:

- Position and direction of the horizontal thrust in the middle of the arch ( $H_{ARC}$ ).
- Position of the new resultant vector ( $R_{ARC}$ ).

The reference lines corresponding to the horizontal thrust vector ( $H$ ) and the resultant of the weight vector ( $P_{ARC}$ ) are extended until they intersect. A new reference ray corresponding to the new resultant vector  $R$  is drawn by connecting the point of intersection of the reference lines  $H$  and  $P_{ARC}$ , with the defined point position for the new resultant vector  $R$ . In this way the direction of vector  $R$  is obtained. The magnitudes for the horizontal thrust vector  $H$  and for the new resultant vector  $R$  are found by sum of vectors.

If following tryouts were needed because a thrust line was not found considering these initial parameters, the following modifications can be assumed:

- New position of the horizontal thrust maintaining the same magnitude. The direction is already defined as “horizontal” as it constitutes the equilibrium with the other half of the arch.
- New magnitude of the horizontal thrust.
- New position of the resultant vector.

Any modification of a parameter will alter the equilibrium “form” of the sum of vectors “shape”, affecting the magnitude and direction of the resultant force vector and the thrust line obtained.

The following images show the results obtained through the analytical and graphical procedures. The difference between both is less than 2% which is an acceptable margin of error.

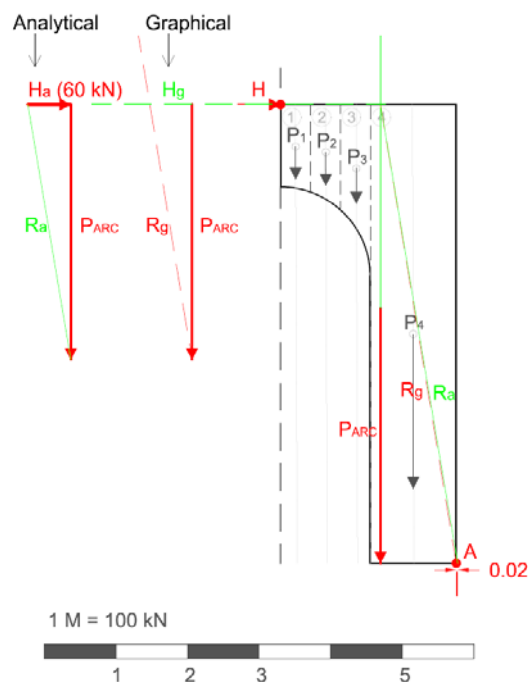


Fig. 67 – Results for H through both analytical and graphical procedures.



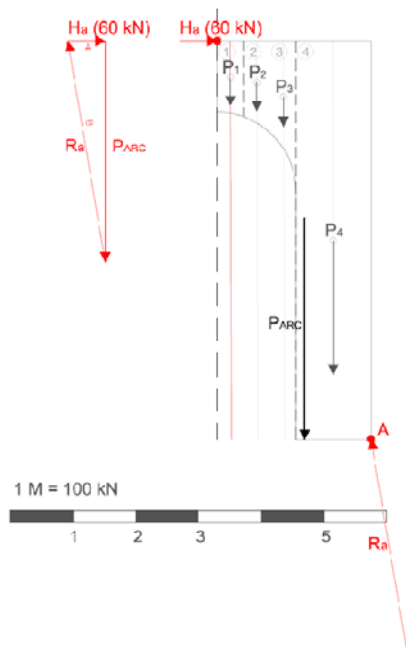


Fig. 68 – Magnitud of vectors (analytical)

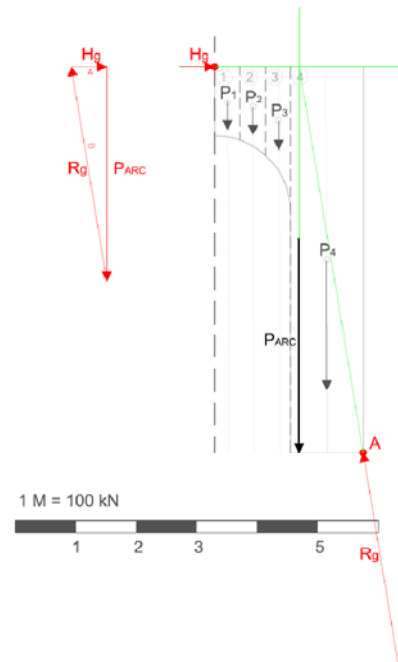


Fig. 69 – Magnitud of vectors (graphical)

- 9) The sum of vectors P, H AND R will define the location of a new origin (O') defining the rays to build the force polygon.
- 10) Draw the THRUST LINE. With the "new origin" (O') defined, the force polygon is constructed over the arch. Each line from origin - O' to each force, is relocated to cross the reference lines of the centroids of each segment of the arch. A sum of vectors is performed.

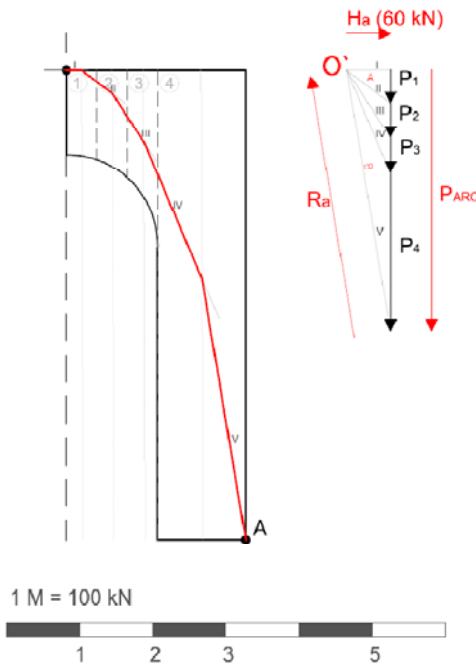


Fig. 70 – Thrust line with H found analytically.

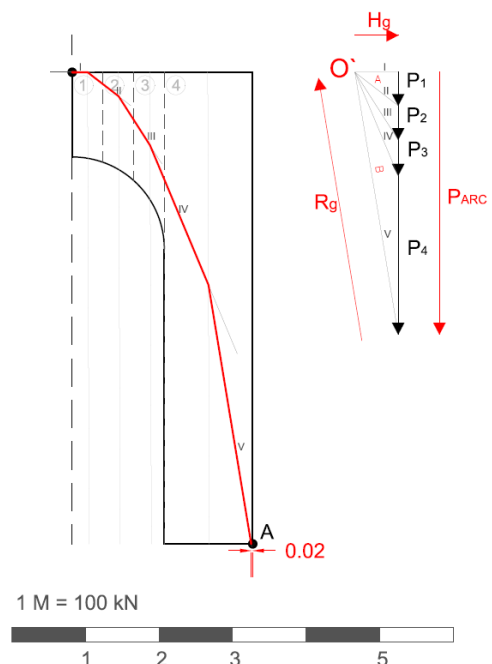


Fig. 71 – Thrustline with H found graphically.

For values of H with a difference of less than 2%, a thrust line is found.



### 3.4 Multiple span arch bridge (Devil Bridge in Spain)

The Roman aqueduct of Tarragona, also known as Devil Bridge, is located near the city of Tarragona in Spain. Tarragona, formerly called Táraco, was an important commercial, religious and administrative Roman city. The Archaeological Ensemble of Táraco was included in the World Heritage List in 2000 by the World Heritage Committee. (United Nations).

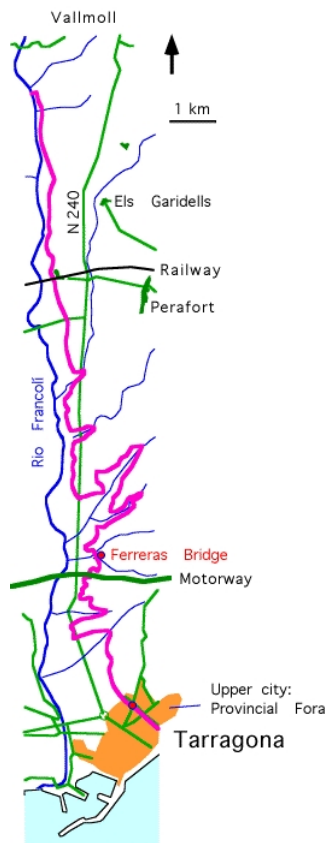


Fig. 72 – Map of the aqueduct of Tarragona (Schram & Passchier, 2005)

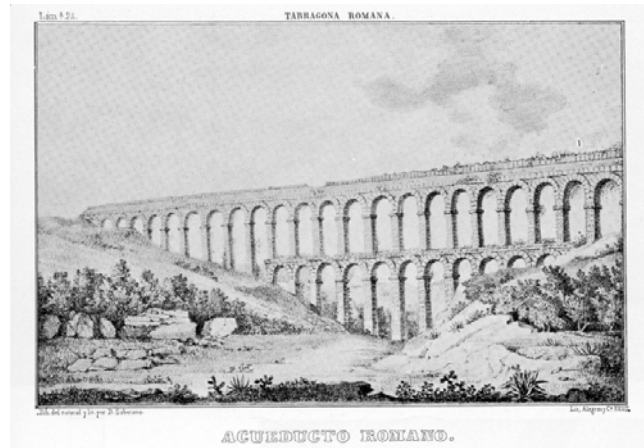


Fig. 73 - Drawing of the Puente de Ferreras bridge of one of the aqueducts of Tarragona (D. Soberano and A&C Reus/casado1972) (Schram & Passchier, 2005)



Fig. 74 – Aqueduct of las Ferreras (Ajuntament de Tarragona)

The Roman Aqueduct of Tarragona was “built in the 1<sup>st</sup> century AD over a natural valley, it carried water from the present-day Puigdelfí to Tarraco. It consists of two rows of superimposed arches built with stone blocks (*opus quadratum*). The lower section has eleven arches, each 6.30 metres wide and 5.7 metres high. The upper twenty-five arches are of a similar size. The maximum height of the aqueduct is 27 metres and it is 217 metres long. The water conduit that runs along the top of the arched structure would originally have been covered. It is waterproofed with a special type of mortar to prevent leaks”. (Ajuntament de Tarragona)

“A special feature of this aqueduct bridge is the stepped nature of the piers below the imposts of the arches. Each step increases the width of the pier by half a roman foot (15 cm), almost certainly to increase stability. Similar stepped piers are known for the aqueduct of Metz in France. The bridge

*probably dates from the time of Augustus. There is a small quarry 100 m North of the bridge which may have provided the building stone". (Schram & Passchier, 2005)*

*"Building of upper archs in line with lower is close to those of first order. Difference stays in pillars: they are not trunks of pyramids, but rectangular prisms.*

*On the last series of archs, conduction is made: the specus, between two walls of covered masonry. Sections with original pavement of opus signinum do remain."* (The History of the Spanish Architecture)



Fig. 75 – Aqueduct of Las Ferreras in Tarragona (The History of the Spanish Architecture)



Fig. 76 – Aqueduct of Las Ferreras detail view (Ajuntament de Tarragona)



Fig. 77 – Aqueduct of Las Ferreras view from the bottom (Ajuntament de Tarragona)



Fig. 78 – Aqueduct of Las Ferreras (Ajuntament de Tarragona)



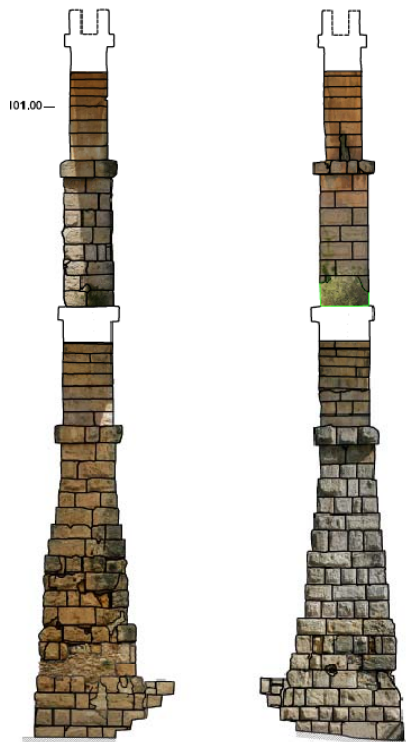


Fig. 79 – Section of Pillars A15-A30. Source: Eng. Pere Roca (UPC)

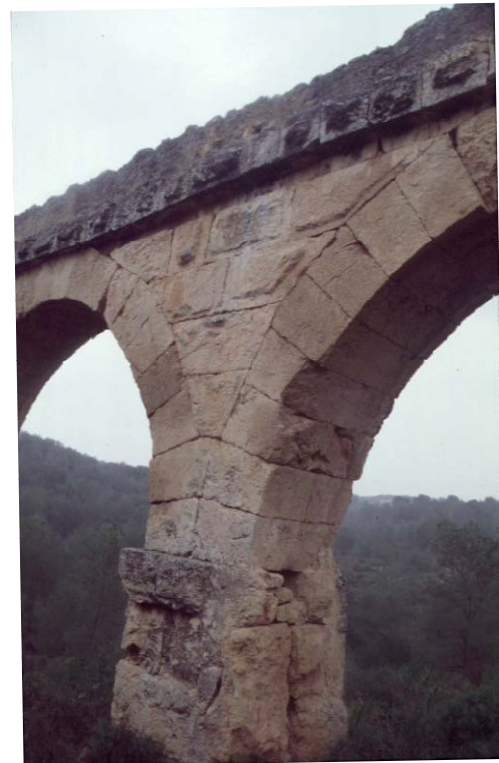


Fig. 80 – Detail of superior arches (Schram & Passchier, 2005)



Fig. 81 – Detail. (Schram & Passchier, 2005)



Fig. 82 – Detail of *specus* (Schram & Passchier, 2005)

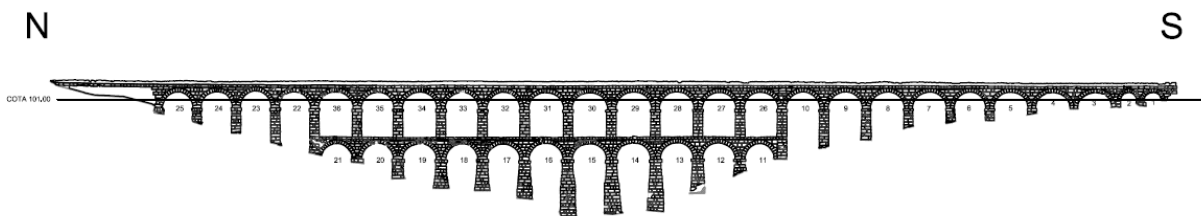


Fig. 83 – Section profile of the Devil's Bridge. Source: Eng. Pere Roca (Universitat Politècnica de Catalunya)

### 3.4.1 Kinematic approach

The transversal section of the arch bridge is evaluated for the global overturning of the transversal section due to seismic actions. The section is analyzed as a simply supported monolithic wall.

An Ultimate Limit State – ULS verification of the local mechanism defined as overturning. The verification was developed following the criteria defined as *simplified verification with structure factor q (linear kinematic analysis)*. (Franchetti, 2009)

The verification is satisfied if:

$$a_0^* \geq \frac{a_g S}{q} \left( 1 + 1.5 \frac{Z}{H} \right)$$

Fig. 84 – ULS verification (Franchetti, 2009)

Where  $a_0^*$  is the spectral *acceleration for the activation of the mechanism*.

The expression  $\frac{a_g S}{q} \left( 1 + 1.5 \frac{Z}{H} \right)$  corresponds to the *acceleration of the elastic spectrum* and is defined by:

- Peak ground acceleration -  $a_g$ .
- Soil type – S.
- Structure factor – q, assumed as 2.
- Height of the center of the masses that generate horizontal forces – Z.
- Height of the whole structure – H.

Safety verification with linear analysis (ULS):

$a_g$ (g)	S	q	Z (m)	H (m)
0.39	1	2	10.44	26.51

$a_0^* \geq 0.31$

Considering this parameter, a value of  $a_0^*$  is to be determined in the following procedure.

- 1) The geometry of the sections is defined. The mechanism will be evaluated in the transversal section, whereas the longitudinal section will be considered for obtaining the areas for calculating the weights. The center of masses is identified for the transversal section. The three assumptions of Limit Analysis are maintained: infinite compressive and no tensile strength for the masonry, and no sliding of the blocks.

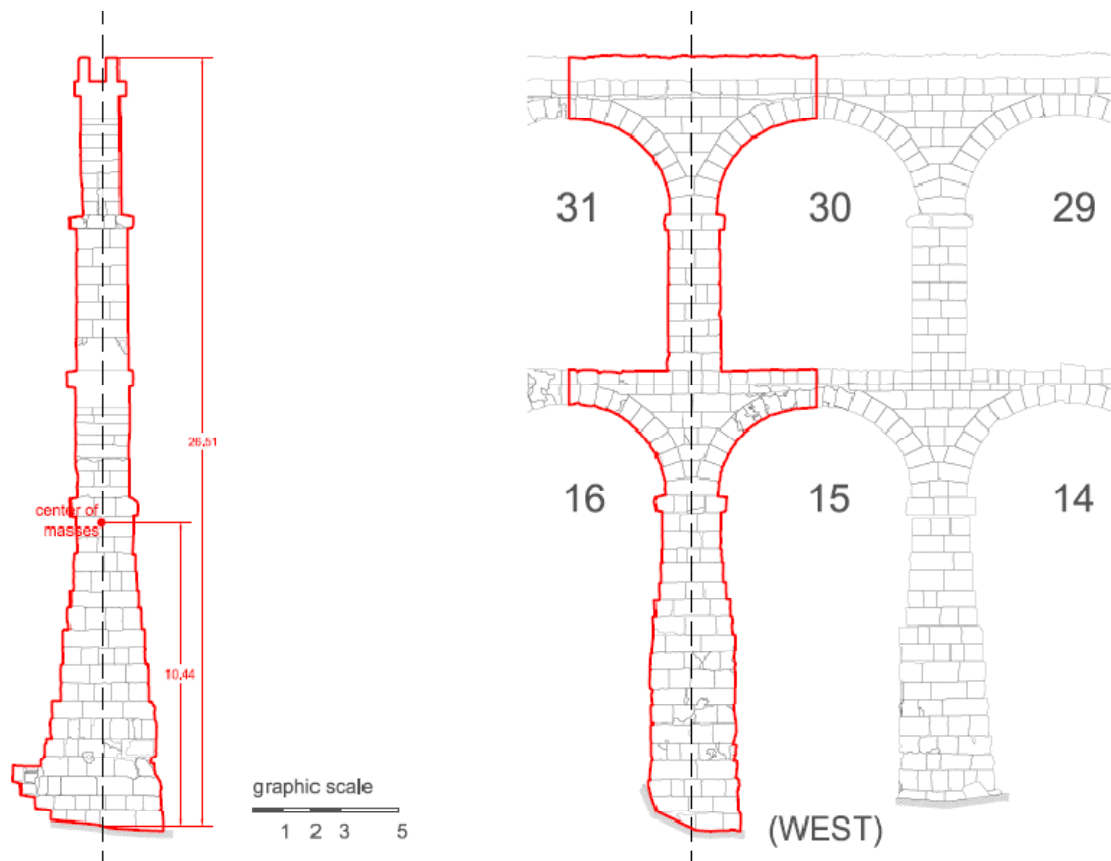


Fig. 85 – Geometry of the transversal section and corresponding area in the longitudinal section.

2) Choosing a collapse mechanism:

An out-of-plane mechanism is defined for analyzing the transversal section of the Tarragona Aqueduct. The section analyzed is located in the center of the bridge length, in sections A15-A30. The action evaluated for the mechanism is perpendicular to the plane of the wall.

- The transversal section is analyzed. A hinge is defined in the base of the section corresponding to the rotation point of the overturning of the wall. An expression considering the equilibrium of moments (resisting and acting) is defined.
- The transversal section is divided in four blocks. The corresponding weight-force is calculated for each block taking the area in the longitudinal section and the height of the transversal section.

Density of the wall	25.00	kN/m <sup>3</sup>		
Area Long-1	28.38	m <sup>2</sup>	Area Long-2	9.86 m <sup>2</sup>
Height-1	5.42	m	Height-2	5.40 m
W <sub>1</sub>	3842.50	kN	W <sub>2</sub>	1330.94
Area Long-3	20.23	m <sup>2</sup>	Area Long-4	30.00 m <sup>2</sup>
Height-3	4.37	m	Height-4	11.32 m
W <sub>3</sub>	2210.98	kN	W <sub>4</sub>	8493.05

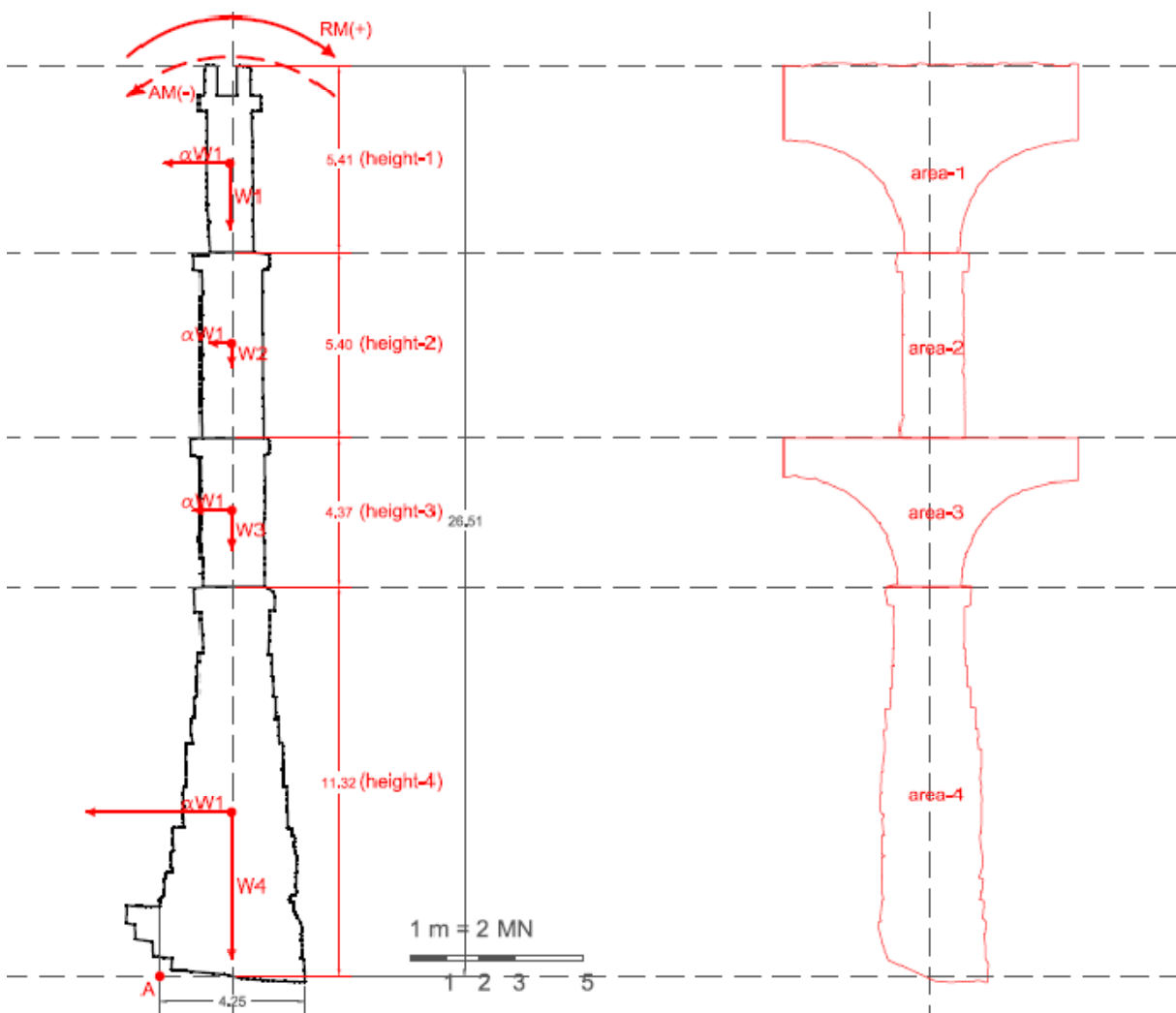


Fig. 86 - Positive Reacting Moment (RM) and negative Acting Moment (AM).

- The horizontal forces are defined as dependent on the corresponding weights by introducing the  $\alpha$  multiplier. The horizontal and weight forces are applied in the center of masses of each defined section of the structure. This is done considering that *“the wall is supposed infinitely rigid, therefore the horizontal forces are the inertial forces”*. (Franchetti, 2009).
- The hinge is defined as point A in the base of the transversal section. Three positions of this hinge were evaluated:
 

0.00 m	1.26 m	1.27 m
--------	--------	--------
- The signs for the moments acting in the structure were defined:  
 Reacting Moment – RM: positive (+); Acting Moment – AM: negative (-)

### 3) Evaluating the horizontal action that activates the mechanism:

- The distances (horizontal and vertical) from the centroids of each block to the hinges are measured. The horizontal distances will be modified by the variation in the



position of the hinge that was mentioned before; therefore three different situations are defined. For the vertical distances the change in the position of the hinge has no effect.

	Horizontal Distance		Vertical Distance
A-hinge (0.00)	A-hinge (1.26)	A-hinge (1.27)	A-hinge (any)
$\Delta_x W_1 A = 2.05 \text{ m}$	$\Delta_x W_1 A = 0.79 \text{ m}$	$\Delta_x W_1 A = 0.78 \text{ m}$	$\Delta_y W_1 A = 23.70 \text{ m}$
$\Delta_x W_2 A = 2.10 \text{ m}$	$\Delta_x W_2 A = 0.84 \text{ m}$	$\Delta_x W_2 A = 0.83 \text{ m}$	$\Delta_y W_2 A = 18.42 \text{ m}$
$\Delta_x W_3 A = 2.11 \text{ m}$	$\Delta_x W_3 A = 0.85 \text{ m}$	$\Delta_x W_3 A = 0.84 \text{ m}$	$\Delta_y W_3 A = 13.57 \text{ m}$
$\Delta_x W_4 A = 2.10 \text{ m}$	$\Delta_x W_4 A = 0.84 \text{ m}$	$\Delta_x W_4 A = 0.83 \text{ m}$	$\Delta_y W_4 A = 4.76 \text{ m}$

Table 8 – Horizontal and vertical distances of centroids from hinge.

- The equilibrium of forces is defined by:

$$\mathbf{RM \text{ (resisting moment-negative) = AM \text{ (acting moment-positive)}}$$

The results for the following steps are presented for each of the locations of hinge-A.

#### A-hinge (0.00)

$RM(W_1) = W_1 \cdot \Delta_x W_1 A$	$AM(W_1) = -\alpha \cdot W_1 \cdot \Delta_y W_1 A$
7871.74 kN*m	-91063.35* $\alpha$
$RM(W_2) = W_2 \cdot \Delta_x W_2 A$	$AM(W_2) = -\alpha \cdot W_2 \cdot \Delta_y W_2 A$
2797.37 kN*m	-24521.54* $\alpha$
$RM(W_3) = W_3 \cdot \Delta_x W_3 A$	$AM(W_3) = -\alpha \cdot W_3 \cdot \Delta_y W_3 A$
4661.63 kN*m	-30001.44* $\alpha$
$RM(W_4) = W_4 \cdot \Delta_x W_4 A$	$AM(W_4) = -\alpha \cdot W_4 \cdot \Delta_y W_4 A$
17843.05 kN*m	-40458.34* $\alpha$
<b>TOTAL RM= 33173.79 kN*m</b>	<b>TOTAL AM= -186044.67 kN*m</b>

#### A-hinge (1.26)

$RM(W_1) = W_1 \cdot \Delta_x W_1 A$	$AM(W_1) = -\alpha \cdot W_1 \cdot \Delta_y W_1 A$
3030.19 kN*m	-91063.35* $\alpha$
$RM(W_2) = W_2 \cdot \Delta_x W_2 A$	$AM(W_2) = -\alpha \cdot W_2 \cdot \Delta_y W_2 A$
1120.39 kN*m	-24521.54* $\alpha$
$RM(W_3) = W_3 \cdot \Delta_x W_3 A$	$AM(W_3) = -\alpha \cdot W_3 \cdot \Delta_y W_3 A$
1875.79 kN*m	-30001.44* $\alpha$
$RM(W_4) = W_4 \cdot \Delta_x W_4 A$	$AM(W_4) = -\alpha \cdot W_4 \cdot \Delta_y W_4 A$
7141.81 kN*m	-40458.34* $\alpha$
<b>TOTAL RM= 13168.18 kN*m</b>	<b>TOTAL AM= -186044.67 kN*m</b>

**A-hinge (1.27)**

$RM(W_1) = W_1 \cdot \Delta_x W_1 A$	$AM(W_1) = -\alpha \cdot W_1 \cdot \Delta_y W_1 A$
2991.77 kN*m	-91063.35* $\alpha$
$RM(W_2) = W_2 \cdot \Delta_x W_2 A$	$AM(W_2) = -\alpha \cdot W_2 \cdot \Delta_y W_2 A$
1107.08 kN*m	-24521.54* $\alpha$
$RM(W_3) = W_3 \cdot \Delta_x W_3 A$	$AM(W_3) = -\alpha \cdot W_3 \cdot \Delta_y W_3 A$
1853.68 kN*m	-30001.44* $\alpha$
$RM(W_4) = W_4 \cdot \Delta_x W_4 A$	$AM(W_4) = -\alpha \cdot W_4 \cdot \Delta_y W_4 A$
7056.87 kN*m	-40458.34* $\alpha$

**TOTAL RM= 13009.41 kN\*m**                      **TOTAL AM= -186044.67 kN\*m**

The multiplier  $\alpha$  is obtained for each of the three cases according to the expression:  $\alpha_0 = -(RM/AM)$  which results from "equalizing the total work made by the external and internal forces applied to the system in correspondence of the virtual displacement" (Franchetti, 2009). The values in each case for  $\alpha$ :

<b>A-hinge (0.00)</b>	<b>A-hinge (1.26)</b>	<b>A-hinge (1.27)</b>
0.18	0.07	0.07

The fraction of the mass participant to the kinematism ( $e^*$ ) needs to be obtained from calculating the participation mass ( $M^*$ ), in order to obtain the spectral acceleration of the defined mechanism ( $a_0^*$ ), that is defined as:

$$a_0^* = \frac{\alpha_0 \sum_{i=1}^{n+m} P_i}{M^*} = \frac{\alpha_0 g}{e^*}$$

Fig. 87 – Spectral acceleration for the activation of the mechanism  $a_0^*$ . (Franchetti, 2009)

- o The participation mass  $M^*$  depends on the virtual displacement ( $\delta_{x,1}$ ) measured from the centroids of the resultant forces of each block ( $W_i$ ). It is defined as:

$$M^* = \frac{\left( \sum_{i=1}^{n+m} P_i \delta_{x,i} \right)^2}{g \sum_{i=1}^{n+m} P_i \delta_{x,i}^2}$$

Fig. 88 – Participation mass  $M^*$  (Franchetti, 2009)

	$P_i \cdot \delta_{x,i}$	$P_i \cdot \delta_{x,i}^2$
$\delta_{x,W_1} = 1$	3842.5	3842.5
$\delta_{x,W_2} = 0.78$	1032.3	800.6
$\delta_{x,W_3} = 0.57$	1264.0	722.6
$\delta_{x,W_4} = 0.20$	1714.7	346.2
<b><math>\Sigma</math></b>	<b>7853.5</b>	<b>5712.0</b>
<b><math>M^* = 10798.0</math></b>		

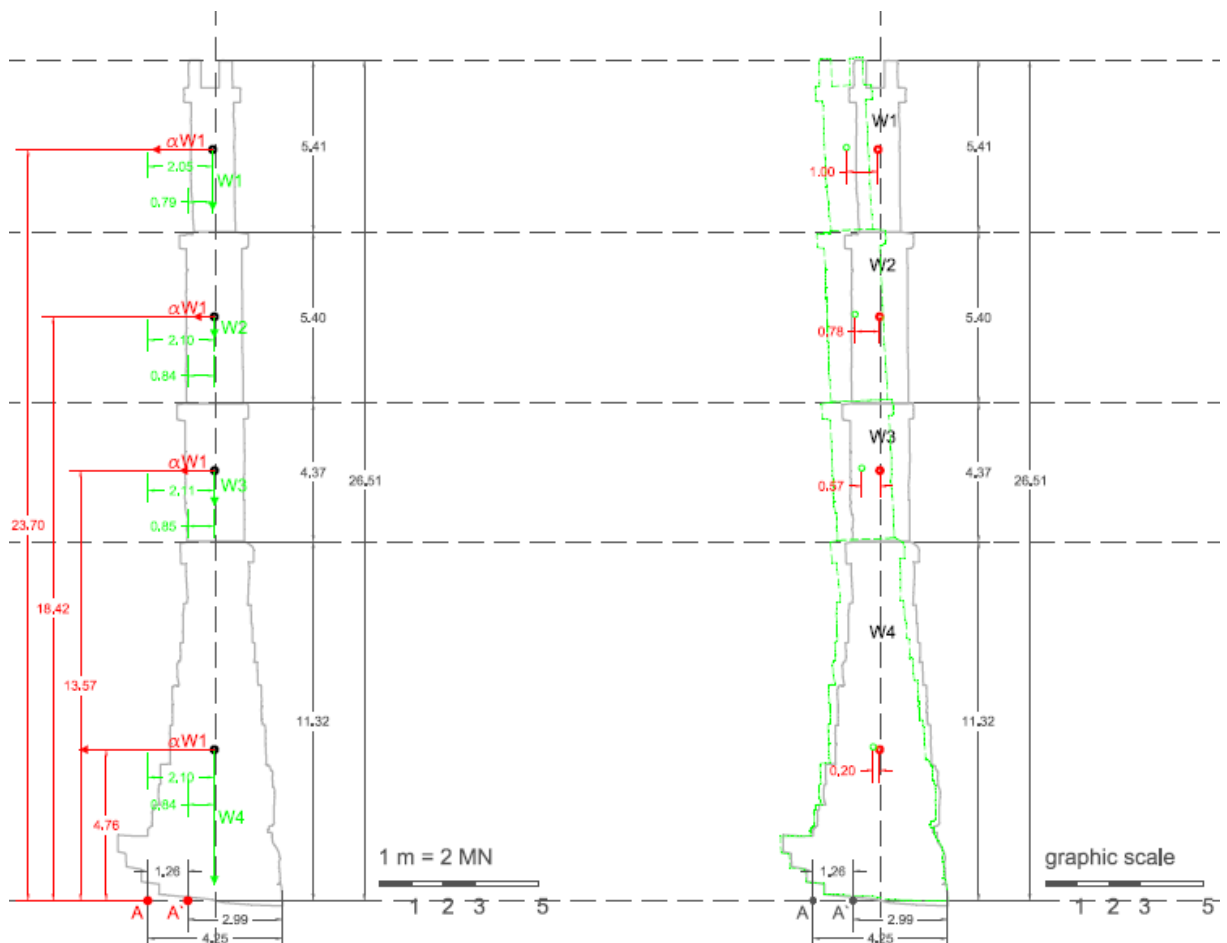


Fig. 89 – Distances from centroids of blocks to hinge-A; Virtual displacements with rotation of structure.

- The *fraction of the mass participant to the kinematism* ( $e^*$ ) was obtained according to the following expression:

$$e^* = \frac{gM^*}{\sum_{i=1}^{n+m} P_i}$$

Fig. 90 – mass participant to the kinematism ( $e^*$ )

**$e^* = 0.68$**

- The *spectral acceleration for the activation of the mechanism* ( $a_0^*$ ) was obtained according to the following expression:

$$a_0^* = \frac{\alpha_0 \sum_{i=1}^{n+m} P_i}{M^*} = \frac{\alpha_0 g}{e^*}$$

Fig. 91 – Spectral acceleration for the activation of the mechanism ( $a_0^*$ )

The results are presented for each of the three cases:

$a_0^*$ (m/s <sup>2</sup> )		
<b>A-hinge (0.00)</b>	<b>A-hinge (1.26)</b>	<b>A-hinge (1.27)</b>
2.57	1.02	1.01

- The safety verification with linear analysis, Ultimate Limit State (ULS) was performed according to the following expression:

$$a_0^* \geq \frac{a_g S}{q} \left( 1 + 1.5 \frac{Z}{H} \right)$$

Fig. 92 – Safety verification for Ultimate Limit State (ULS)

- The safety verification with linear analysis, Ultimate Limit State (ULS) was performed according to the following expression:

Safety verification with linear analysis (ULS):

$a_g$	<b>S</b>	<b>q</b>	<b>Z</b>	<b>H</b>
0.39	1	2	10.44	26.51
<b><math>a_0^* \geq 0.31</math></b>				

The values obtained for each of the three cases evaluated, and the safety conditions in result are:

<b>Position hinge-A</b>	<b><math>A_0^*</math> (m/s<sup>2</sup>)</b>	<b>Safety verification</b>
0.00	2.57	<i>SAFE</i>
1.26	1.02	<i>SAFE</i>
1.27	1.01	<i>STRENGTHENING IS REQUIRED</i>

### 3.5 FAÇADE WALL (Quintela Tower in Portugal)

A safety evaluation was performed for one of the granite walls of the façade in Quintela Tower, for the SA7 report during the coursework of the present master. (Abacilar, Manrique, Roberts, & Taneri, 2010)

A detail explanation of the procedure is now performed and is presented as the last case study of application of Limit Analysis.

The Quintela Tower is located in the city of Vila Real in the north of Portugal. The tower was constructed during the XIII-XIV centuries and constitutes an example of romanic and gothic residential architecture. The building is classified as a National Monument since 1910.

The structure of the tower consists of three-leaf granite masonry walls. A simply supported timber lintel system exists for the two levels of floor slabs and the hip roof.

The geometry of the tower is a rectangular plan and a height:side ratio of approximately 2:1.

The tower has been subjected to several interventions, being of importance the fact that the slabs and roof we observe today are from 1982, which indicate that the masonry walls have been exposed for a long time without protection to the changing weather conditions of the area.

At present the use of the tower is classified as cultural.

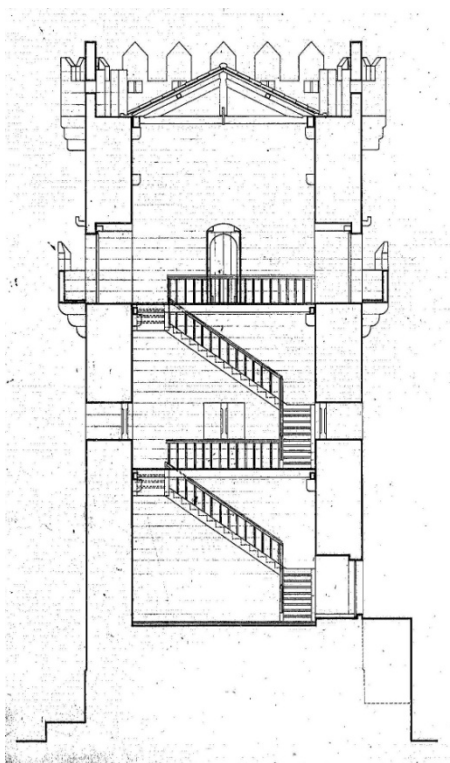


Fig. 93 – Section (SIPA - Sistema de Informação para o Património Arquitectónico (IHRU, Instituto da Habitação e Reabilitação Urbana, IP))



Fig. 94 – Quintela Tower in 1907 (Museu de Arqueologia e Numismática de Vila Real)

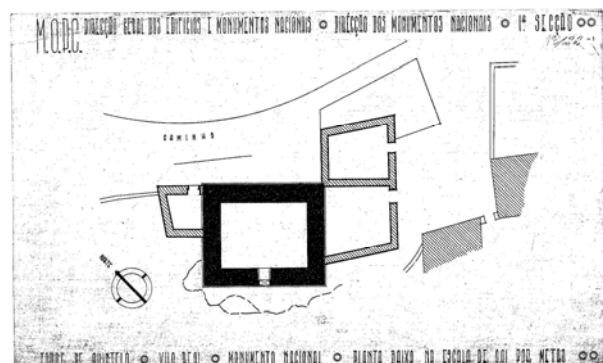


Fig. 95 – Orientation and plan geometry (IGESPAR IP - Instituto de Gestão do Património Arquitectónico e Arqueológico (former IPPAR))

### 3.5.1 Kinematic approach

The objective of the safety evaluation of one of the façade walls in Quintela Tower was influenced by a previous structural analysis that suggested a possible out-of-plane collapse mechanism. Therefore, the Limit Analysis kinematic approach was used in order to determine if strengthening by the use of ties were needed.

Assumptions were made that make the approach conservative, such as neglecting the contribution of the orthogonal walls. However, a simplification consisting in considering the three-leaf wall as monolithic can be assumed as compensation.

The difference of this example with the Devil's Bridge in Spain, is the fact of using the kinematic approach beyond safety evaluation by applying the procedure to a simplified design of a strengthening technique.

The transversal section of one of the granite three-leaf walls is evaluated for the global overturning due to seismic actions. The section is analyzed as a simply supported monolithic wall.

An Ultimate Limit State – ULS verification of the local mechanism defined as overturning. The verification was developed following the criteria defined as *simplified verification with structure factor q (linear kinematic analysis)*. (Franchetti, 2009)

The verification is satisfied if:

$$a_0^* \geq \frac{a_g S}{q} \left( 1 + 1.5 \frac{Z}{H} \right)$$

Fig. 96 – ULS verification (Franchetti, 2009)

Where  $a_0^*$  is the spectral *acceleration for the activation of the mechanism*.

The expression  $\frac{a_g S}{q} \left( 1 + 1.5 \frac{Z}{H} \right)$  corresponds to the *acceleration of the elastic spectrum* and is defined by:

- Peak ground acceleration from -  $a_g$ .
- Soil type – S.
- Structure factor – q.
- Height of the center of the masses that generate horizontal forces – Z.
- Height of the whole structure – H.

Safety verification with linear analysis (ULS):

$a_g$	<b>S</b>	<b>q</b>	<b>Z</b>	<b>H</b>
1.28	1	2	10	20
$a_0^* \geq$	<b>1.12</b>			

Considering this parameter, a value of  $a^*_0$  is to be determined in the following procedure.

- 1) The geometry of the section is defined. The mechanism will be evaluated for the cross section of the front façade. The center of masses is identified for the defined section. The three assumptions of Limit Analysis are maintained: infinite compressive and no tensile strength for the masonry, and no sliding of the blocks.

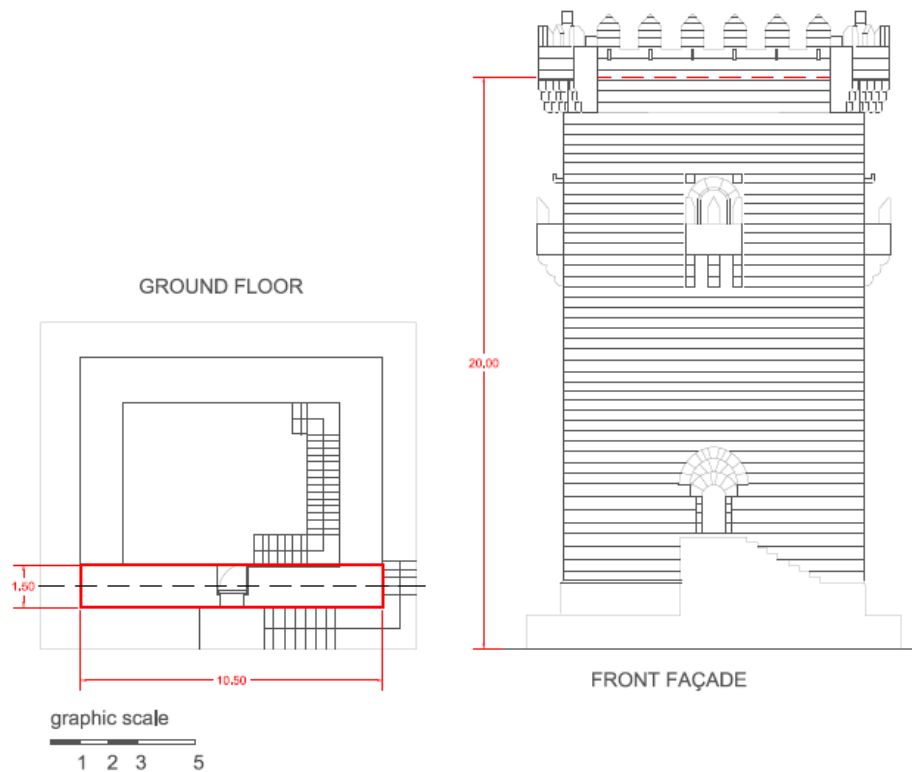


Fig. 97 – Plan and section view of Quintela Tower showing the wall that will be verified.

- 2) Choosing a collapse mechanism:

An out-of-plane mechanism is defined for analyzing the wall of the front façade of the Quintela Tower. The action evaluated for the mechanism is perpendicular to the plane of the wall.

- The cross section of the wall is analyzed. A hinge is defined in the base of the section corresponding to the rotation point of the overturning of the wall. An expression considering the equilibrium of moments (resisting and acting) is defined.
- The cross section is divided in three blocks. The corresponding weight-force is calculated for each block taking the area in the plan section and the height of the wall.

**Total weight of masonry wall:**

Density of the granite	2300 kg/m <sup>3</sup>	Depth of the wall	10.5 m
Density of the infill	800 kg/m <sup>3</sup>	Height of the wall	20 m
Thickness outer leaf	0.4 m		

Thickness inner leaf 0.4 m

Thickness infill 0.7 m

**W<sub>t</sub>-Total weight of masonry wall 504000 kg (4939.2 kN)**

**Weight per level of masonry wall:**

Height level-1 7.68 m

**W<sub>1</sub> = 1896.7 kN**

Height level-2 5.34 m

**W<sub>2</sub> = 1318.8 kN**

Height level-3 6.98 m

**W<sub>3</sub> = 1723.8 kN**

- The weight-forces contributing from the two slab levels and the roof level are also calculated:

**Weight from timber slabs:**

Permanent and live loads 2.0 kN/m<sup>2</sup>

Tributary area 30.6 m<sup>2</sup>

**T<sub>2</sub>-weight of slab second floor 91.7 kN**

**T<sub>3</sub>-weight of slab second floor 91.7 kN**

**Weight from timber roof:**

Permanent and live loads 2.0 kN/m<sup>2</sup>

Tributary area 33.1 m<sup>2</sup>

**T<sub>4</sub>-weight of slab second floor 66.2 kN**

- The horizontal forces are defined as dependent on the corresponding weights by introducing the  $\alpha$  multiplier. The horizontal and weight forces are applied in the center of masses of each defined section of the structure. This is done considering that *"the wall is supposed infinitely rigid, therefore the horizontal forces are the inertial forces"*. (Franchetti, 2009).
- The hinge is defined as point A in one corner of the base of the cross section.
- The signs for the moments acting in the structure were defined:  
Reacting Moment – RM: positive (+); Acting Moment – AM: negative (-)
- Considering that with this example the need of strengthening with TIE-RODS will be evaluated, a horizontal force F is defined in the top of the wall. For the initial verification this value will be zero (0). The force of the Tie Rod F is calculated as following:

**Strengthening with tie rods:**

Number of tie rods 0

Diameter of tie rods - D 0.016 m

Yielding strength of stainless steel F<sub>y</sub> 3.16E+08 N/m<sup>2</sup>

To calculate the force of the tie rod:

Area of stainless steel tie rods-A<sub>s</sub> 0.00E+00 m<sup>2</sup>

Force of Tie rod F=A<sub>s</sub>\*F<sub>y</sub> 0.0 N

The variables for the number of tie rods and the diameter of tie rods will be the ones to be modified for designing the strengthening.



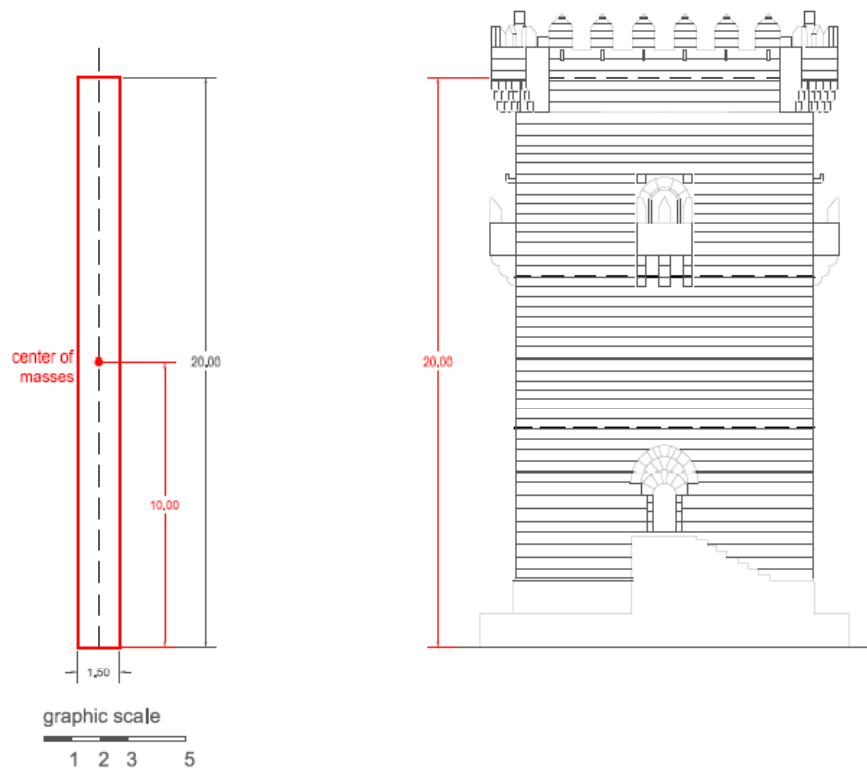


Fig. 98 – Geometry of the cross section with location of the center of masses

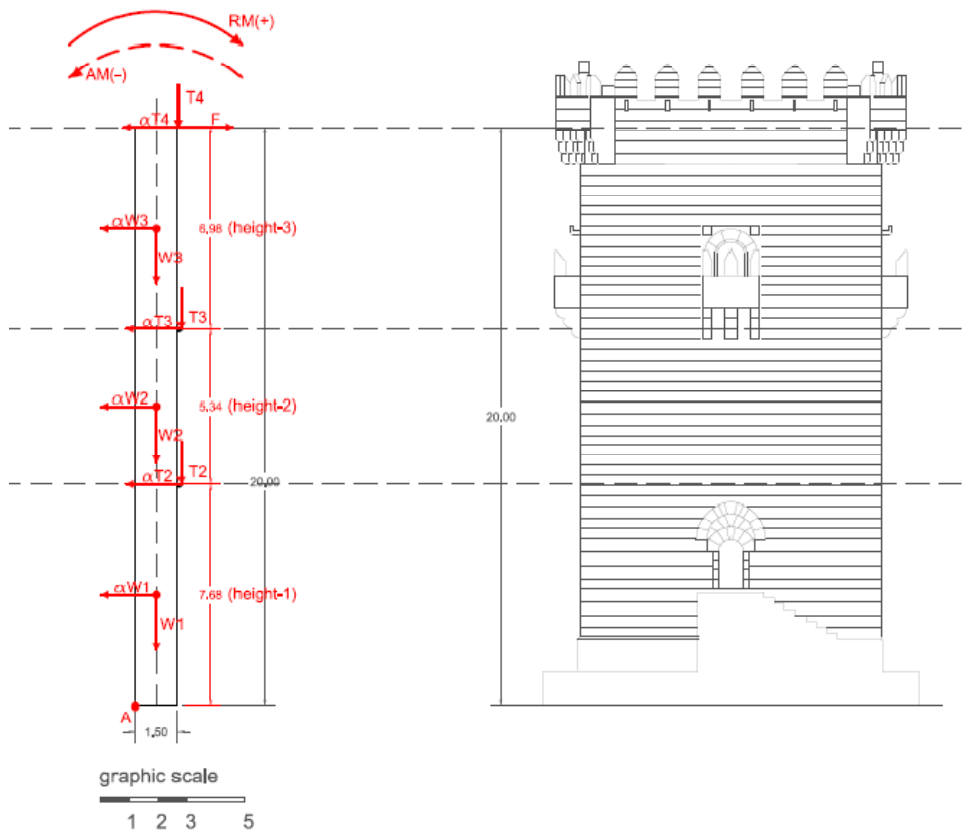


Fig. 99 - Location of the vertical and horizontal forces acting in the mechanism.

## 3) Evaluating the horizontal action that activates the mechanism:

- The distances (horizontal and vertical) from the point of application of each force to the hinges are measured and considered for calculating the Acting and Resisting moments.
- The equilibrium of forces is defined by:

$$\mathbf{RM \text{ (resisting moment-negative) = AM (acting moment-positive)}}$$

**Equilibrium of forces without tie-rod strengthening**

RM( $W_t$ )= $-W_t^*(t/2)-A$ -3704.40 kN*m	AM( $W_t$ )= $\alpha^*W_t^*10$ 49392 * $\alpha$
RM( $T_4$ )= $-T_4^*(t+0.1-A)$ -105.84 kN*m	AM( $T_4$ )= $\alpha^*T_4^*20$ 1323 * $\alpha$
RM( $T_3$ )= $-T_3^*(t+0.1-A)$ -146.66 kN*m	AM( $T_3$ )= $\alpha^*T_3^*13$ 1191.645 * $\alpha$
RM( $T_2$ )= $-T_2^*(t+0.1-A)$ -146.66 kN*m	AM( $T_2$ )= $\alpha^*T_2^*7.7$ 705.8205 * $\alpha$
RM(TR)=- $F^*H$ 0.0 kN*m	

$$\mathbf{TOTAL \ RM \ (kN^*m)=-4103.57}$$

$$\mathbf{TOTAL \ AM \ (kN^*m)=52612.4655^*\alpha}$$

The multiplier  $\alpha$  is obtained according to the expression:

$\alpha_0 = -(RM/AM)$  which results from “equalizing the total work made by the external and internal forces applied to the system in correspondence of the virtual displacement” (Franchetti, 2009). The value for  $\alpha$ :

$\alpha$  for no tie-rods

$$0.08$$

The fraction of the mass participant to the kinematism ( $e^*$ ) needs to be obtained from calculating the participation mass ( $M^*$ ), in order to obtain the spectral acceleration of the defined mechanism ( $a_0^*$ ), that is defined as:

$$a_0^* = \frac{\alpha_0 \sum_{i=1}^{n+m} P_i}{M^*} = \frac{\alpha_0 g}{e^*}$$

Fig. 100 – Spectral acceleration for the activation of the mechanism  $a_0^*$ . (Franchetti, 2009)

- The participation mass  $M^*$  depends on the virtual displacement ( $\delta_{x,i}$ ) measured from the centroids of the resultant forces of each block ( $W_i$ ). It is defined as:

$$M^* = \frac{\left( \sum_{i=1}^{n+m} P_i \delta_{x,i} \right)^2}{g \sum_{i=1}^{n+m} P_i \delta_{x,i}^2}$$

Fig. 101 – Participation mass  $M^*$  (Franchetti, 2009)

	$P_i \delta_{x,i}$	$P_i \delta_{x,i}^2$
$\delta_{x,TR} = 1$	0.0	0.0
$\delta_{x,T_4} = 1$	66.2	66.2
$\delta_{x,T_3} = 0.65$	59.6	38.7
$\delta_{x,T_2} = 0.38$	34.8	13.2
$\delta_{x,W_3} = 0.83$	1574.2	1306.6
$\delta_{x,W_2} = 0.52$	685.8	356.6
$\delta_{x,W_1} = 0.19$	327.5	62.2
<b><math>\Sigma</math></b>	<b>2748.1</b>	<b>1843.5</b>
<b><math>M^* = 4096.4</math></b>		

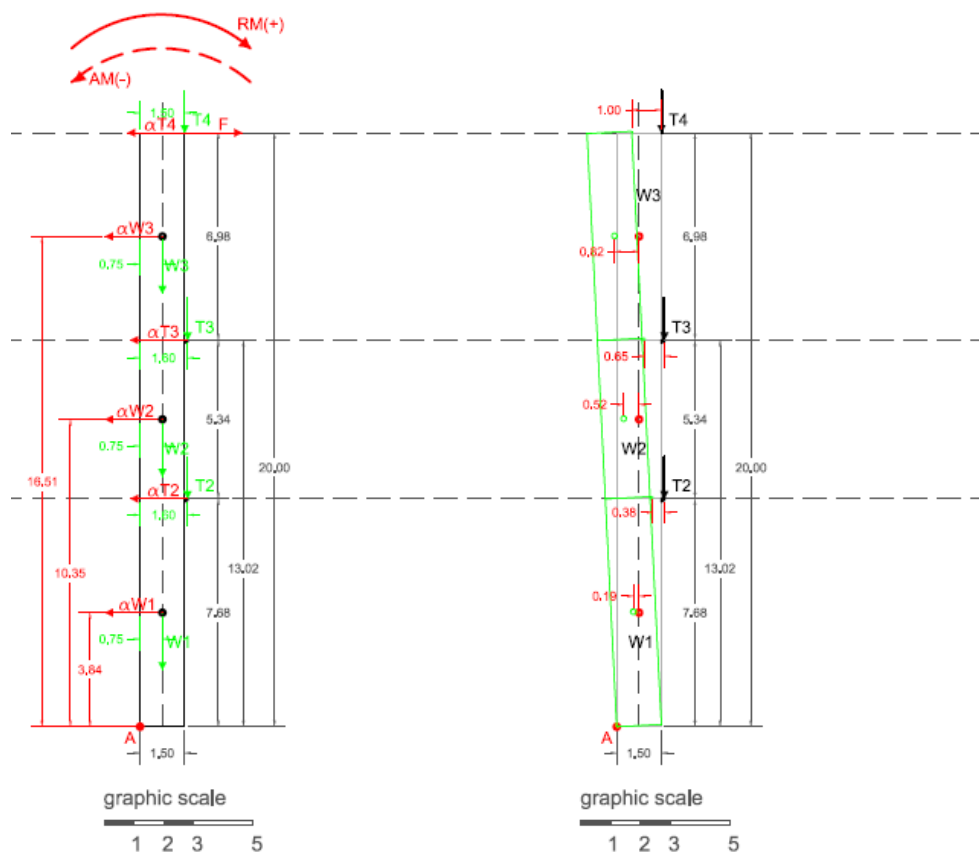


Fig. 102 - Distances from centroids of blocks to hinge-A; Virtual displacements with rotation of structure.

- The *fraction of the mass participant to the kinematism* ( $e^*$ ) was obtained according to the following expression:

$$e^* = \frac{gM^*}{\sum_{i=1}^{n+m} P_i}$$

 Fig. 103 – mass participant to the kinematism ( $e^*$ )

$$e^* = 0.79$$

- The *spectral acceleration for the activation of the mechanism* ( $a_0^*$ ) was obtained according to the following expression:

$$a_0^* = \frac{\alpha_0 \sum_{i=1}^{n+m} P_i}{M^*} = \frac{\alpha_0 g}{e^*}$$

 Fig. 104 – Spectral acceleration for the activation of the mechanism ( $a_0^*$ )

The result obtained for the verification without tie-rod strengthening is:

$$a_0^* \text{ (m/s}^2\text{)}$$

$$0.97$$

- The safety verification with linear analysis, Ultimate Limit State (ULS) was performed according to the following expression:

$$a_0^* \geq \frac{a_g S}{q} \left( 1 + 1.5 \frac{Z}{H} \right)$$

Fig. 105 – Safety verification for Ultimate Limit State (ULS)

- The safety verification with linear analysis, Ultimate Limit State (ULS) was performed according to the following expression:

Safety verification with linear analysis (ULS):

$a_g$	<b>S</b>	<b>q</b>	<b>Z</b>	<b>H</b>
1.28	1	2	10	20

$$a_0^* \geq 1.12$$

The value obtained for each the case verification without tie-rod and the safety condition in result is:

<b>Tie - rod</b>	$a_0^* \text{ (m/s}^2\text{)}$	<b>Safety verification</b>
0.00	0.97	<i>STRENGTHENING IS REQUIRED</i>

The same procedure was performed modifying the number of tie-rods and the location of hinge-A:

	$\alpha$	$M^*/g$	$e^*$	Tie Force	$ao^*$ m/s <sup>2</sup>	Min( $ao^*$ ) m/s <sup>2</sup>	Status
<b>V</b>	0.08	4096.4	0.79	0.0	<b>0.97</b>	1.12	Not safe
<b>S5-t20</b>	0.11	4194.8	0.81	127.1	1.29	1.12	Safe
<b>S4-t15</b>	0.11	4194.8	0.81	127.1	1.35	1.12	Safe
<b>S3-t10</b>	0.12	4194.8	0.81	127.1	1.41	1.12	Safe
<b>S2-t5</b>	0.12	4194.8	0.81	127.1	1.47	1.12	Safe
<b>S1-t0</b>	0.13	4194.8	0.81	127.1	1.53	1.12	Safe

Table 9 – Results of the verification without tie-rods and five tryout for strengthening with tie-rods modifying the hinge of the mechanism proposed.

S1 refers to “strengthening tryout-1” and t0 refers to the hinge in position 0.0 meters. The strengthening S1 through S5 are proposed with two tie-rods with a diameter of 0.016 meters.

Strengthening with tie rods:

Number of tie rods	2
Diameter of tie rods - D (m)	0.016
Yielding strength of stainless steel $F_y$ (N/m <sup>2</sup> )	3.16E+08

To calculate the force of the tie rod:

Area of stainless steel tie rods- $A_s$ (m <sup>2</sup> )	4.02E-04
Force of Tie rod $F=A_s \cdot F_y$ (N)	127.1



## 4. CONCLUSIONS

Limit Analysis techniques have a wide application for a simplified assessment of historical structures. The graphic approach allows understanding the concepts involved in structural analysis in order to be able to interpret the results that are obtained with computational limit analysis being developed and available today.

The examples previously presented constitute a starting point for the development of a compilation guide of detailed case studies applying Limit Analysis for the safety evaluation of historical constructions. Different typologies of historical constructions were evaluated in order to understand the specific considerations in each case such as loading conditions and behavior of the macro elements when defining the collapse mechanisms. The cases were presented in a step-by-step scheme in order to follow the sequence being performed and to be able to complement the figures and analytical procedures in order to be used by future students interested in the use of limit analysis for the assessment of historical constructions.

With each case study new variables were introduced allowing the application of the theory involved in the kinematic and static approaches for different targets.

For Bridgemill Bridge, the objective was known from previous reports documenting results for the collapse load being obtained experimentally and analytically. Therefore in this case the value for the true solution was already known. This was important as it was the first example being solved and a reference allowed to verify and to optimize the procedure.

In the example of Cuernavaca Church, it was important to compare two possible mechanisms and understanding the parameters to define which was more critical.

The last arch in a series within a façade of one of the buildings in Praça Reial was performed in order to understand the effect of the loads imposed by several stories in an exterior buttress.

The Roman Aqueduct of Tarragona suggested the challenge of evaluating an out-of-plane mechanism of the transversal section.

One of the façades of Quintela Tower was evaluated also for an out-of-plane mechanism and additionally a design of reinforcement was proposed using the limit analysis technique.

The software`s that were used such as computer-aided design and spreadsheets simplified some of the tasks in terms of time but are not needed for the procedures being performed; these can be done by hand. The software RING© was used for quick verifications in two of the cases. The graphic procedure was tedious in the start but with each new example it was possible to notice a reduction in the time that was needed.

The methodology that was followed suggests the possibility of further examples to be developed which can include different types of structures (natural and artificial), further parameters of comparison

between mechanisms, among others. Furthermore, it constitutes a learning technique not only as a reference abacus when more examples are included and classified, but as an approach for understanding de concepts during the step-by-step process of solving each case.

The assessment of historical constructions requires integrating the knowledge of structural engineering and architecture. In order to propose the best possible solutions, complex concepts from both disciplines must be understood by each professional in order to be able to understand the problem as a whole.

In some undergraduate programs, architecture education has reduced to the minimum the basic contents of the sciences, therefore the language necessary to understand and explain the physic world becomes very limited and speculative. Furthermore the possibility to communicate with engineers is reduced.

However, initiatives like the MSc-SAHC program, has evidenced the growing interest of each side towards integration. From my point of view as an architect this has been a unique opportunity to interact with engineers from different parts of the world and being able to see how a common abstract language allows understanding and solving real problems. With basic tools I have seen how new techniques were learned and used in practical matters. Within the techniques introduced Limit Analysis has been the bridge to start understanding basic concepts that were presented during the courses, and with each case study I have developed for this thesis the fragments have started to come together.

Leonardo da Vinci used to say: *“un arco è la somma di due debolezze che genera una fortezza”*<sup>2</sup>.

---

<sup>2</sup> Italian version from a quote in (Huerta Fernández, 2004)



## 5. REFERENCES

Abacilar, P., Manrique, C., Roberts, G., & Taneri, C. (2010). *Quintela Tower - Integrated Project*. Guimaraes.

*Aero-plano*. (n.d.). Retrieved Junio 28, 2010, from Producciones audiovisuales

Ajuntament de Tarragona. (n.d.). *Museu d'Historia de Tarragona*. Retrieved June 11, 2010, from <http://www.museutgn.com/monumentos.asp?id=11>

*Alcolea Antigüedades*. (n.d.). Retrieved June 29, 2010, from <http://www.alcoleaantigüedades.com/images/Plaza-Real-81-x-60.jpg>

archINFORM. (n.d.). *International Architecture Database*. Retrieved June 28, 2010, from Francesc Daniel Molina i Casamajó: <http://spa.archinform.net/arch/108346.htm>

Block, P. (2005). *Equilibrium systems: Studies in Masonry Structure*. Cambridge: MIT.

Block, P., & Ochsendorf, J. *Lower-bound Analysis of Masonry Vaults*. Cambridge.

Block, P., DeJong, M., & Ochsendorf, J. (2006). As Hangs the Flexible Line: Equilibrium of Masonry Arches. *Nexus Network Journal* 8 , 13-24.

Franchetti, P. (2009). Damage and collapsing mechanisms in existing (particularly historical) structures. *MSc-SAHC*. Guimaraes.

Gilbert, M. (2007). Limit analysis applied to masonry arch bridges: state-of-the-art and recent developments. *ARCH'07 – 5th International Conference on Arch Bridges*, (pp. 13-28).

Gilbert, M. (2005). *RING: Theory and Modelling Guide*. Computational Limit Analysis and Design Unit. The University of Sheffield.

Heyman, J. (1996). *Elements of the Theory of Structures*. New York: Cambridge University Press.

Heyman, J. (1995). *The Stone Skeleton: Structural Engineering of Masonry Architecture*. Cambridge: Cambridge University Press.

Huerta Fernández, S. (2004). *Arcos, bóvedas y cúpulas: Geometría y equilibrio en el cálculo tradicional de estructuras de fábrica*. Madrid: Instituto Juan de Herrera.

Huerta, S. (2003). El cálculo de estructuras en la obra de Gaudí. *Ingeniería Civil* 129 , 121-133.

Huerta, S. (2001). Mechanics of masonry vaults: The equilibrium approach. *Historical Constructions* (pp. 47-69). Guimarães: P.B. Lourenço, P. Roca (Eds.).

*IGESPAR IP - Instituto de Gestão do Património Arquitectónico e Arqueológico (former IPPAR)*. (n.d.). Retrieved 2010, from <http://www.igespar.pt/pt/patrimonio/pesquisa/geral/benscomproteccaolegal/detail/70323/>

*La Praça Real*. (n.d.). Retrieved June 28, 2010, from <http://www.lareial.com/>

Lourenço, P. B. (2001). Analysis of historical constructions: From thrust-lines to advanced simulations. *Historical Constructions* (pp. 91-116). Guimarães: P.B. Lourenço, P. Roca (Eds.).

Marcari, G., Maca, J., & Oliveira, D. (2009). Seismic Behaviour and Structural Dynamics. *SA3\_11\_2009 MSc-SAHC*. Guimaraes: MSc-SAHC.

Massachusetts Institute of Technology - Building Technology Program - Masonry Research Group. (n.d.). *Interactive Thrust*. Retrieved June 3, 2010, from <http://web.mit.edu/masonry/interactiveThrust/examples.html>

Massachusetts Institute of Technology - MIT. (n.d.). *Interactive Thrust*. Retrieved June 17, 2010, from <http://web.mit.edu/masonry/interactiveThrust/>

Meli, R. (2009). On Structural Bases for Building the Mexican Convent Churches From the Sixteenth Century. *International Journal of Architectural Heritage* (3), 24–51.

Molins, C. (June 1998). Capacity of Masonry Arches and Spatial Frames. *Journal of Structural Engineering*.

*Museu de Arqueologia e Numismática de Vila Real*. (n.d.).

O. P. C. M. 3431. (2005). *Ordinance of the Prime Minister. 3rd of May*.

Orduña, A., & Lourenço, P. B. (2001). Limit analysis as a tool for the simplified assessment of ancient masonry structures. *Historical Constructions* (pp. 511-520). Guimarães: P.B. Lourenço, P. Roca (Eds.).

Roca, P. (2010, June). Acueducto Romano de Tarragona-croquis. Barcelona, España.

Roca, P. (2009-2010). Ancient Rules and Classical Approaches- Part 1-4. SA1 Lectures. *Advanced Masters in Structural Analysis of Monuments and Historical Constructions*. Guimaraes.

Roca, P. (2009-2010). Damage and Collapse Mechanisms - Part 1. *Advanced Masters in Structural Analysis of Monuments and Historical Constructions*. Guimaraes.

Roca, P. (2009-2010). Damage and Collapse Mechanisms - Part 2. *Advanced Masters in Structural Analysis of Monuments and Historical Constructions*. Guimaraes.

Schram, W. D., & Passchier, C. W. (2005, March 25). *Roman Aqueducts*. Retrieved June 11, 2010, from Tarragona (Spain): <http://www.romanaqueducts.info/aquasite/tarragona/foto3.html>

*SIPA - Sistema de Informação para o Património Arquitectónico (IHRU, Instituto da Habitação e Reabilitação Urbana, IP)*. (n.d.). Retrieved 2010, from Direcção-Geral dos Edifícios e Monumentos Nacionais [DGEMN]: [http://www.monumentos.pt/Monumentos/forms/002\\_B1.aspx](http://www.monumentos.pt/Monumentos/forms/002_B1.aspx)

*The History of the Spanish Architecture*. (n.d.). Retrieved June 11, 2010, from Aqueduct of Las Ferreras (Tarraco):

[http://www.spanisharts.com/arquitectura/imagenes/roma/i\\_tarragona\\_acueducto.html](http://www.spanisharts.com/arquitectura/imagenes/roma/i_tarragona_acueducto.html)

United Nations. (n.d.). *UNESCO*. Retrieved June 11, 2010, from World Heritage Centre: <http://whc.unesco.org/en/list/875/>

United Nations. (n.d.). *UNESCO*. Retrieved June 11, 2010, from World Heritage Centre: <http://whc.unesco.org/en/news/184>



## 6. ANNEXES

### 6.1. Limit Analysis using RING©

A verification of two of the selected cases was done with the use of RING© software.

#### 6.1.1. Bridgemill bridge: Limit Analysis using RING©

The objective was to replicate the test performed experimentally in order verify the collapse load, the location of the produced hinges and the shape of the thrust line.

The geometry, material and loading parameters were defined as following (report output of RING©):

#### Geometry (all distances in mm, angles in radians)

Global:	No. of spans	Bridge width	Fill depth	LHS abut	RHS abut		
	1	8300	3754	None	None		
Span 1:	Shape	Span	Rise	Auto angle	LHS angle	RHS angle	No of Rings
	Segmental	18290	2840	No	0,969	0,969	1
Ring	No of Blocks	Thickness					
1	40	711					

#### Material Properties (unit weights in kN/m<sup>3</sup>, stresses in N/mm<sup>2</sup>, angles in radians)

Masonry:	Unit Weight	Radial friction	Tangential friction	Crushing Strength		
	20	0,6	0	Infinite		
Backfill:	Unit weight	Fill/arch frictn	Disp angle	Disp type	Horizontal pressure	
	18		0	uniform	None	

#### Load Cases (all distances in mm)

No.	Vehicle	Position
1	L1	4572,5

#### Vehicles (all distances in mm, forces in kN)

Name	Axle no.	Axle position	Axle width	Axle intensity
L1	1	0	10	2740

The maximum external vertical load applied at  $\frac{1}{4}$  of the span that was obtained is 2740kN for a Critical Load Factor = 1.

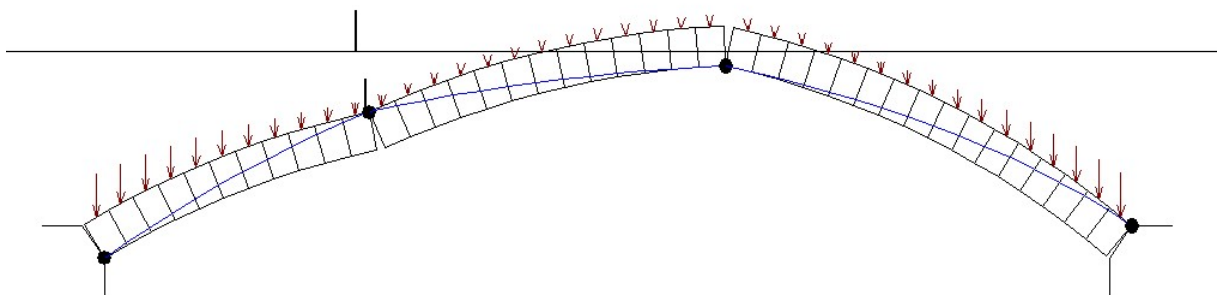


Fig. 106 – RING© output showing a four-hinge mechanism and the corresponding thrust line.

A modification of the Axle width (750 mm) of the applied vertical load at  $\frac{1}{4}$  of the span was done according to the parameters shown in another reference found about the Bridgemill Bridge.

### Vehicles (all distances in mm, forces in kN)

Name	Axle no.	Axle position	Axle width	Axle intensity
L1	1	0	750	2890

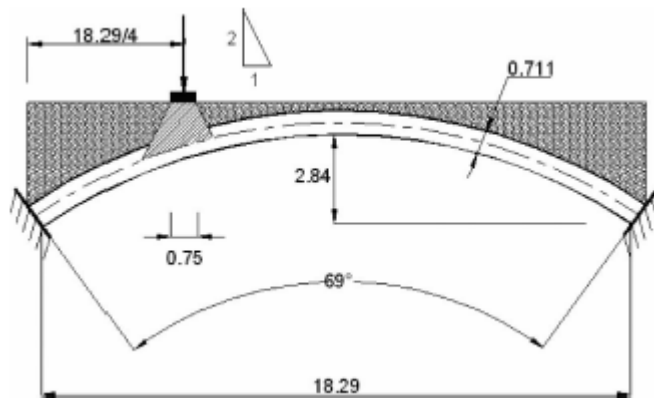


Fig. 107 – Bridgemill bridge geometry with an axle width of 0.75 meters (Meli, 2009)

In this case, the maximum external vertical load applied at  $\frac{1}{4}$  of the span that was obtained is 2890kN for a Critical Load Factor = 1.

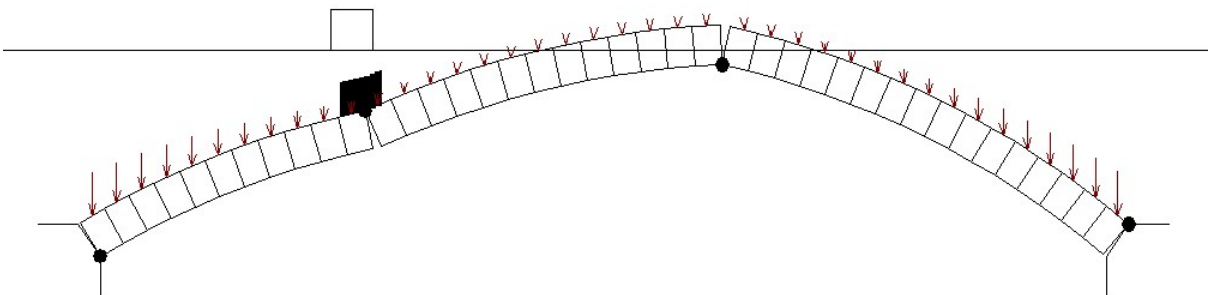


Fig. 108 - RING© output showing the same four-hinge mechanism with a modified axle width for the vertical load.

For the Kinematic approach using computer-aided design software and a spreadsheet, the conditions were according to the first case which takes into account the vertical load applied without a surface distribution. Even though the differences between the results in the maximum external vertical load applied, the locations of the hinges are the same in both cases. According to these considerations, the reference collapse load will be 2740kN.

For the same parameter of loading (2740 kN), the geometry and material properties were modified to consider the structure without infill in order to see the effect in the result for the Critical Load Factor.

The value obtained was 0,59. Without the infill, the maximum vertical load in  $\frac{1}{4}$  of the span that could be applied will be 1617 kN. For an applied load of 1617 kN it was observed the relocation of the third hinge nearer to the support of the arch (two voussiors closer).

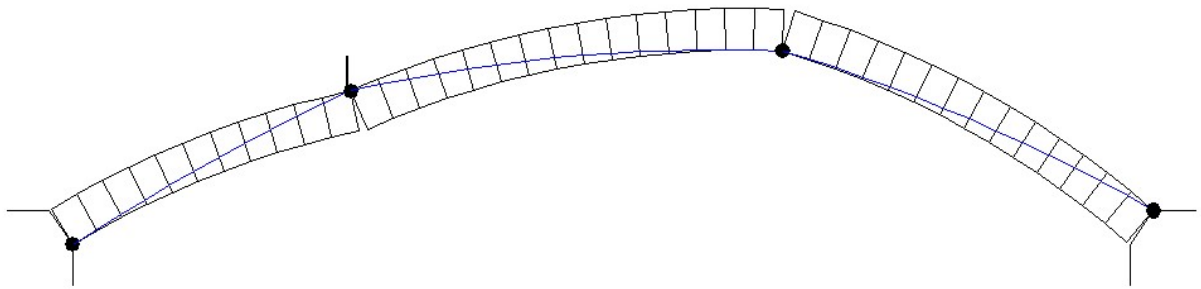


Fig. 109 - RING© output showing the relocation of the third hinge for the arch without infill.

In order to visualize why the location of the load was applied in  $\frac{1}{4}$  of the span, a verification was performed with the same loading value (2740 kN) in the center of the arch. The result obtained for the Critical Load Factor was 13,84, demonstrating that the former case is more critical, therefore corresponding to the load location that must be considered, and the asymmetrical four-hinge mechanism the one to be assumed (as opposed to the symmetrical four-hinge mechanism obtained for the load applied in the center of the arch).

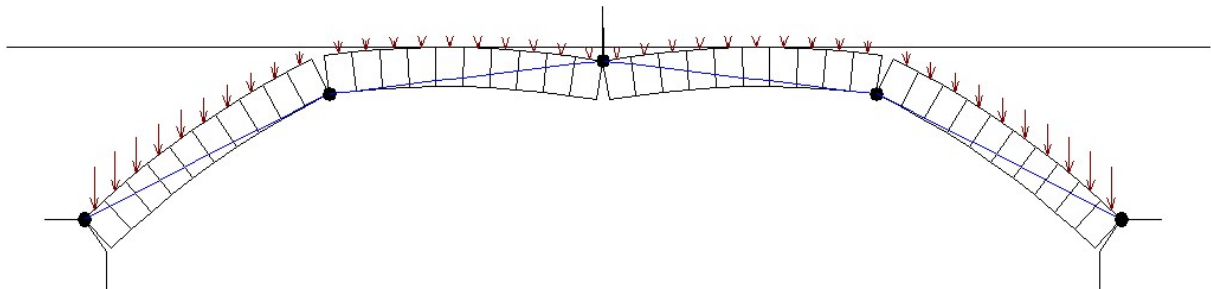


Fig. 110 - RING© output showing the mechanism obtained for the load applied in the center of the arch.

### 6.1.2. Cuernavaca Church: Limit Analysis using RING©

The mechanism obtained for a vertical load in the key of the arch was of an isolated arch with five hinges. The buttresses made no contribution. The “T” section of the arch and buttress was not simulated for this analysis, therefore it represents a massive wall of 4,25 x 10,00 meters. However, as the mechanism that was found was of an isolated arch, this does not affect the result.

The input data was defined as following:

#### Geometry (all distances in mm, angles in radians)

<b>Global:</b>	<b>No. of spans</b>	<b>Bridge width</b>	<b>Fill depth</b>	<b>LHS abut</b>	<b>RHS abut</b>		
	1	10000	0	Yes	Yes		
<b>LHS Abut:</b>	<b>Abut Height</b>	<b>Width(top)</b>	<b>Width(base)</b>	<b>No of blocks</b>			
	13650	4350	4350,00435	10			
<b>Span 1:</b>	<b>Shape</b>	<b>Span</b>	<b>Rise</b>	<b>Auto angle</b>	<b>LHS angle</b>	<b>RHS angle</b>	<b>No of Rings</b>
	Segmental	13500	6749,9325	Yes	0	0	1
	<b>Ring</b>	<b>No of Blocks</b>	<b>Thickness</b>				
	1	40	1000				
<b>RHS Abut:</b>	<b>Abut Height</b>	<b>Width(top)</b>	<b>Width(base)</b>	<b>No of blocks</b>			
	13650	4250	4250,00425	10			

#### Material Properties (unit weights in kN/m<sup>3</sup>, stresses in N/mm<sup>2</sup>, angles in radians)

<b>Masonry:</b>	<b>Unit Weight</b>	<b>Radial friction</b>	<b>Tangential friction</b>	<b>Crushing Strength</b>	
	15,69	0,6	0,5	Infinite	
<b>Backfill:</b>	<b>Unit weight</b>	<b>Fill/arch frictn</b>	<b>Disp angle</b>	<b>Disp type</b>	<b>Horizontal pressure</b>
	0	,524	0	uniform	None

#### Load Cases (all distances in mm)

<b>No.</b>	<b>Vehicle</b>	<b>Position</b>
1	1kN Single Axle	6750

#### Vehicles (all distances in mm, forces in kN)

<b>Name</b>	<b>Axle no.</b>	<b>Axle position</b>	<b>Axle width</b>	<b>Axle intensity</b>
1kN Single Axle	1	0	1	1

A Critical load factor of **315,38** was obtained for the load case defined.

For analyzing the second mechanism which includes the buttresses, RING© was not used as the section plan of the contributing area could not be simulated, therefore the buttress volume of 4,25 \* 10,00 \* 13,65 is not realistic.



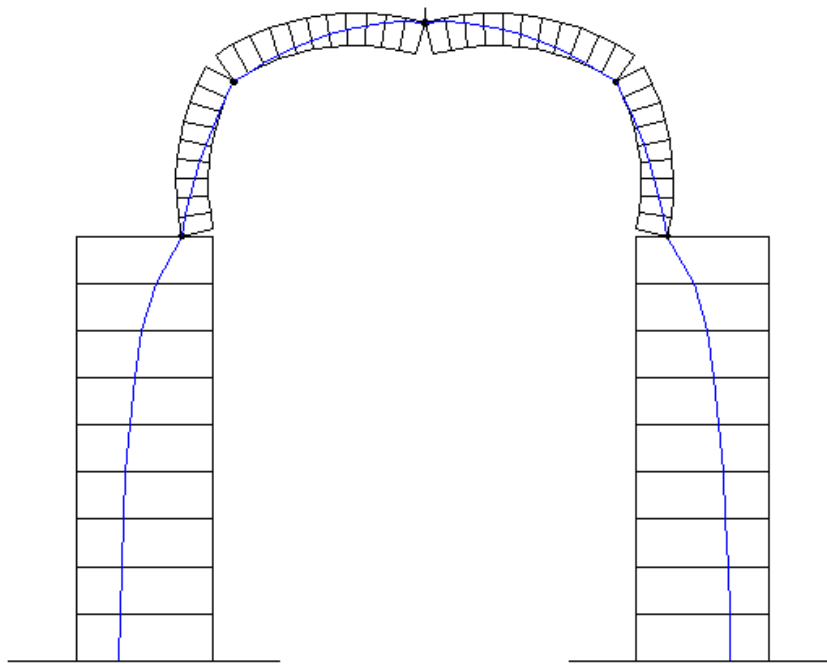


Fig. 111 - RING© output showing the mechanism obtained for the load applied in the center of the arch.